

SOME STUDIES
ON
SEMICONDUCTING AND STRUCTURAL PROPERTIES
OF
VACUUM DEPOSITED FILMS

1966

R. H. JOG, M.Sc.

SOME STUDIES
ON
SEMICONDUCTING AND STRUCTURAL PROPERTIES
OF
VACUUM DEPOSITED FILMS

A THESIS SUBMITTED TO THE
UNIVERSITY OF POONA FOR THE
DEGREE OF
DOCTOR OF PHILOSOPHY
IN
PHYSICS

By
R. H. JOG, M.Sc.
National Chemical Laboratory,
Poona-8.

August, 1966.

C O N T E N T S

	<u>Pages</u>
<u>CHAPTER - I</u> : <u>GENERAL INTRODUCTION</u>	
A : Thin films, their nature, structures and properties.	.. 1
B : Theory of conductivity.	.. 3
C : Thermoelectric power	.. 21
D : Hall effect, photoelectric effect, etc.	.. 24
<u>CHAPTER - II</u> : <u>EXPERIMENTAL TECHNIQUES</u>	
A : Preparation of films.	.. 27
B : Thickness measurement.	.. 28
C : Resistivity measurement.	.. 30
D : Thermoelectric power.	.. 34
E : Temperature coefficient of resistance (TCR) and Hall effect	.. 35
F : Electron diffraction	.. 36
<u>CHAPTER - III</u> : <u>A DEVICE FOR MEASURING SEMICONDUCTING PROPERTIES OF THIN FILMS AND TEMPERATURE OF DISCONTINUITY (T_d)</u>	.. 38
<u>CHAPTER - IV</u> : <u>SEMICONDUCTING PROPERTIES OF TELLURIUM FILMS</u>	
A : <u>Introduction</u>	.. 46
B : Experimental	.. 53
C : Results	.. 55
i) Annealing of tellurium films.	.. 56
ii) Effect of deposition rate	.. 57
iii) resistance ^{of} resistance of films.	
iv) resistivity and activation energy	.. 57

	iv) Thermoelectric power.	.. 89
	v) Temperature coefficient of resistance (TCR).	.. 60
	vi) Resistivity and activation energy of tellurium pellets.	.. 61
	vii) Surface structure	.. 62
	D : Discussion	.. 63
CHAPTER - V	<u>SEMICONDUCTING PROPERTIES OF SnSe, Sn₂Se₃, SnS and SnTe FILMS</u>	
	A : Introduction	.. 72
	B : Experimental	.. 77
	C : Results	.. 78
	i) Resistivity and activation energy	.. 78
	ii) Thermoelectric power	.. 82
	iii) Temperature coefficient of resistance	.. 84
	iv) Electron diffraction patterns	.. 85
	D : Discussions	.. 86
CHAPTER - VI	<u>ELECTRON DIFFRACTION STUDIES OF THE GROWTH OF SnSe, Sn₂Se₃ AND SnTe FILMS</u>	
	A : General introduction	.. 89
	B : Experimental	.. 97
	C : Results	..100
	SnSe and Sn ₂ Se ₃ on:	..100
	Rock salt(100),(110),(111)	
	Mica (0001), Collodion and Glass	

SnFe on:	..	106
Rock salt(100),(110), (111)		
Mica(0001), Colloidion and glass		
D : Discussion	..	107
<u>CHAPTER - VII</u> : <u>SUMMARY AND CONCLUSION</u>	..	110
<u>ACKNOWLEDGEMENT</u>		116
<u>REFERENCES</u>		

CHAPTER - I

GENERAL INTRODUCTION

A : Thin films, their nature, structures and properties

During the last two decades, tremendous development has been made in the electronic devices for power supply, rectification, amplification, detection system, storage of energy and its release on demand, miniaturization of such devices etc. This has been possible due to the development of a new class of materials known as the semi-conductors. Intense researches are going on, throughout the world, to find out newer and better materials with special and desirable properties so as to use them in various electronic equipments.

During the last world war not only selenium, tellurium, sulphides, selenides and tellurides of metals etc. were used in various detection and amplification systems, but also other materials especially single crystals of germanium and silicon with appropriate doping were developed. The developments in these last two semiconductor-materials have revolutionised the entire electronic industries and widened their applications.

In many of the devices, the above materials were used in the form of thin films especially in photocells, resistors,

memory system, thin film transistors (TFT) etc. It is also well known that ~~the~~ material in thin film state behave quite often differently from that of ^{the} bulk. Even highly conducting metals like, sodium, potassium, rubidium and cesium, behave as semiconductors with negative temperature coefficients of resistance, when they are in thin film state (Mayer 1959, 1961). Similar semiconducting behaviour was also observed in silver, gold and nickel (see Holland 1966). Resistivity of a material which is a non-variant parameter, depending entirely on the purity of the sample is no longer constant in thin film state but depends on various factors like, film thickness, rate of deposition etc.

The science of "Physics of Thin Films" is a subject which as yet is much less understood compared to that of the bulk material. Over and above this, further complications are introduced in the understanding ^{of} "Thin Film Physics" by the appearance of new phases, in ^{the} change of structures and also of orientations, surface asperities, etc., during the preparation of films by vacuum deposition methods. Despite these apparent draw-backs, intensive work is being carried out throughout the world, especially in 'USA' and 'USSR' to understand the electron transport phenomena in thin films mainly because of their wide applications in various fields. Most of these results are being kept as guarded secrets.

It is, therefore, of great interest not only to make a thorough study on the electron transport process of thin films and compare them with those of bulk material, but also to have a corresponding study on the structure and the crystal growth process of thin films under different conditions of evaporation. Further as there has not so far been any attempt to standardise the thin film parameter-measurement and ^{to} correlate with the corresponding structure, a systematic investigation has been made here not only to standardise the measurement of parameters, but also to make detail structural studies by electron diffraction method. In subsequent chapters all these details are given.

B: Theory of conductivity

Many of the physical properties of a solid depend not only upon the crystalline nature but also on the electronic structure. The theory of electrical conductivity was initially developed to explain the conduction process particularly for solid metals and later it was extended to explain the properties of semiconductors and insulators.

The first electron theory was postulated by Drude as early as in 1894 and it was further developed by Lorentz (1904-1905). In this theory known as "free electron" theory, it is assumed that extranuclear electrons ^{in metals,} like gas molecules are quite free in the crystal lattice without

much hindrance to one another. A metal is thus considered to consist of positive ions forming the lattice and the valence electrons, giving rise to electron gas. These electrons can move in any arbitrary directions within the metal. The interaction between the electrons and the potential field of the metal lattice, as well as the electro-static repulsion between electrons themselves is considered to be very small and hence, neglected. Though the "free electron" theory could account for many of the properties of metals, in general it could not satisfactorily explain the specific heat of metals, a major weakness of the theory. Further, it did not even suggest any basis for calculating or estimating the value of mean free path (l) of electrons for different metals. Because of this main drawback and also to improve it, Sommerfeld (1928) applied quantum mechanical concepts to the "free electron" theory, assuming that electrons did not make frequent collisions with the atoms or ions and they could move in field-free space, the field of force due to atomic interaction with other electrons being smoothed out except at the boundary of the solid. Though these electrons are indistinguishable the state of each electron i.e. its energy level, is determined by its quantum numbers, such as X, Y, Z and also by the spin quantum numbers with positive as well as negative values. A monovalent metal contains about 10^{23} atoms per unit volume (per c.c.) and the possible energy levels of valence electrons lie very close to each other. Sommerfeld also applied Fermi-

bracket

Dirac statistics to explain the conduction phenomena.

Thus the probability of occurrence of a certain quantum state of an electron is given by the expression:

$$P_e(E) = \frac{1}{\text{Exp} \left[\left(\frac{E-E_f}{kT} \right) + 1 \right]} = f \left\{ \frac{E-E_f}{kT} \right\} \quad \dots(1)$$

where 'E' represents the energy associated with a particular level and 'E_f' is the energy associated with the Fermi-level. In deriving the above expression Pauli's exclusion principle was also taken into account and formula was valid for a non-degenerate system. For a degenerate system, considering the degeneracy of 'g' the above can be modified to:

$$P_e(E) = 'g' \times \text{Exp} \left[\frac{1}{\left(\frac{E-E_f}{kT} \right) + 1} \right]^{-1} = 'g' \times f \left\{ \frac{E-E_f}{kT} \right\} \quad \dots(2)$$

where $f(x) = \frac{1}{e^{x+1}}$

From above expression depending upon the values of 'x' three possibilities exist, namely:

(i) If 'x' is large and positive, then the corresponding value of f(x) will be small *this* leads to a conclusion that when $(E-E_f) \gg kT$, thus the probability of occupation of an energy level is very small.

(ii) If 'x' is large and negative then $f(x) \simeq 1$, which suggests that when $(E-E_F) \ll kT$, the level is almost occupied.

(iii) If $x = 0$ then $f(x) = 1/2$ and in this case the probability of occupation is only half.

From the above discussion it can be seen that the energy levels are most likely to be empty when all levels have energy much greater than ' E_F ' and likely to be occupied when less than ' E_F '.

Actual contribution of electrons in the available states is given by Fermi-Dirac distribution law as follows:

$$n(E)dE = 2Nc(E) P_e(E)dE \quad \dots (3)$$

where $n(E)dE$ = number of electrons in the conduction bands having energies between ' E ' and ' $E + dE$ ' and $Nc(E)dE$ - allowed energy levels per unit volume in the conduction band between the energy levels ' E ' and ' $E + dE$ ', and finally factor ' 2 ' in the above expression accounts for the degeneracy of each level arising from the spin. The final formula obtained by applying Fermi-Dirac statistics for the conduction and carrier concentration per unit volume is given by:

$$\zeta = \frac{ne^2}{m\bar{v}} \cdot l. \quad (4)$$

and

$$n = \frac{8\pi}{3} \left\{ \frac{m\bar{v}}{h} \right\}^3 \quad (5)$$

where:

e - represents charge on an electron

m - mass of an electron

h - Plank's constant, and

\bar{v} - velocity of electrons at the surface of Fermi level

l - mean free path of free electrons.

Sommerfeld's modification of the original theory of Drude not only explains the conductivity but also the contribution arising out of specific heat, since the mean-free path ' l ' could be determined more accurately than before. In spite of this advantage, the Sommerfeld's theory fails to distinguish between metals and insulators. The theory was hence further modified by Bloch(1928). He introduced the concept of periodic potential instead of smoothed out potential of Sommerfeld, by taking into account the interaction between electrons and atomic cores, situated at lattice points of a crystal. It was assumed that the periodicity of such potential was the same as that of lattice.

The solutions of the wave function for such a periodic field are of the form:

: 8 :

$$\psi = U_k(r) e^{ikr} \quad \dots (5)$$

where $U_k(r)$ represents the periodicity of the lattice. On the basis of the original free-electron model all the values of energies were possible. But now by introducing the concept of periodic potential there appear "forbidden ranges" of energies of electrons, where the solutions representing movement of electrons through lattice do not exist. Thus ^{the} energy levels are restricted, so that electrons can occupy only those levels other than the forbidden energy levels. The above theory known as "band theory" introduces also the concept of effective mass (m^*) of an electron moving in a periodic potential field and is given by:

$$\frac{1}{m^*} = \frac{1}{\hbar^2} \cdot \frac{\partial^2 E}{\partial k^2} \quad \dots (7)$$

where:

$$\hbar = h/2\pi$$

E - Kinetic energy, and

k - A wave vector.

In the case of anisotropic bodies m^* is a function of directions. With the Sommerfeld's modification alone, the energy levels of valence electrons of a metal lie very close to each other, thus forming a continuous band, but on the basis of periodic potential of lattice these bands are separated by a energy band gap. On the basis of the above theory, it is now possible to explain the conduction

phenomena in metals and insulators as well as to distinguish between them.

Let us consider the case of a mono-valent alkali metal crystal, which has only one electron at the outer most 's' level. Considering the electrons of opposite spin as per Pauli's exclusion principle, if there are 'N' states possible, only (N/2) states will be filled by electrons of alkali metals, so that each band will be half-filled. Under an applied field the electrons will hence move thus showing conductivity. Alkali earth metals like Ca, Mg, etc. will have similar 'N' states and since there will be two electrons per atom, all the 'N' states will be filled up. Hence under a similar electrical field electron *can* no longer move easily because there is no unfilled space to occupy and the material will thus behave as an insulator. In actual fact, these metals are bad conductors, but not insulators. To explain this, Wilson (1931) proposed ~~his~~ 'zone theory', where he assumed that an array of divalent atoms would show metallic conduction as long as there was an over-lap of wave functions such as s, p, d. These will fill a zone. In three dimensional case of metals the wave functions over-lap on each other, and hence under potential field, slight conductivity is shown, even though, the valence band is filled up.

In a crystal, electrons occupy different states like s, p, d, etc. The inner electrons are firmly bound with the nucleus, whereas the outer most electrons known as valence electrons are not being so, contribute to the conduction phenomena. The bands that lie above the inner electron-shell can be divided mainly into two groups (a) valence, and (b) conduction bands. In the valence band all the available states are occupied by valence electrons, whereas the vacant states in the conduction band can be occupied by the electrons, thus giving rise to electrical conductivity. These two bands are separated by a gap known as "forbidden gap". In case of the insulators the forbidden gap is too large to allow a thermally excited electron to jump from valence band to the conduction band. In the case of monovalent metals, only half the states, in the conduction band, are occupied and because of high concentration of electrons in the band, the electrical conductivity is much higher than that of an insulator.

Semiconductors

As discussed before the solid materials can broadly be classified as conductors and insulators. There, however, exists another class of materials known as semiconductors, conductivities of which are in between those of metals and insulators. Fig.1 gives an idea of the range of resistivity

for metals, semiconductors and insulators. In extreme cases the resistivity of a semiconductor can be as high as an insulator and as low as that of a poor metallic conductor. Resistivity of semiconductors generally lie between $10^{-3} \Omega \text{ cm}$ to $10^6 \Omega \text{ cm}$. These semiconductors show some peculiar properties such as negative temperature coefficient of resistance (TCR), sensitivity to light giving rise to photovoltage and photocurrent or change in the resistance etc.

On the basis of the band theory of solids the behaviour of such semiconducting materials can also be explained. As already discussed, at absolute zero the valence band is filled up and the lower most unfilled band known as conduction band is empty. These bands are separated by forbidden energy gap ΔE . With the rise of temperature, when the thermal energy is sufficient enough to overcome the forbidden energy gap, the electrons can be excited the valence band to the conduction band, leaving behind vacant sites in valence band, thus creating holes equivalent to a positive charge in the valence band. With an applied field both electrons in the conduction band as well as the holes in the valence band take part in the conduction process, though they will move in opposite direction. With the increase of temperature, the creation of electron-hole pairs also

increases and conductivity will also rise. The number of electrons or holes thus created by thermal excitation is given by:

$$n \simeq p = A \exp. \left\{ \frac{\Delta E}{2kT} \right\} \quad \dots (8)$$

n and p = number of electrons and holes.

ΔE = Forbidden band gap.

k = Boltzmann's constant.

T = Temperature in degree absolute.

A = A constant depending upon mass of electron or hole and also to some extent on temperature.

From the above relation it can be seen that the number of electrons or holes created, generally depends upon the exponential term. Thus in the case of a pure semiconductor the conduction is due to the creation of electron hole pairs due to the thermal excitation. The above expression takes the following form when all the factors for 'A' are taken into account:

$$n_1 = 2 \left[\frac{2 \pi kT}{h^2} \right]^{3/2} \times \left[m_e^* \cdot m_h^* \right]^{3/4} \times \exp.(- \Delta E/kT) \quad \dots (9)$$

where

m_e^* and m_h^* represent the effective mass of electrons and holes, respectively. Since holes and electrons arise from different bands the effective mass of an electron may not be necessarily same as that of hole. According to

Sommerfeld's consideration conductivity (σ)

$$\sigma = n_e \cdot \frac{e \ell}{m v} = n_e \mu \cdot e \quad \dots (10)$$

where μ is the mobility of the carrier when only one type of carrier is present. If there are two types of carriers then:

$$\sigma = (n_e \mu_e + p_e \mu_h) \cdot e \quad \dots (11)$$

n and p represent carrier concentrations of electrons and holes. In this expression it is assumed that the mobility of the electrons or holes is small as compared with the exponential factor, then the expression for conductivity can be written as:

$$\sigma = \sigma_0 \exp. (- \Delta E/2kT) \quad \dots (12)$$

where σ is proportional to number of carriers. Semiconductors which obey the above variation are known as 'intrinsic' type. It is also possible to have electrical conduction primarily by the formation of electrons or holes ^{alone} without the creation of electron hole pairs. The situation can be visualized in the following way. In an ideal crystal each atom is surrounded by other atoms in a perfect periodic lattice so that electrostatic neutrality is attained every where. But in reality crystal contains

many defects such as vacancies, atoms at interstitial sites, incorporation of foreign atoms, etc. often imparting peculiar electrical behaviour. The defects due to missing of atoms, addition of impurities etc. will give rise to new levels depending upon the nature of substance, in the forbidden energy band gap in the crystal. Such defects will also give rise to conductivity as was first observed by Gudden (1926, 1934). These impurity levels will be situated near the top of the forbidden gap and will serve as sources as donors of electrons. This type of semiconductors are called 'n' type. On the other hand, when these levels are near the bottom of forbidden energy band they will act as the reservoirs for accepting electrons from the valence band and they are known as acceptors. This type of semiconductors is called 'p' type. Since the energy band heights of these newly created levels are small, there will be large conduction for a small thermal change. Fig. 2 shows the donor and acceptor levels in two types of semiconductors in the forbidden gap. The donor level is just below the bottom of conduction band whereas the acceptor level is just above the top of valence band. The concentration of electrons (n) in the conduction band (c) and holes (p) in the valence

band is given by the relations:

$$n = N_c \cdot \text{Exp. } (E_f/kT) \quad \dots (13)$$

$$p = N_v \cdot \text{Exp. } \left\{ - (\Delta E + E_f)/kT \right\} \quad \dots (14)$$

$$n \cdot p = F(T) \cdot e^{-\Delta E/kT} \quad \dots (15)$$

where $F(T) = AT^{3/2}$

The band structure is applied to periodic array of atoms in the crystal. The concentration of impurity atoms which is low in the semiconductor crystals, will be randomly disposed in the lattice. The disordered lattice thus created by the presence of impurity provides the free electrons for conductivity. In the case of very high concentration of impurities, disposed randomly in the crystal lattice, these will add to the residual resistance. Wilson's (1931) classification was insufficient as reported by Verway et.al. (1948). Mott (1949), for the above class of materials suggested that the description of electronic configuration in terms of Bloch wave functions was not correct and therefore the use of London-Heitler wave function was also necessary.

From the above survey of conduction mechanism it can be seen that though the details of Drude-Lorentz theory and the band theory differ, still the physical phenomena of conduction is more or less similar in both the cases.

Mean free path of electrons is an important factor governing the conduction phenomena.

The theories developed above are valid for metal crystals, solid semiconductors and insulators. Since many of the solid state devices involve the use of thin films it will be worthwhile to consider the theory of conduction as applied to thin films.

An ideal thin film is a limiting case of a solid where one dimension of the material is reduced very much as compared to the other two dimensions, namely length and breadth and since this may vary from atomic ~~size~~ dimension to the order of mean free path of electrons or even larger than that. From formula (10) it can be seen that conductivity depends upon mean free path ' l '. In the case of thin films since the thickness parameter may be comparable to the mean free path of electrons, the behaviour of conductivity of films is likely to differ from that of bulk materials. Fuchs (1938) gave a detailed analysis of the mechanism of electrical conduction in thin but ideal films. He considered a spherical Fermi surface where ' p ' fraction of electrons incident on the boundary-surface are specularly reflected, then the conductivity is given by:

$$\frac{\sigma_0}{\sigma} = \frac{\phi(k)}{1} \quad \dots (16)$$

: 17 :

where: $k = \frac{\text{Thickness}}{\text{Mean free path}} = \text{Reduced thickness.}$

σ = Conductivity of a metal film.

σ_0 = Conductivity of bulk material.

By considering $\sigma(k)$, a final expression for conductivity of thin metal films was given by Sondheimer (1952) as follows:

$$\frac{\rho}{\rho_0} = \frac{1}{1 + \frac{3k}{4} \left\{ 1 - \frac{k^2}{120} \left(E_1(-k) \right) - \frac{3}{8k} (1 - e^{-k}) - \left\{ \frac{5}{8} + \frac{k}{16} - \frac{k^2}{16} \right\} e^{-k} \right\}} \dots 1$$

From the above, an approximate formula for thin films where thickness is much smaller than the mean free path is given by:

$$\frac{\rho}{\rho_0} = \frac{4}{3 \frac{d}{\lambda} \left\{ \ln \frac{1}{d} + 0.4228 \right\}} \dots (18)$$

and for thicker films where thickness is much larger than mean free path is also given by:

$$\frac{\rho}{\rho_0} = \left[1 + \frac{3}{8} \frac{l}{d} \right] \dots (19)$$

or

$$\frac{\rho}{\rho_0} = \frac{1}{d} \left[d + \frac{3l}{8} \right] \dots (20)$$

or

$$\rho \cdot d = \rho_0 \left\{ d + \frac{3}{8} l \right\} \dots (21)$$

In deriving above formulae it was assumed that scattering of electrons at the surface was entirely diffuse. Sondheimer (1952) further obtained the expression in terms of 'p' the fraction of electrons scattered at the surface, as given below:

$$\frac{\rho}{\rho_0} = \frac{\sigma_0}{\sigma} = \left[1 + \frac{3}{8K} (1-p) \right] \quad \dots (22)$$

where $K = \text{Reduced thickness} \gg 1$.

It can be clearly seen from the above expression that:

(i) $p = 1$ for all electrons specularly reflected, the effective conductivity is independent of thickness since above expression reduces to $\sigma = \sigma_0$.

(ii) $p < 1$ conductivity decreases with the decreasing thickness which generally is the case when thickness of the film is comparable to the mean-free path. This theory was further extended by Ham and Mattis (1960), Price (1960) and applied vector mean-free path by considering the general ellipsoidal energy surface for the cases (i) $p \neq 1$ and (ii) $p = 0$.

The above expression for the resistivity of films as derived by Sondheimer has recently been used by Mayer (1959). In all above discussions it was implied that the film was of ideal type and continuous. But in reality no films are

continuous as reported by many electron microscopy studies.

During the formation of a vacuum deposited film it is well known that in the initial stage nuclei are formed which later on with time of deposition give rise to islands. The size of these islands increases with thickness during the deposition process and finally a continuous film is formed but with certain asperities depending upon the deposition conditions. Basset, Menter and Pashley (1959) and many others showed, the formation of island with the increase of thickness. As the size of island increases, the average distance between decreases. According to Neugebauer (1962, 1964) conductivity of a film involves:

(i) Thermal activation of the charge carrier, creation process involving removal of electron from initially neutral island leaving it positively charged, and

(ii) The drift of free charges by tunneling through gaps between islands.

Neugebauer and Webb (1962) gave the following expression for conductivity of a vacuum deposited film.

$$\sigma = \frac{A \cdot \sqrt{2m\phi}}{h^2 d} \text{Exp.} \left\{ -\frac{4\pi d \cdot \sqrt{2m\phi}}{h} \right\} \times B \cdot \text{Exp.} \left\{ -\frac{e^2 / \epsilon r}{kT} \right\} \text{cm}^{-1} \text{cm}^{-1} \dots (23)$$

where:

A and B are constants.

ϕ = is potential barrier between islands.

e is the electronic charge.

m electronic mass.

ϵ dielectric constant of the substrate.

r Average radius of the island, and

k Boltzmann's constant.

The first term $\text{Exp.} \left\{ - \frac{4 \pi d}{h} \sqrt{2m \phi} \right\}$

in the above expression contributes to conductivity because of tunneling effect whereas the second term

$\text{Exp.} \left\{ - \frac{e^2 / \epsilon r}{kT} \right\}$ contributes due to the size of islands and dielectric constant of the substrate.

On the basis of island structure it is possible to see that for smaller size of island there will be a greater activation energy, and larger the distance between the islands lower is the probability of tunneling, and lower conductivity.

When contribution arising from the tunneling effect is negligible as compared with $\frac{e^2 / \epsilon r}{kT}$ conductivity can

be written as:

$$\sigma = \sigma_0 \left\{ \frac{-e^2 / \epsilon r}{kT} \right\} \quad \dots(24)$$

which can be qualitatively compared with:

$$\sigma = \sigma_0 \exp(-\Delta E / 2kT) \quad \dots(25)$$

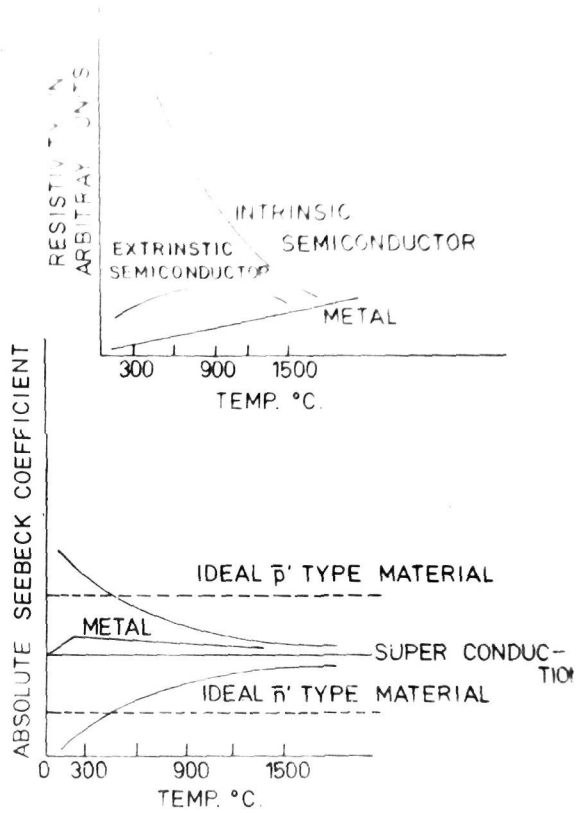


Fig. 3.

C: Thermoelectric power (α)

It is well known that if a temperature difference is maintained between two ends of a semiconductor or a metal, a thermal e.m.f. is produced. This effect was first observed by Seebeck (1822) and therefore known as Seebeck effect. The measurement of this effect also gives information about the electron transport process. Thermoelectric power has great applications in devices as thermoelectric generators. For such uses the materials should have a large value of thermoelectric power. Electrical resistivity, thermal conductivity and Seebeck coefficient all depend on each other, and from their knowledge it is possible to estimate carrier concentration, mobility, etc. It is also found that the Seebeck coefficient of metals, ranges from extremely small values to approximately $80 \mu\text{volts}/^\circ\text{C}$, however, for semiconductors, this range is $50 \mu\text{volts}/^\circ\text{C}$ to $\simeq 400 \mu\text{volts}/^\circ\text{C}$. The materials having Seebeck coefficient $\simeq 100$ to $400 \mu\text{volts}/^\circ\text{C}$ are generally selected for thermoelectric operations.

In an ideal case the thermoelectric power should have invariant optimum values and these values should not depend on temperature of observation. The situation is shown in the Fig. 3. From graphs it can be seen that Seebeck effect leads to zero at very high temperatures for materials whether metals or semiconductors.

Thermoelectric power (α) is expressed approximately in terms of Boltzmann's constant (k) and charge of free carriers (e) as follows:

$$\alpha \cdot e = C_v / N = k \quad \dots(2)$$

where C_v is sp. heat of system of charge carriers and N = number of charge carriers, taking part into conduction.

The reverse of Seebeck effect is termed Peltier effect, where heat is evolved at one junction and absorbed at the other when electric current is passed. Seebeck coefficient (α) and Peltier coefficient (π), depend on absolute temperature ($T^\circ K$) and the relation between them is given by:

$$\alpha = \pi / T \quad \dots(27)$$

The cause of Seebeck effect can be expressed in the following way. When one end of the specimen is at a higher temperature than its other end, the concentration and velocities of electrons at the hot end will be increased. This situation will cause a diffusion of electrons from the hot end to the cold end, along the thermal gradient. This flux of negative charges sets a potential difference between two ends. The concentration, velocities of electrons at hot end and their diffusion, depends upon the thermal gradient between hot and cold ends. Thermoelectric power (α) depends upon the temperature difference between the two ends of the specimen. In the case of a mixed semiconductor

there is a diffusion of electrons and holes, along the thermal gradient from the hot end to the cold end. In a metal the carrier concentration of free electrons does not change with the temperature, whereas in a semiconductor, temperature is one of the most important factors, which control the carrier concentration of electrons and holes taking part in the diffusion process. In general the expression for thermoelectric power (α) for a non-degenerate system is given by:

$$\alpha_{np} = -\frac{k}{e} \left[\frac{n \mu_e \left\{ \left(\frac{5}{2} - s \right) + n \left(\frac{N_c}{n} \right) \right\} - p \mu_h \left\{ \left(\frac{5}{2} - s' + n \left(\frac{N_v}{p} \right) \right) \right\}}{n \mu_e + p \mu_h} \right] \dots (28)$$

and for a degenerate semiconductor:

$$\alpha'_{np} = -\pi^2 \frac{k}{e} \left[\frac{n \mu_e \left\{ \left(\frac{1}{2} - \frac{1}{3} s \right) \left(\frac{kT}{E_f} \right) \right\} - p \mu_h \left\{ \left(\frac{1}{2} - \frac{1}{3} s' \right) \left(\frac{kT}{E_f} \right) \right\}}{n \mu_e + p \mu_h} \right] \dots (29)$$

In the above expression it is assumed that the time of relaxation for electrons and holes is a function of energy which depends upon the scattering mechanism. Ioffe (1957) gave different values for the term $(5/2 - s)$ in above expressions for different scattering centres. Further the occurrence of thermoelectric power was also explained on the basis of phonon-drag effect and finally expression for thermoelectric power is given as:

D: Hall effect, Photoelectric effect, etc.

One of the important parameters, which determine the mobility factor of electrons and holes, is Hall coefficient. If electric field and magnetic field is applied perpendicular to each other on the specimen, then a voltage is produced along a third mutually perpendicular direction. This voltage is known as 'Hall voltage'. This is given by:

$$V_H = V_L = \frac{R_H \cdot I_x \cdot H_y}{d} \times 10^{-8} \quad \dots(31)$$

where:

I_x = current in amperes passed through specimen

H_y = Magnetic field in oersted perpendicular to the direction of current.

$V_L = V_H$ = Hall voltage developed along the direction perpendicular to both current and magnetic field.

R_H is called 'Hall coefficient'. It is a constant depending upon the nature of the semiconductor. Hall effect mainly arises from the deviation of electrons or holes taking part in the conduction process, by magnetic field and the electric field. Hall coefficient is given by:

$$R_H = \pm \frac{\gamma}{n_e} \quad \dots (32)$$

where positive and negative sign indicate the value arising from holes and electrons respectively and ' γ ' a constant depending upon the degeneracy of the system. In a particular semiconductor where holes and electrons both take part, Hall effect is given by the expression:

$$R_H = - \frac{\gamma}{e} \left[\frac{(nb^2 - p)}{(nb - p)^2} \right] \quad \dots (33)$$

where 'b' represents the ratio of mobility of electrons to those of holes namely $b = \frac{\mu_e}{\mu_h}$. The above expression can be applied in the intrinsic region where the concentration of holes and electrons is nearly equal i.e. $n \simeq p$.

This is -ve sign

$$R_H = \frac{\gamma}{ne} \cdot \frac{b-1}{b+1} - \frac{\gamma}{pe} \cdot \frac{b-1}{b+1}$$

$$R_H \simeq \frac{\gamma}{ne(b-1)} \left\{ \frac{\mu_e}{\mu_h} - 1 \right\} = - \frac{\gamma}{pe(b+1)}$$

Thus factor $\left\{ \frac{\mu_e}{\mu_h} - 1 \right\}$ determines the sign of R_H

whether positive or negative. The sign of R_H is taken positive for holes and negative for electrons.

Finally the parameters like Hall coefficient (R_H) and conductivity (σ) give the idea of Hall mobility

H related by:

$$\mu_H = R_H \cdot \epsilon = \frac{R_H}{\rho} \quad \dots (36)$$

Photoelectric effect

One of the important properties exhibited by semiconductors is 'Photoelectric effect', which was discovered near the end of last century. Semiconductors when exposed to monochromatic ^{or any} source of light, show an increase in the electrical conductivity. This phenomena was soon demonstrated and termed as "Photoelectric effect". The materials like selenium, sulphides, selenides and tellurides, exhibit the above properties. In recent years, sulphides and selenides are very often used as materials for photocells.

CHAPTER IIEXPERIMENTAL TECHNIQUESA: Preparation of films by vacuum deposition

Thin films used for the study of semiconducting properties were prepared from vapour-phase, in an evaporation unit, fabricated in this laboratory, evacuated by an oil diffusion pump and a rotary pump. The bulk materials were evaporated in vacuo ($\approx 10^{-4}$ mm. Hg.), from a microconical silica basket on to glass substrates placed at suitable distance above the basket, which was heated by a tungsten wire coiled around it. Before putting any sample in the basket for evaporation, the tungsten coil was flushed several times in order to remove surface impurities, if any. Substrates were made from gold-seal glass slides or from cleaned mica of size ($4 \times 0.5 \text{ cm}^2$) and placed over a mask in such a way that the effective deposit area was $\approx 3 \times 0.5 \text{ cm}^2$. The basket was generally put at one end, and below the mask, and the distance of which could be varied from $\approx 2 \text{ cm.}$ to $\approx 10 \text{ cm.}$ depending upon the experimental conditions. A chromel-p. alumel thermocouple was also placed in an appropriate position to measure the substrate temperature, during the deposition process. Further, the geometrical arrangement of the glass-substrates was such that there was a gradual



Fig. 4.

decrease in the thickness of the deposit, from one substrate to the other. Thus under the same conditions of deposition the films of graded thickness were obtained on the substrates. This was of particular importance for comparing the properties of films of different thickness, since no two evaporation conditions are exactly similar. All other variables, except the thickness, were generally kept fixed. It was also possible to have many samples of same thickness by altering the geometrical arrangement. Figure (4) shows the arrangement of substrates for varying deposit thickness.

The rate of deposition was controlled, either by controlling the current passing through the filament, or by appropriate adjustment of distance between the basket and the substrate position.

Before the deposition, the glass substrates were cleaned with chromic acid solution, washed thoroughly in running distilled water and finally dried at $\approx 100^{\circ}\text{C}$.

B: Thickness measurement

Unlike bulk material, many of the semiconducting parameters of the film are influenced by the film thickness. Hence a knowledge of thickness is very important. An accurate measurement of thickness involves many difficulties,

since films are rarely of uniform thickness, especially when they are ultra-thin. In the case of thick films, because of surface irregularities caused by evaporation conditions, the film thickness is again not uniform from point to point.

An approximate knowledge of the film thickness can be obtained (by using of the following methods:

(i) Multiple beam interferometry (Tolansky 1948, Hennin 1956, Gontier et.al. 1956, Benjamin, 1966, Leonard and Faney 1964).

(ii) From the knowledge of mass of material evaporated from the filament (Williman and Backus 1949, Ghosh 1961, Ramazanov 1962).

(iii) From the knowledge of mass of film deposited during deposition process (Wait 1922, Steinberg 1923, Brattain and Briggs 1949, Moss 1952, Gillham et.al. 1955, Clark 1956).

In the present study, the last method was used.

An approximate measurement of thickness was calculated from the knowledge of difference in weight of substrate before and after deposition and also from the deposited area, assuming that the density of deposit films is same as that of bulk material. It has been reported by many workers

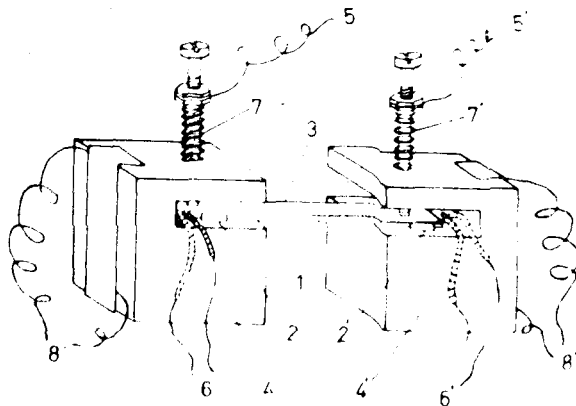


Fig 5.

Experimental set-up for measuring the semiconducting properties of thin films:

1, glass substrate with deposits;
 2 and 2', platinum foils; 3, glass cover;
 4 and 4', brass blocks; 5 and 5', electrode leads;
 6 and 6', thermocouples; 7 and 7', springs; and
 8 and 8', microheater leads.

(Sennett and Scott 1950, Philip and Trompette 1955, Ramaznov 1962) that thickness thus measured by this method agrees well within 10% with the other methods. Though the deposits were uniform in each of the specimen there would be a slight variation in thickness, which could, however, be minimised either by slow rate of deposition or by increasing the distance between the substrate and the source.

Film thickness was calculated by using the relation

$$d = \frac{m}{l \cdot b \rho} \quad \dots (37)$$

where: m = mass deposited on substrate

$l \cdot b$ = deposit area

ρ = density of film \approx density of bulk.

C: Resistivity measurement

In order to study the different semiconducting parameters of vacuum deposited film-semiconductors, the device developed in this laboratory (Fig.5) was used (Goswami and Jog 1964). One of the important parameters is the resistivity or conductivity of a semiconductor. Platinum foil contacts were made at the two ends of the film and introduced into the slots of two brass-blocks. The arrangement was then put in a pyrex boat and then put into a tube of

dia. $\simeq 2.5$ " and 16" in length, continuously evacuated (vacuo $\simeq 10^{-2}$ to 10^{-3} mm Hg.). About 12 terminals were taken out of this tube, the two of them are the silver leads for resistance measurements. In order to study the variation of resistance with increase or decrease of temperature an external coaxial heater controlled by variac was used and the temperature inside the tubular-chamber was measured by a thermocouple (chromel-p. alumel type), the details are described in Chapter III.

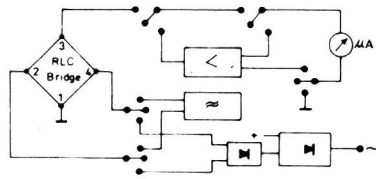
A. C. as well as D.C. resistance was measured by using universal RLC Tessel Bridge operating at 400 cycles/sec. This bridge is suitable for the measurements of resistance, capacitance and inductance. The instrument has four main components namely, the bridge proper, amplifier, A. F. oscillator and power pack. The bridge itself consists of a series of standard resistances of two capacitance standard and two potentiometers for loss factor compensation. A switch is provided for placing the resistors, capacitance standards and compensating potentiometers in the appropriate arms of the bridge as required for the particular measurements intended. According to the actual requirements, an A.C. voltage at a frequency 400 cycles/sec. or a D.C. voltage may be connected to the bridge.

For D. C. measurements a galvanometer is connected directly to the bridge. For A.C. measurements, a two stage A.F. amplifier is inter-posed between the bridge and the galvanometer. Its first valve functions as a normal resistance coupled amplifier. This is followed by a two stage L.C. filter which attenuates the lower frequency components. The sensitivity control is placed between the filter and the next-stage. One section of second valve acts as a triode amplifier, the other section as a diode rectifier of the out-of-balance current supplied to the galvanometer, provided with zero current compensation. The A.F. oscillator used to supply the bridge is of conventional design. Wide range of measurements, facilities for D.C. and A.C. measurements, loss factor compensation, simple operation, direct reading of observed value, are some of the advantages of this bridge. The basic diagram is shown in Figure (6).

An arrangement for low temperature measurements on resistivity of films

In order to measure the resistivity at temperatures below the room temperature, an arrangement was designed and used in our measurements.

The experimental set-up in fig.(5) was introduced in a vertical tube closed at one end dia. ≈ 2.5 " and leads through the other end fitted with rubber cork were taken



BASIC DIAGRAM
 TESLA UNIVERSAL BRIDGE
 T.M. 393

Fig. 6.

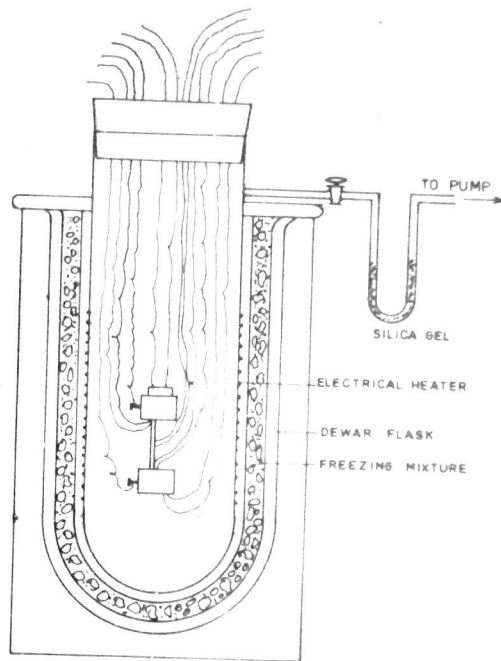


Fig 7.

out which were further connected to the external measuring instruments for A.C. bridge and a D.C. potentiometer. The tube was continuously evacuated by oil rotary pump through a 'U' tube trap containing silica gel to absorb moisture in the experimental tube if any. An electric heater was wound around this tube and finally introduced into an other pyrex tube of slightly bigger size (3" dia.) and this set-up was then introduced vertically in a Dewar-flask containing freezing mixture namely ice and salt. Open top of Dewar-flask was carefully covered by a sheet of non-conductor of heat (Fig.7). This arrangement could give temperature as low as $\approx -10^{\circ}\text{C}$ to $\approx -12^{\circ}\text{C}$. The measurements for resistance were made in usual way as mentioned before during fall of temperature namely from room temperature to low temperature ($\approx -12^{\circ}\text{C}$), and when lower fixed temperature was reached an electrical heater arranged around the experimental tube was used in order to heat the freezing mixture uniformly thereby getting steady increase in temperature, slightly above the room temperature. The measurements of resistance were also done during heating from $\approx -12^{\circ}\text{C}$ to room temperature. Thus from room temperature to low temperature (-12°C), and back to room temperature also

caused cooling and heating curves and hysteresis loop could be minimised by a good control, during cooling and heating process. This measurement was used practically for all the films studied.

D: Thermoelectric power (α)

One of the most important basic parameters in the semiconductor study is the thermoelectric power, which throws light on the conduction mechanism and hence the ionic mobility. For the above purpose, a set-up, similar to the one used in resistance measurements was used. To create a thermal gradient between two ends, one end of the film was heated by a micro-heater and other was kept, comparatively at cold temperature i.e. at room temperature in vacuo $\simeq 10^{-2}$ to 10^{-3} mm Hg. The E.M.F. thus produced was measured by a potentiometer method. The record of E. M. F. was done with the rise, as well as, the fall of temperature below T_d . The rate of heating was maintained by controlled heating, $\simeq 2^\circ\text{C}/\text{min.}$, and readings for E.M.F. developed were taken when a practically steady temperature was reached. Some times the cold junction was also kept at the temperature of melting point of ice (0°C) and other end was heated, and the E.M.F. thus created by the thermal gradient was recorded in the usual way. The slope of the graph namely e.m.f. generated Vs temperature difference

between two ends gives the thermoelectric power.

$$\text{Thermoelectric power } (\alpha) = \frac{\text{e.m.f. between two ends}}{\text{Temperature difference between two ends.}}$$

The type of semiconductor was determined from the sign of polarity, namely when the cold junction was positive, it was of 'p' type, and when cold junction was negative, the semiconductor was of 'n' type.

E: Temperature coefficient of resistance (TCR) and Hall effect

Another parameter equally important is the temperature coefficient of resistance (TCR) which is defined as the change in resistance, per unit, resistance, per unit change of temperature. Resistances at different temperatures on resistance Vs temperature graph were noted and the slope $\frac{dR}{dT}$ at the temperature obtained, and TCR i.e. $\frac{1}{R} \frac{dR}{dT}$ was calculated. In some cases, two points on the graph, resistance VS temperature were taken, where the mean resistance was $R = \frac{R_1 + R_2}{2}$ and $dR = R_1 - R_2$, $dT = T_1 - T_2$. A plot of resistance Vs temperature was made for all the samples and TCR calculated for each of the films and variation of TCR with temperature was also calculated.

Hall effect is measured by noting the voltage when passing a direct current of about several m.A; through the specimen subjected to the magnetic field at right angles to the direct current.

F: Electron diffraction

The vacuum deposited films used for the electrical measurements were examined in the Electron Diffraction Camera, (cold cathode type), fabricated in this laboratory, for their structures. The films were examined by reflection method, both before and after the electrical measurements. In most of the cases the surface layers were polycrystalline in nature and developed one degree orientation depending upon the thickness of the film. It was, however, observed that higher thickness of the films favoured one degree orientation. "Tilted orientation" of deposits was often observed because of asymmetrical deposition from the source, with respect to the substrate and consequently the change in the angle of incidence of vapour with the substrate. In many cases especially during the study of crystal growth process the deposits were formed on the single crystal substrate as described in Chapter VI. The method of interpretation

of all these electron diffraction patterns was similar to those already mentioned by Beeching (1936), Finch and Wilman (1937), Thompson and Cochrane (1939), Pinsker (1953), Vainshtein (1964).

These electron diffraction patterns can be broadly classified in the following main categories:

(i) Patterns due to single crystals (mosaic) or two-degree orientated deposit crystals mostly consisting of spots some times with slight spread depending on the degree of perfection of orientation.

(ii) Ring patterns not showing any change in the intensity distribution along the rings with the change of beam direction, are due to unoriented polycrystalline deposits.

(iii) Patterns consisting of arcs or with a change in intensity distribution along the rings but remaining unchanged with change of beam direction are normally due to polycrystalline deposits having preferred orientation (one degree).

CHAPTER III

A DEVICE FOR MEASURING SEMICONDUCTING PROPERTIES
OF THIN FILMS AND TEMPERATURE OF DISCONTINUITY(T_d)

Experimental methods to study the different parameters of semiconductors in bulk form have more or less been standardized (Ioffe 1957, 1960), but the same cannot be said of the vacuum deposited films (Levinstein 1949, Scanlon and Lark-Horvitz 1947, Abele's 1956, Ghosh 1961, McKay, ^{and} Gravelle 1961). The difficulties involved in dealing with thin films, which are practically of two dimensions in nature arise from their flimsy character as well as high reactivity even at room temperature. The high reactivity ~~of thin films~~ of thin films, demands that all the measurements should be carried out as far as possible in vacuo especially when the measurements are carried out at temperatures higher than the room temperature.

In order to determine different parameters like resistivity, activation energy, thermoelectric power, etc., of semiconductors the first requirement is the suitable electrical contact of the film with the electrodes. These contacts with films can be made by a number of methods. In one of them, heavy deposits of metals such as gold, silver or platinum (or with aqua-dag) are made at two ends of the insulating substrates, like glass or quartz and then semiconducting films are deposited over them.

(Holmes 1923, Luis Harris 1946, Bonfigliotti 1956, Reimer, 1957). Another procedure is to deposit the film first and the electrodes later on, at two ends of the film (Holland 1956). In some other variations of making the electrical contacts, however, the semiconducting layers are sandwiched between two metal film electrodes. All these methods suffer from a major defect, namely the formation of alloy layers or of compounds at contact region of electrodes due to the high reactivity of films. These layers spread by the diffusion process with the rise of temperature. Any measurement like resistivity or thermoelectric power, will also include the contribution from these layers and hence, unless corrected for, eventually will result in a serious error.

Further, it is well known that a bulk material evaporates partially or even completely, when it is in thin film state, at temperatures much below its melting point. This leads to a practical difficulty i.e. the continuous evaporation of material from the surface layers of thin films, with the rise of temperature. The extent of evaporation increases with the temperature and unless, proper precautions are taken, the resistance measurements will not yield reproducible results during

heating and cooling cycles. Other factors to be taken into account are stress, inhomogeneity, etc. present in the films. These can, however, be removed by appropriate annealing at a suitable temperature. Again the temperature at which the annealing is done should be such that the loss of material due to evaporation should be minimum. The above difficulties have considerably been reduced in the apparatus designed and experimental set up used for measurement of resistivity (ρ) and thermoelectric power (α) is described below.

The experimental set-up used is shown in Fig. 5. The thin films of semiconducting material were deposited in vacuum, on glass-slides (gold-seal) cut into size $\approx 4 \times 0.6$ cm² after proper cleaning. Two flexible platinum foils (thickness ≈ 0.02 mm) of size about 1.5×0.6 cm² were placed over the film with a 'U' turn and over them, another glass-slide of the same size, without any deposition was put. The two ends of this set up were then inserted into the slots of two brass-blocks provided with leads and tightened by means of screws controlled by springs. The leads thus automatically made contact with two platinum foil electrodes.

The top glass-slide not only protects the film from damage, as will be seen later, but also prevents the evaporation of deposit-films to some extent without any

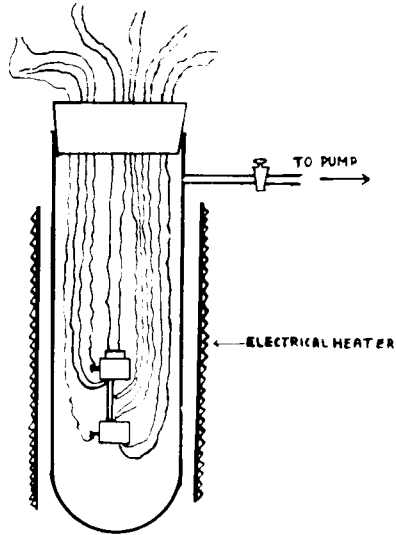


Fig 8.

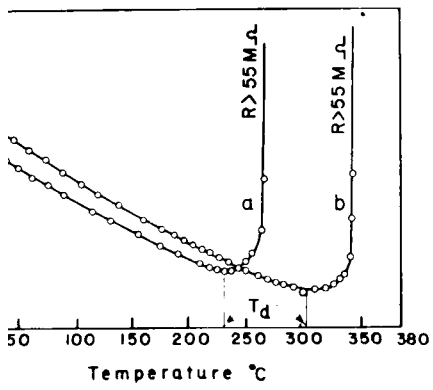


Fig 9.

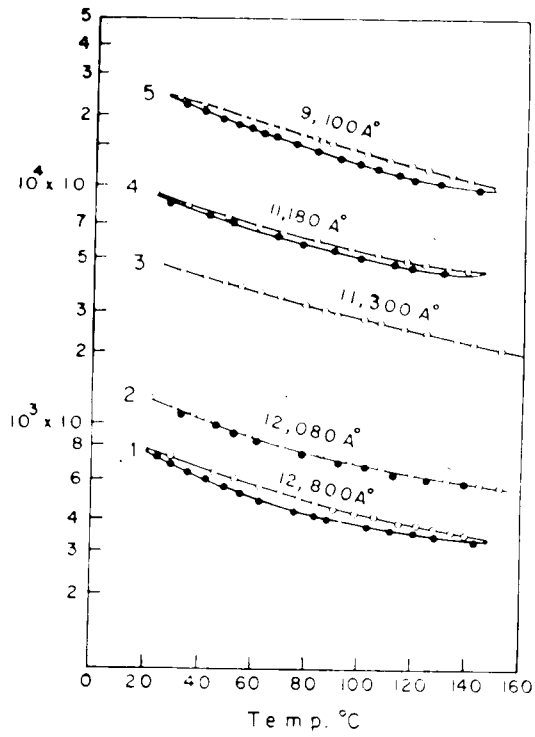


Fig 10.

hindrance to the evacuation of the set-up during the subsequent measurements. Two micro-heaters were attached to the brass-blocks to heat the film at the ends and two thermocouples also introduced for the measurement of temperature. A third thermocouple was also introduced in between the two ends. The whole set-up was then put in a pyrex tube dia. \approx 2.5 cm. in diameter and 16 cm. in length with one end closed and other end fitted with a rubber cork with appropriate holes to allow different leads. The tube was continuously evacuated by rotary and oil diffusion pump to a pressure of $\approx 10^{-4}$ mm Hg. (Fig.8).

'12' terminal/ were taken out for the measurements, (6 for thermocouple, 4 for heaters, and 2 for electrodes). The glass tube with the set-up inside was uniformly heated by an external electric heater controlled by a variac. For the measurements of the temperature below room temperature this tube with the set-up was put into a thermos-flask containing a freezing mixture and the mouth was covered by thermocouple (Fig.7). With this arrangement the measurements could be made down to $\approx -12^{\circ}$ C.

The set-up, with the film on the substrate was put in a glass chamber and evacuated continuously. The tube was heated by an external heater and the ~~for~~ A.C. resistance measurements were carried out with an Universal Tesla Bridge during heating cycle. Fig.(9) shows the typical variation of resistance of

semiconducting films (in the case of tellurium films) with the rise of temperature (measured in vacuo). It was also found that the film resistance decreased with the gradual increase in the temperature and at a certain temperature region, the resistance instead of decreasing with the further rise, remained more or less steady and suddenly became infinitely large. This sudden rise of resistance was found to be due to a break in the continuity of the film. This behaviour was found to be universal for all films (semiconducting) studied so far. The temperature region beyond which the resistance suddenly increased, was termed as "temperature of discontinuity" (T_d). It was also found that the resistance measurements were repeatable both during the heating, as well as cooling cycles, for any temperature, provided the maximum temperature was below the ' T_d ' temperature. If on the other hand, the temperature once rose beyond the ' T_d ' temperature, measurements were irreproducible. Thus to have reproducible and meaningful results of resistance measurements T_d temperature was the upper limit for any semiconducting parameter measurements. It was also found that this ' T_d ' temperature was much lower than the m.p. of the corresponding solid materials for tellurium, lead sulphide, lead telluride, lead selenide, etc

respectively. Since this T_d temperature is low for films compared to m.p. of bulk it will be useful, if possible, to increase this limit to higher value. It has been found by Coswami and Jog (1964) that if a top glass cover of the same size as the substrate, is placed over the platinum foil as shown in the experimental set-up, the T_d region increased by about 80-100°C, thus increasing the useful range of measurements. The curve 'b' in Fig.(9) shows such an increase. Similar increase was also found for many other semiconducting films. If the resistance measurements are now carried out upto T_d temperature during the heating cycles, followed by a similar measurement during the cooling period, the heating and cooling curves lie very close together. With the careful control of heating and cooling cycles these two curves even merged to one curve as shown in Fig.(10).

Generally, resistance was measured in running temperature, such a procedure ⁱⁿ the heating and cooling showed a hysteresis, in the heating and cooling curve (Fig.10). The width of the hysteresis loop was, however, governed by the rate of heating and cooling of the film as controlled by the variac. With the slow rate of heating and cooling, the width of the loop was much smaller (Fig.10). Repeated

measurements of resistance showed that the paths were repeated for any number of heating and cooling process. In actual practice, therefore, moderate rate of heating and cooling was adopted, say 2°C in 5 minutes, with the help of the variac, and a mean of heating and cooling path was taken for the necessary graphs. It was observed that such a mean path was very very close to the equilibrium steady temperature path for the two heating and cooling cycles. Using this dynamic method, it was however possible to make several measurements through out the day, without waiting for a long period to attain the steady equilibrium temperature. Further, since the aim of the measurements was to have some relative idea of the variation of resistance with the temperature gradient, but not so much of the absolute values, as would be seen in the subsequent chapters, the slight error associated with the measurements, would cancel out during evaluating the semiconducting parameters.

The above device clearly shows the limitation of temperature to which the film can be subjected to the measurements. This limitation is no doubt, due to the rapid evaporation of the films at slightly elevated temperatures, unlike the bulk materials. Since the films are restricted in one dimension i.e. thickness, even a slight evaporation of material from the surface will reflect in a greater change, in the film properties.

It has, however, been assumed here that since the film properties such as resistance, resistivity etc. were reproducible below T_d temperature, for many repeated heating and cooling cycle measurements, the semiconducting films did not lose any appreciable amount of material to affect its properties and hence the thickness remained practically unaltered. This assumption is consistent with the idea of many workers, who used the film resistance as an indication of thickness.

CHAPTER IV

SEMICONDUCTING PROPERTIES OF TELLURIUM FILMS

A: INTRODUCTION

Tellurium occurs in group VIb in the periodic table, its group state being $5s^25p^4$. The elements of the VIb group in the order of increasing atomic number comprise, the insulator oxygen and sulphure, the semiconductor selenium and tellurium and finally the metal polonium (po). The properties of selenium and tellurium, especially the latter, is of great interest since the elements lie intermediate between the metal and the insulator. The study of physical properties of semiconductors was started as early as in 1833 by Faraday. He observed a negative temperature coefficient in the case of silver sulphide, a characteristic behaviour quite different from the conductor namely metals. Becquerel (1839) however observed a photovoltage produced by shining light, later on Smith (1873) also observed the fall of resistance of selenium due to light falling on it and the effect was understood as photovoltaic effect. The first photoelement of modern type from selenium was prepared by Adams and Day (1876). Fritts (1883) prepared first rectifier from selenium. Thus by 1885 workers on different parts of the world determined the

important parameters like negative TCR, rectification, photoconductivity, photoelectromotive force, Bose(1904), Dumwoody (1906), Austis (1907), Pierce (1907-1909) found out that point contact on galena, silicon carbide, tellurium, silicon, etc. were good detectors of radio waves.

transport

Electron ^{transport} properties and mechanism of semiconductivity of tellurium were studied by Hawley, Cartwright, Harberfeld-Schwarz(1948). Unusually high value of Wiedemann Franz ratio of tellurium was quite successfully explained by the above authors. It has been found that in the case of tellurium most of the heat is transferred by bond atoms and comparatively small by free electrons. Thus the heat transferred by free electrons in tellurium is especially small. This itself indicated that tellurium differed from true metals, in that the density of free electrons is much small. Classical statistics was applied to explain the conductivity of tellurium, given by:

$$\sigma = \frac{4}{3} e^2 l n (2 \pi m k T)^{-1/2}$$

where 'n' the density of free conduction electrons.

Specific resistance at R.T. was $\approx 0.3 \Omega \text{cm}$ and corresponding mean free path l was $\approx 5.3 \times 10^{-6} \text{ cm}$ which agreed well with Sommerfeld's value of mean free path for silver using Fermi-Dirac statistics. The density of free electrons (n)

calculated from above considerations was $\approx 2.9 \times 10^{16}/^{\circ}\text{C}$ about one free electron per million tellurium atoms, in contrast to good conductors in which there is approximately one free electron per atom even in limiting case, with mean free path $l \approx 3. \times 10^{-3}$ cm. It was, however, suggested that anomalous electron transport properties *might* be due to a change in small electron density (Cartwright et.al. 1933). It seems reasonable to assume that the mean free path of electrons in tellurium is of same order as in ordinary metals and is not changed very much. Cartwright ~~and~~ et.al. (1934) suggested that the anomalous properties arising in experimental work might be, due to the impurities. Cartwright (1935) also studied the effect of small impurities of common metals on the electrical conductivity and thermoelectric power of purest tellurium single crystal rods. He observed that the conductivity of tellurium was increased which was expected from Wilson's theory (1931). Both measurement of specific resistance and thermoelectric power showed that there was an increase in conductivity with the addition of small metal atoms. The increase in the conductivity was independent of specific resistance of metal added, but was certainly dependent, on the amount of metal added, as impurity in tellurium. Pure tellurium had a negative TCR which became less negative by the addition of metal impurities like, copper or antimony. Haken (1910) reported a very strong evidence for two allotropic modifications of tellurium. One *from* stable at

about 352°C with melting point 452°C , specific resistance $0.2 \text{ } \Omega \cdot \text{cm.}$ and thermoelectric power $\alpha \approx 500 \mu\text{volts}/^{\circ}\text{C}$, and other ~~from~~ which was observed stable at lower temperatures having specific resistance $\approx 5.6 \times 10^{-3} \Omega \cdot \text{cm.}$ and thermoelectric power $\approx 160 \mu\text{volts}/^{\circ}\text{C}$. In contrast to Haken's results, many other investigators (Cohen and Kroner, 1913, Wold, 1916, Lange and Heller, 1929) did not find any influence due to heat treatment. Most convincing evidence that there is only one modification of metallic tellurium is obtained from x-ray analysis by many workers, Groth (1906), Bradley (1924), Stattery (1925), Olshausen (1925) and also from electron diffraction studies of thin films.

Electrical conductivity for pure homogeneous material was then given by the relation:

$$\rho = C \frac{NZ}{NE} ; \rho = C \cdot \frac{NZ+A}{NS+B} \quad (\text{For nonhomogeneous system})$$

where C = constant depending upon the statistics applicable, namely Maxwell's for tellurium. $N = 3.0 \times 10^{22} \text{ atoms/cm}^3$ for tellurium, Z = average number of free electrons per atom for tellurium, S = reciprocal of mean free path, A = density of free electrons and B = scattering of free electrons.

The main interest among the investigators was to know whether the electrical properties exhibited by tellurium were due to the impurity or the allotropic modification due

to heat treatment as reported by Haken (1910), Cartwright (1934, 1935).

Batton (1952) reported tellurium to be 'p' type semiconductor at low, as well as, as at high temperatures, but in the samples of adequate purity there was a range of temperatures within which the sign of Hall coefficient was negative. This anomalous behaviour was also reported by earlier investigators Wold (1916), Middleton (1944), Scanton (1948). It was found that samples containing carrier concentration fewer than $\approx 10^{17}$ carrier/cm³, the Hall coefficient was negative within a certain range of temperatures. At low temperatures Hall coefficient was always positive, changing to negative, at temperature, depending upon the extrinsic carrier concentration. Hall coefficient remains negative between this temperature and 230°C near which, sign becomes positive and remains so upto m.p. of tellurium. The upper reversal temperature is related to the carrier concentration by empirical relation:

$$\ln R' = A + \frac{b}{T_r}$$

where: R' = Hall coefficient, T_r = temperature of reversal, a and b, constants.

In samples cut from single crystals of tellurium, neither the value, nor the sign, of Hall coefficient depended on the orientation of the sample with respect to magnetic field or crystallographic axis. Measurements of Hall coefficient showed that the anomalous behaviour was not due to Ettingshausen effect. This conclusion was also verified by the direct measurements of thermoelectric power (α) and Ettingshausen effect. The intrinsic resistivity for a number of polycrystalline samples was $\simeq 0.5 \Omega \cdot \text{cm.}$ at $\simeq 27^\circ \text{C}$ and the slope of the curves of resistivity as a function of temperature, in the intrinsic range showed ^{that} the forbidden gap $\simeq 0.33 \pm 0.01 \text{ eV.}$

The resistivity was also measured in the form of single crystals. Resistivity was $\simeq 0.56 \Omega \cdot \text{cm.}$ at $\simeq 27^\circ \text{C}$ in the direction perpendicular to the principal axis and $0.29 \Omega \cdot \text{cm.}$ in parallel direction. Since, the samples were well in the intrinsic region at room temperature, these values observed were much higher than those previously reported by Bridgman (1926), Schmidt and Stafflbach (1937). The electrical properties of single crystals of tellurium, were studied extensively by Schmidt and Wasserman (1927), Bottom (1949, 1952), Fukurai (1949, 1952), Allen Nassbaum (1954). Results of these workers showed that tellurium was a 'p' type semiconductor below -40°C , it reversed to 'n' type at about $\bar{2}$ temperature, depending upon impurity concentration and it

changed back to 'p' type at about 230°C , the latter temperature being independent of concentration. The forbidden gap from resistivity vs $1/T$ curves was found to be $\simeq 0.32$ eV.

Loferski (1952) also studied the optical properties and values of forbidden gap determined from his observations were $\simeq 0.32$ eV and $\simeq 0.36$ eV by observing polarization, parallel and perpendicular to 'c' axis respectively.

Not much work has been carried out to study the semiconducting properties of tellurium films obtained from vacuum deposition on glass. Optical properties were studied by many workers (Moss and others, 1949, 1951, 1952). Refractive index was confined to visible or ultraviolet region of spectrum by reflection methods (Van-Dyke 1922, Miller 1925). Transmission method was also adopted by other workers namely Rutter (1930), Pfund (1933), Soezima (1949), Bartlett (1925). Thin films of known thickness were formed from specpure samples of tellurium. It was evaporated in high vacuum and films were prepared of thickness down to $\simeq 0.26 \mu$. The measurements on bulk material indicated the presence of absorption edge in the region $\simeq 3 \mu$ to $\simeq 3.5 \mu$, which was approximately coinciding with the threshold wave length of photoconducting effect in tellurium films (Moss 1951). Tellurium films are also being used for preparing thin films transistors (TFT_s)

(Weiner 1964). It was observed that the evaporated tellurium films were 'p' type semiconductors and the characteristics were as good as those of cadmium sulphide (CdS) films. The drift mobility was also studied by them which was as high as ≈ 200 $\text{cm}^2/\text{volts cm.}$ It was about 10 to 100 times larger than ^{those} reported by the earlier workers. Ghosh (1961) also made some study on tellurium films and found that the band gap was ≈ 0.34 eV.

It is apparent from the above survey that no systematic studies of thin films of tellurium ~~film~~, have been undertaken to correlate the behaviour of semiconducting properties of the film with evaporation conditions, variation of film thickness, etc. A ^{detailed} systematic study has been made on the resistivity, energy band gap, thermoelectric power, TCR, with evaporation conditions and at the same time, the crystal growth process.

B: EXPERIMENTAL

(1) Preparation of tellurium films

Tellurium powder obtained from E. Merck & Co. was evaporated from a micro-conical silica basket in a vacuum chamber as described in Chapter II. Glass and cleaved mica slides of size 4×0.5 cm^2 used as substrates were put on a mask and placed horizontally at a distance about 10 cm. away,

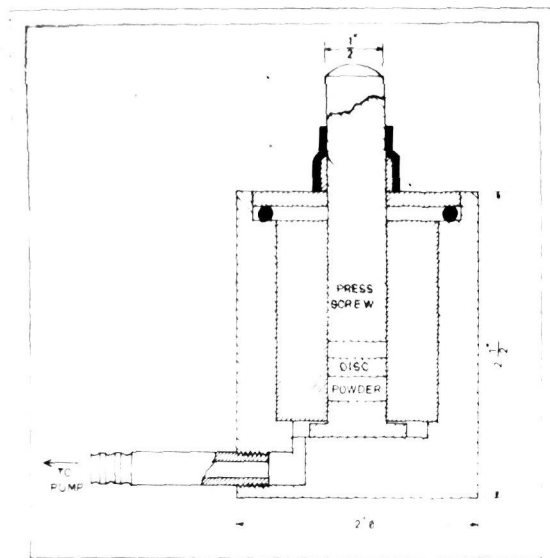


Fig 11.

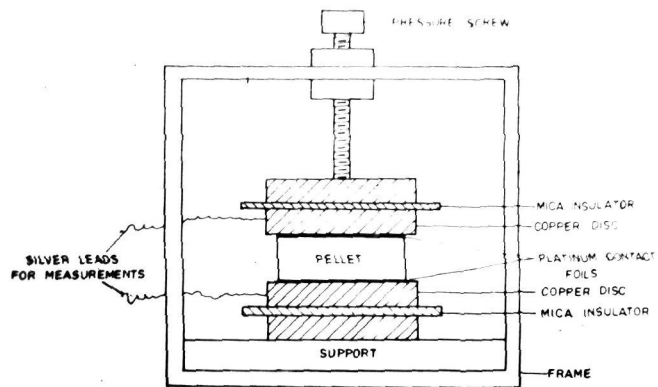


Fig 12.

above the micro-conical basket. The rate of deposition was practically maintained constant by controlling the current passing through the coil, used for heating the silica basket, containing tellurium powder. In each set of evaporation a number of samples of different thickness *was* made, for the measurements of semiconductor parameters and the study of evaporation rate. All the measurements were carried out with a set-up already described in Chapter III.

(ii) Preparation of tellurium pellets

In order to compare parameters of thin films, with those of bulk tellurium, tellurium pellets were also prepared from the tellurium powder by the technique similar to that usually used for the preparation of ABr pellets for infrared studies. Requisite amount of tellurium powder was put in the cylindrical cavity and covered by a disc, ~~first~~ fitting in the cavity. The disc was then pressed by a pressure screw operated by a handle. The lower end of the cylindrical cavity was closed by a block with a suitable arrangement for the continuous evacuation by a rotary pump. All the pressing surfaces which came into contact with the powder were prepared from hard steel to stand heavy pressure and were also plated, to prevent any corrosion. The tellurium pellets of sizes about 1.2 cm. diameter and 0.4 cm. thickness were prepared under pressure of about 10,000 lbs/inch². The

For the study of resistivity and activation energy etc. for the bulk, pressure contacts, different from those used for thin films, were used. Fig.12 shows the pressure contacts for pellets. The tellurium pellet was placed between two platinum foils of nearly the same diameter. The pellet with platinum foil was then placed between two copper discs and silver wires as contact leads, were taken out from copper discs. The whole set-up was finally put in a rectangular frame in which a pressure contact by platinum foil is caused with the help of a pressing screw. Mica was used as an insulator to prevent any contact between the metal frame and the experimental pellet.

C: RESULTS

It is well-known that the evaporation conditions in the vacuum chamber affect considerably the semiconductor parameters like resistivity (ρ), thermoelectric power (α) carrier concentration (n), temperature coefficient of resistance (TCR), etc. Some initial experiments were therefore carried out to study the effect of strain, deposition rate, film thickness, etc, on the resistivity of films. In order to have consistent and reproducible results, the effects due to the deposition conditions were minimised as far as possible by using appropriate methods.

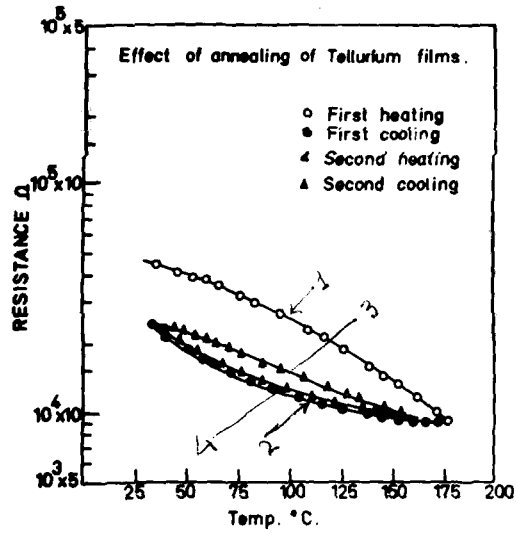


Fig 13.

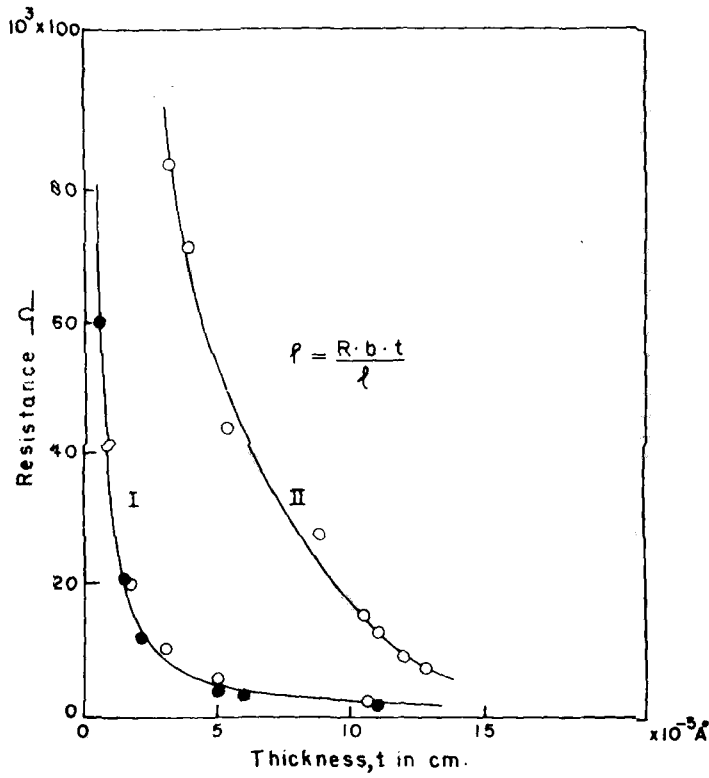


Fig 14.

(1) Annealing of tellurium films

Tellurium films prepared in vacuum unit, were annealed for an appropriate period of time at a suitable temperature below T_d temperature in vacuo, in order to remove strain in the films produced during deposition. It was, however, observed that annealing at $\simeq 70^\circ\text{C}$ for about 1/2 hours in vacuum ($\simeq 10^{-2}$ mm Hg.), or simply heating to $\simeq 160^\circ\text{C}$ during the first heating cycle and cooling to room temperature, removed most of the defects. (Fig.(13) shows the effect of heating of an unannealed tellurium film during the first heating cycle and then, cooling back to room temperature. Curve (1) of the graph shows the variation of $\log R$ with temperature during the first heating, whereas curve (2) shows the corresponding variation during the cooling back to room temperature. Curves (3) and (4) show the path followed during the subsequent heating and cooling cycles. It is interesting to point out that several repeated measurements were made and the paths followed along the curves 3 and 4. In all cases the room temperature resistance remained unchanged. If, however, the sample was annealed at $\simeq 70^\circ\text{C}$, the starting point of the curve on the graph of $\log R$ vs temperature followed the same path of curves (3) and (4) as above, without any change in room temperature resistance. It is also observed that if tellurium films were kept in a desiccator for ^a few days the samples

become self-annealed, and did not require any annealing treatment. The nature of curves was similar to those mentioned in Fig.(10).

(ii) Effect of deposition rate on the resistance of tellurium films

Some initial experiments were made to study the effect of rate of deposition on the resistivity or conductivity of films. Fig.(14) shows the resistance vs thickness curves for two rates about $650\text{\AA}/\text{min.}$ to $\approx 300\text{\AA}/\text{min.}$ respectively. It is apparent from the nature of curves that the slopes are different in different regions and also different for different rates of deposition. Both the curves attained nearly constant value, with the increase of thickness (Fig.15). This change in the nature of curves is seen much more clearly in curves of resistance vs reciprocal of thickness. The slopes are distinctly different for two rates of deposition. The samples prepared at a slower rate had higher resistivity whereas the samples prepared at a higher rate had comparatively smaller resistivity (Fig15).

(iii) Resistivity and activation energy

Typical $\log R$ vs $\frac{1}{T}$ curves for tellurium films of different film thickness varying between 500\AA to 1500\AA obtained from the same set of deposition, both for heating and cooling cycles are shown in the Fig.(13). It is seen that $\log R$

decreased linearly with the increase of temperature through out the range of temperature studied, namely from room temperature to about 180°C during the present measurements. It is also seen that slopes of graphs are nearly equal for thickness greater than 5000\AA whereas for lower thickness it is slightly higher.

ΔE was measured from the slopes of graph resistivity or resistance vs $\frac{1}{T}$ in the following way:

$$\text{Since } R_0 = \rho_0 \frac{l}{b.d.}$$

$$\log R_0 = \log \rho_0 + \log \left\{ \frac{l}{b.d.} \right\}$$

Hence at two different temperatures

$$\log R - \log R_0 = \log \rho - \log \rho_0 \quad \dots (1)$$

$$\rho = \rho_0 e^{\frac{\Delta E}{2kT}}$$

$$\log \rho = \log \rho_0 + \frac{\Delta E}{2kT}$$

$$\frac{\log \rho - \log \rho_0}{\frac{1}{T}} = (2k) = \Delta E$$

OR

$$\Delta E = \frac{\log \rho - \log \rho_0}{\frac{1}{T}} \cdot (2k) \cdot 2.303 \quad \dots (11)$$

$$\text{From (1) and (11), } \Delta E = \frac{\log R - \log R_0}{\frac{1}{T}} \times 2k \times 2.303 \quad \dots (37)$$

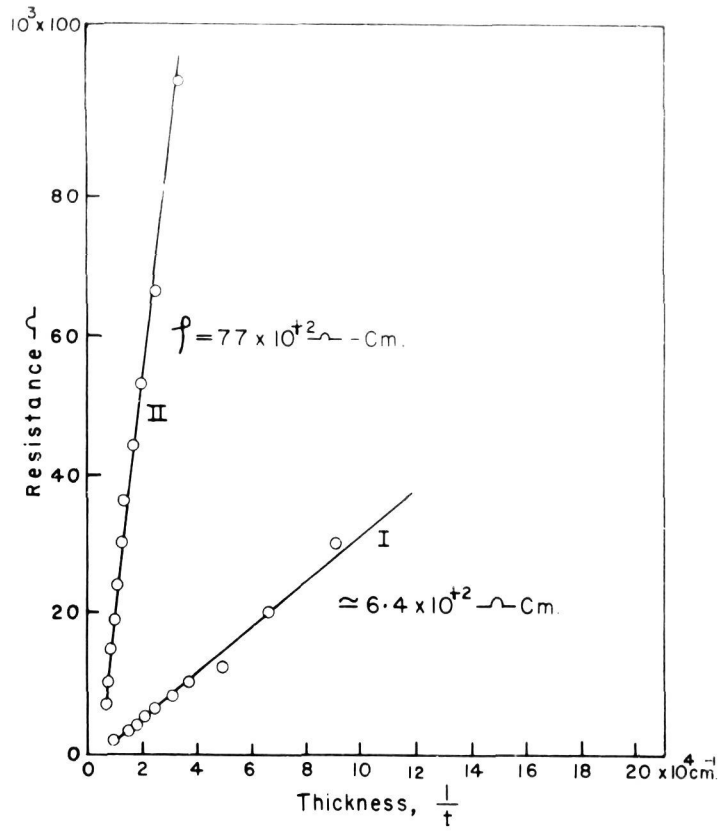


Fig 15

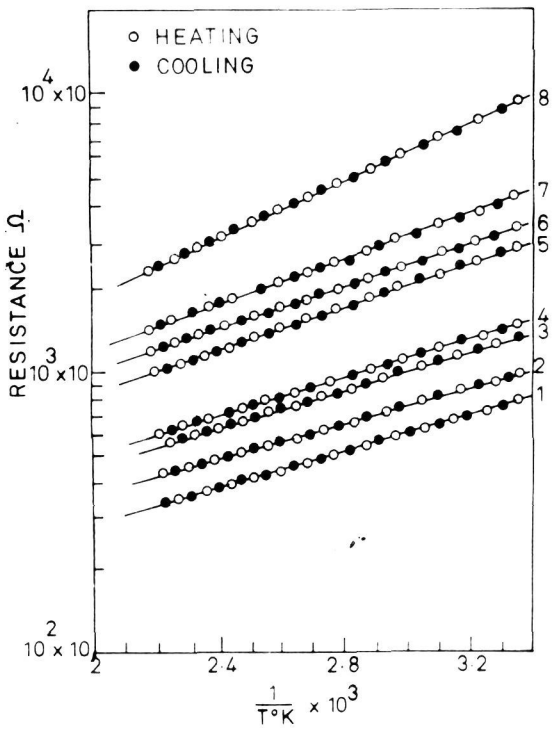


Fig 16.

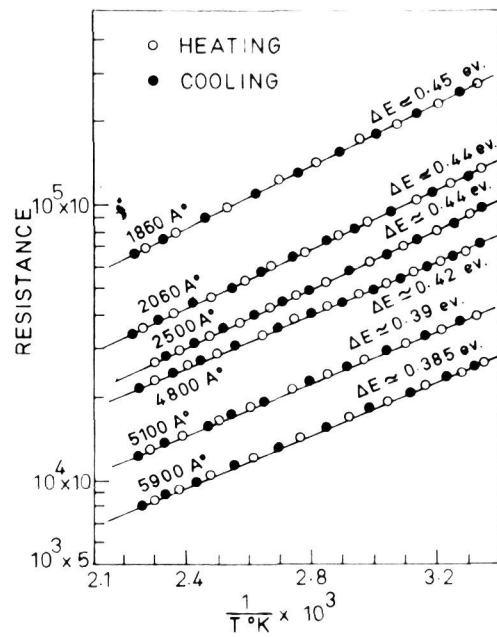


Fig 17

Table 1

Film thickness \AA	Activation energy (ΔE) eV
5900	0.385
6100	0.390
4800	0.42
2500	0.44
2500	0.44
1850	0.45

Table 2

Film thickness \AA	Activation energy (ΔE) eV
15000	0.324
10000	0.325
5030	0.33
3000	0.33
1500	0.41
500	0.44

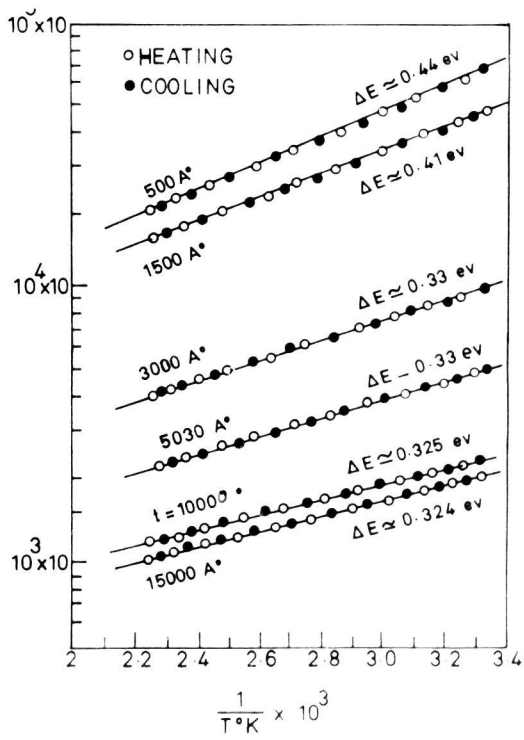


Fig 18

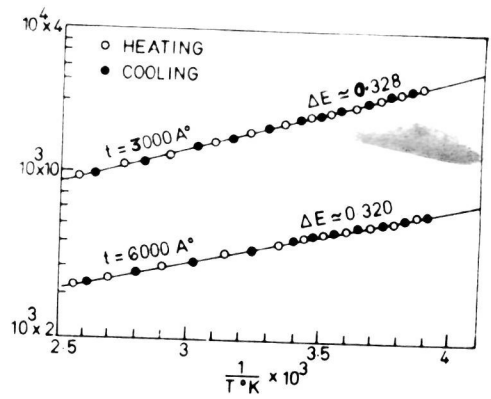


Fig 19.

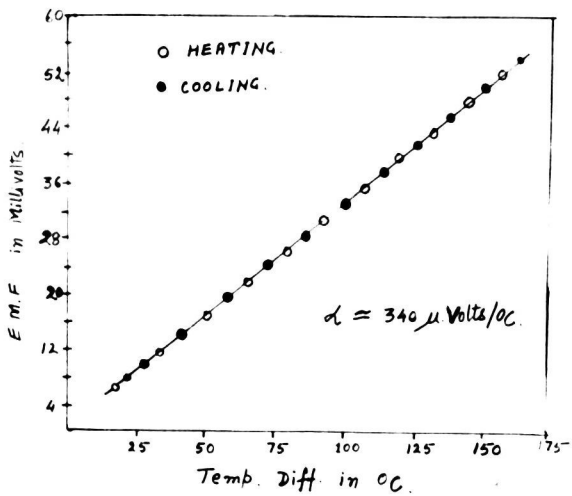


Fig 20.

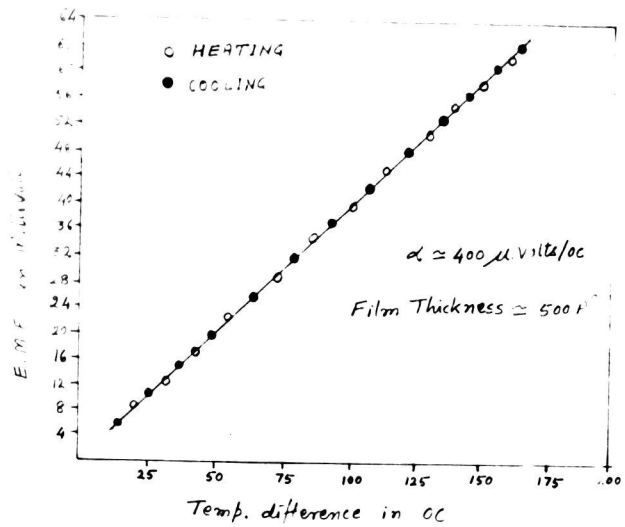


Table (1) shows ΔE for different film thickness.

ΔE varied from 0.32 eV for thicker films to 0.44 eV for thinner films of about 500\AA . Fig. (17, 18) show the variation of $\log R$ vs $\frac{1}{T}$ for two rates of evaporation.

Table 2, shows ΔE for corresponding film thickness for fig 18.

In order to see if there is any change in the slope of curves $\log R$ vs $\frac{1}{T}$, at temperatures below room temperature experiments were carried out in the manner discussed before, to measure resistivity upto $\simeq -12^{\circ}\text{C}$. Fig. (19) shows such curves for film thickness $\simeq 6000\text{\AA}$ and 3000\AA between the temperature range of $\simeq -12^{\circ}\text{C}$ to 180°C and $\Delta E \simeq 0.32$ eV. It is clearly seen that the slopes of curves remained same even below room temperature indicating that the tellurium films behave as an intrinsic semiconductor between temperature range $\simeq -12^{\circ}\text{C}$ to $\simeq 180^{\circ}\text{C}$.

(iv) Thermoelectric power (α)

Thermoelectric power as defined before, (the change in thermal e.m.f. with the change in temperature,) was measured by integral method upto maximum temperature of 130°C . Fig. (20) shows the variation of thermal e.m.f. with change of temperature keeping the cold end more or less at room temperature, while increasing the thermal gradient between the ends for different film thickness. It is seen, except for very thin films, the slopes of curve were practically constant for all the film thickness. The thermoelectric power varied from $340 \mu\text{volts}/^{\circ}\text{C}$

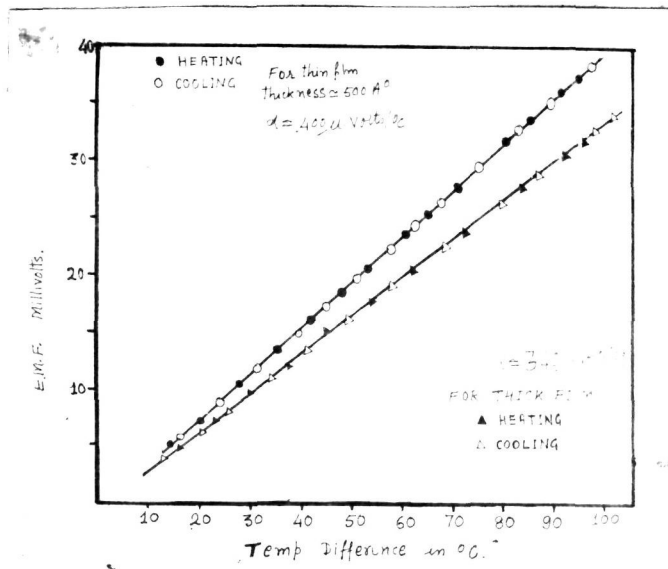


Fig 21.

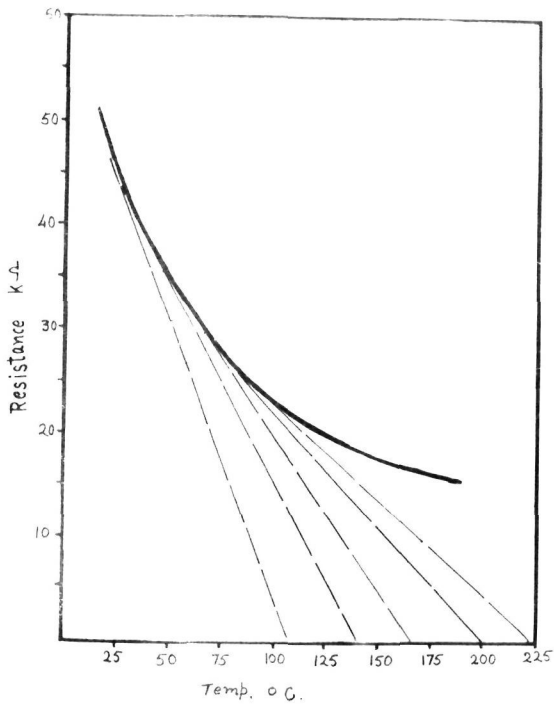


Fig 22.

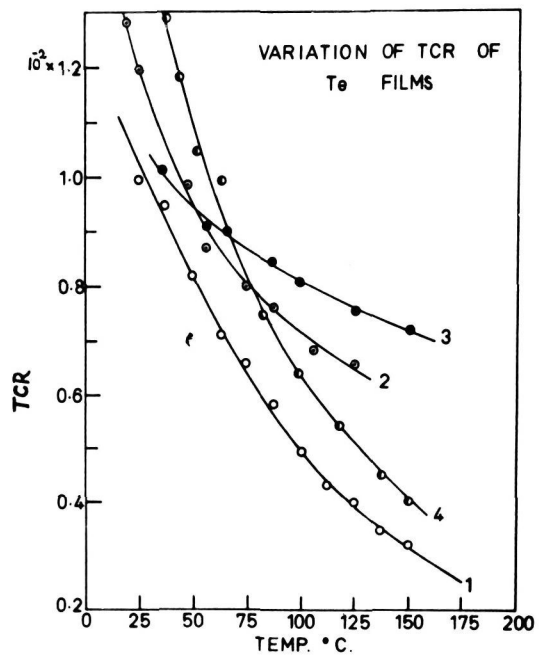


Fig 23.

Table 3

Film No.1(thickness) ($\approx 1500\text{\AA}$)		Film No.2(thickness) ($\approx 1000\text{\AA}$)		Film No.3(thickness) ($\approx 300\text{\AA}$)		Film No.4(thickness) ($\approx 150\text{\AA}$)	
Temp. °C	TCR per °C	Temp. °C	TCR per °C	Temp. °C	TCR per °C	Temp. °C	TCR per °C
25	0.01	20	0.013	35	0.013	37.5	0.013
37.5	0.0095	30	0.012	55	0.0092	45	0.012
50	0.0082	40	0.011	65	0.0090	50	0.0103
62.5	0.0070	55	0.0086	87.5	0.0084	52.5	0.0098
75	0.0067	75	0.0081	100	0.0081	80	0.0075
87.5	0.0058	87.5	0.0076	125	0.0075	100	0.0064
100	0.0049	105	0.0069	150	0.0072	120	0.0053
112.5	0.0043	125	0.0056			132.5	0.0045
125	0.0040					150	0.0040
137.5	0.0035						
150	0.0032						

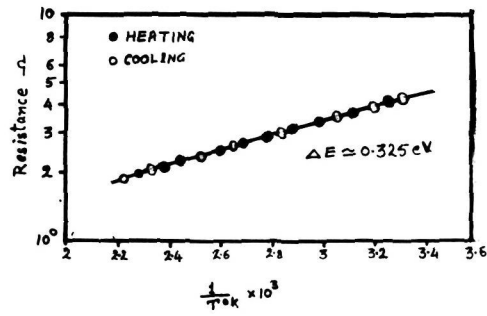


Fig 24.

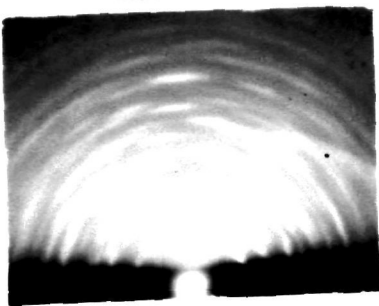


Fig 25.

for thicker film $\simeq 15000\text{\AA}$, to $\simeq 400 \mu\text{volts}/^\circ\text{C}$ for films $\simeq 500\text{\AA}$ thick. Fig.(21) shows thermoelectric power(α) for different film thickness of tellurium films. It is clearly seen that thermoelectric power (α) is independent of temperature through out the range of measurements. Adopting both the methods integral as well as differential lead to a similar conclusion. It is interesting to point out^{that} unlike PbS or PbSe no inversion temperature was observed, showing thereby that the contribution from the minority and the majority carriers was equal with the rise of temperature.

All the samples of tellurium films measured by thermo-electric test set, were found to be 'p' type i.e., the electrical conduction was mostly due to holes even though no intentional impurity was added to the film. It seems that this was due to the presence of defects, inter-crystalline boundaries into the film, which are inherent in the film formation process.

(v) Temperature coefficient of resistance (TCR)

Temperature coefficient of resistance (TCR) which is given by $\frac{1}{R} \cdot \frac{dR}{dT}$ is obtained for different film thickness from the actual measurements, using the resistance Vs temperature curves as shown in the Fig.(22). From graphs, resistance vs temperature, dR/dT is obtained from the slope of curve, point to point with resistance as shown in the Fig.(22). Fig.(23) and table (3) show the variation of TCR with temperature. It is

interesting to note here that TCR was decreasing throughout the range of temperature studied. The curves decreased continuously, finally attaining constant value in the higher range of temperature (max. temp. $\simeq 180^{\circ}\text{C}$). This general feature was observed for all the films of different thickness of tellurium films studied.

(vi) Resistivity and activation energy of tellurium pellets

For a comparison with film ^{properties}, some studies have also been made on the resistivity (ρ) and activation energy (ΔE) of tellurium pellets made from the powder, as mentioned before in Chapter IV B. Fig.(24) shows a typical curve of $\log R$ vs $1/T$ for tellurium pellets of diameter 1.2 cm. and 0.4 cm. thickness between the temperature range room temperature to $\simeq 180^{\circ}\text{C}$. Both for heating and cooling cycles, the measurements were repeated several times. It is clearly seen that the graph is a linear one, with activation energy $\Delta E \simeq 0.325$ eV which is nearly equal to the values obtained for the higher film thickness. It may be mentioned here that activation energy (ΔE) obtained for bulk of pure samples, reported by different authors varied from 0.33 eV to 0.41 eV. Higher values were, however, obtained by optical methods. The resistivity observed

was $\simeq 12 \Omega \text{ cm.}$ which was comparable to that of pure sample ($\simeq 10 \Omega \text{ cm.}$). It may be pointed out that the resistivity for thin films, however, varied widely for different film thickness, but it was of the order of $10^2 \Omega \text{ cm.}$

(vi) Surface structure

Tellurium films as deposited on glass substrate especially those which were nearest to the source of evaporation, exhibited preferred orientation when examined by electrons diffraction methods (Fig.25). It was also found that as the distance of glass substrate increases from the filament the film thickness also decreased and consequently there was less tendency for preferred orientation. Ultimately for these specimen the deposit films were practically polycrystalline without any preferred orientation. It was also interesting to note that except at the substrate which were placed right above the source, deposits not only developed a preferred orientation but showed asymmetric electron diffraction patterns, no doubt, due to oblique angle of incidence to the substrates. This results in developing crystals with one of their axes along with direction of incidence. Whatever be the type of orientation developed, the deposit crystals had hexagonal structure ($a_0 \simeq 4.46 \text{ \AA}$, $c_0 \simeq 5.93 \text{ \AA}$) similar to those observed by Aggarwal (1958).

D: DISCUSSIONS

From the results of resistivity, thermoelectric power, temperature coefficient of resistance of vacuum deposited tellurium films, it is seen that there is a considerable difference between the bulk properties and corresponding properties in thin film state. Our experimental results for bulk tellurium pellets showed resistivity $\simeq 12 \Omega \text{ cm}$. whereas the vacuum deposited films of tellurium had resistivity of the order of $\simeq 10^2 \Omega \text{ cm}$. It can further be noted that in bulk material resistivity is independent of dimensions of the specimen whereas in vacuum deposited films resistivity is no longer constant, but depends on the thickness of the film, rate of deposition, temperature of substrate, order of vacuum in the deposition unit etc. During one set of the evaporation, it was found that when all other variables except thickness were kept more or less constant, then the resistivity decreased with the increase of film thickness ultimately reaching a constant value often different from the bulk material. Similar results were also observed by many workers, (Steinberg, 1923, Vincent, 1900, Longden, 1900, Patterson, 1902, Weber and Costerhuis, 1917, Kind 1917, Gillham et.al. 1955, Naugebaur and Webb, 1962, 1964). It has already been pointed out in Chapter I that according to the modern theory of conductivity, the electrical resistance is primarily due to imperfections in the lattice (Bloch 1928, Mayer, 1959).

For a macroscopic material the resistance arises as a result of hindrance in the passage of electrons by the following process, namely;

- (1) Scattering of electrons caused by the thermal vibrations of atoms or ions about their mean position i.e. scattering caused by phonons.
- (2) Scattering by lattice defects such as missing atoms, interstitials, impurity atoms, etc. Therefore, the resistance of a bulk material may be thought to be composed of two parts:

- (a) Ideal part strongly dependent on temperature, and
- (b) Residual part due to lattice defects but generally independent of the temperature. Hence the resistance is given by the relation:

$$\rho_{\text{Total}} = \rho_{\text{Ideal}} + \rho_{\text{Residual}}$$

which is known as Mathiessen's rule.

In the case of bulk materials the conductivity depends upon ^{the} mean free path (ℓ) of electrons in the lattice, but if one dimension is reduced very much, ultimately reaching and becoming smaller than the mean free path (ℓ) then resistance and hence resistivity is likely to increase with the decrease of film thickness.

The above concept of dependence of resistivity on film thickness was first introduced by Thompson (1901) and finally developed by Sondheimer and others (1952). By considering Sondheimer's concept, the total resistance of the material in the film state can be modified as:

$$\rho_{\text{Total}} = \rho_{\text{Ideal}} + \rho_{\text{Residual}} + \rho_{\text{Thickness}}$$

The above relation satisfactorily explains the dependence of film resistivity on its thickness which ^{was} also observed in our experimental results on tellurium films. But the increase of activation energy (ΔE) with the decrease of film thickness, which was experimentally observed in all cases cannot be satisfactorily accounted for, from the above consideration. On the basis of theory of island structure, developed by Naugebauer and Webb (1962, 1964), it is possible to explain some of the properties of thin films, at least qualitatively. It has already been pointed out in Chapter I that with the increase of film thickness ^{the} island-size also increases and hence the distance between islands decreases. The size of islands and distance between them often depend upon the nature of the substrate, its temperature, geometry of the substrate with respect to the source of vapour and many a times, the distance between the substrate and the source during the deposition process.

In the case of vacuum deposited films often there is a high density of defects such as dislocations stacking faults, microtwins etc. (Pashley, 1959, Mathew, 1959, Philips, 1960). Since these defects are inherent in the process of growth of films, not formed in the ideal conditions of deposition, these will consequently also affect the resistance of the films. Annealing of films at suitable temperature will, however, remove some of these defects with the result that there will be a decrease in the resistance. By ^{the} annealing process the films are also homogenised. Measurements on annealed films confirmed the above view. This shows more clearly, why ~~resistance variation~~, generally the decrease of resistance, occurs on annealing the films. Ghosh (1961) also observed that conductivity Hall mobility and field effect mobility varied with the thickness of the evaporated films in ^{the} case of tellurium. The ^{low} values of Hall mobility are due to scattering carriers at the intercrystalline boundaries.

During the present investigations, it was also found that ^{the} rate of evaporation also produced a considerable effect on the resistivity of the films, Fig (15) shows two ^{such} curves. A curve with ^a higher slope is for the films formed at slow rate of depositions, whereas second curve is for films formed at comparatively fast rate of deposition. This results into higher resistivity for films of slow rate of deposition and smaller resistivity for films of comparatively high rate of

deposition. The above experimental results suggest that the film of similar thickness prepared under different rates had different granular structure as far as porosity morphology, grain boundaries etc. were considered.

During the study of metallic films, similar results were also obtained by DeBoer and Krank (1936), Levinstein (1949), Senett and Scott (1950). These workers have suggested that there is a relation between the morphological *features* and electrical conductivity. Neugebauer (1964) gave a relation between the size of islands, and number of impinging atoms. At a certain fixed substrate temperature higher rate of evaporation *will cause more nucleation but due to high surface n* ~~cause less nuclei~~ *for bigger* islands, *leading to a* ~~causing~~ *into* decrease in intercrystalline boundaries and therefore the conductivity is more. On the other hand at slow rate of deposition at room temperature, *less* ~~more~~ nuclei of smaller islands are formed causing thereby the increase in the intercrystalline boundaries and thus decrease in the conductivity.

It has already been pointed out that unannealed samples exhibit extra resistance which disappeared, when subjected to heating and cooling cycles in vacuo. This process is analogous to annealing process. Annealing was also observed even at room temperature when the films were kept under vacuum for about 8 to 10 days at room temperature. Activation energy for tellurium films varied between 0.32 eV to 0.44 eV. All

the films gave practically same value except for very thin films. It can be noted here that resistivity of tellurium films was much higher ($\approx 10^2 \Omega\text{-cm.}$) as compared with corresponding bulk tellurium ($\approx 12 \Omega\text{-cm.}$). Moss (1961) studied ^{the} optical properties and showed that it was photo-conducting element, the value of activation energy determined was ≈ 0.36 eV. He also studied reflectivity in infrared region and value of ΔE was ≈ 0.37 eV. Wayne Scanlon and Lark-Horovitz (1947) however, reported ^a reversal of sign for Hall coefficient, similar to that of bulk material. The activation energy reported by these workers was ≈ 0.36 eV at temperature $\approx 25^\circ\text{C}$ and ≈ 0.039 eV at liquid air temperatures. In our studies of tellurium films, the activation energy did not depend on the temperature even upto $\approx -10^\circ\text{C}$.

The higher values of activation energy (ΔE) for thinner films and vice versa, can be satisfactorily explained on the basis of island structure of films. Once the nuclei for the islands are formed the size of island goes on increasing with time of deposition, causing a decrease in their average distance of separation. In ^{the} case of very thin films the intercrystalline boundaries are more, the distance between islands is comparatively very large and tunneling effect for the conduction is less, thus causing an increase in the resistance of thinner films and also ~~the~~ increase in the activation energy (ΔE).

Naugebauer and Webb (1962) on the basis of island structure of films explained the variation in electrical conductivity of films. According to them the conductivity of an 'island structure' metal film, depends on the distance (d) between islands and their radius (r) as stated by the formula:

$$\sigma = A' \text{Exp} \left[\frac{4\pi d}{h} \left(\sqrt{2m\phi} \right) + \frac{2e^2 / \epsilon r + \Delta E}{2 kT} \right]$$

Activation energy for the conduction can be considered as the energy required to transfer charge from one initially neutral island to other at some distance. Only electrons or holes (excited) will be able to tunnel from the neutral island to the other. Such an activated process leads to an equilibrium number of islands changed to potential $\text{Exp.} \left(- \frac{e^2}{\epsilon r / kT} \right)$. The transfer of a charge from a charged island to a neutral island is not an activated process because it does not lead to net increase in energy of the system. Thus according to island structure, the activation energy observed in the electrical conduction of island films is determined by the size of islands, and conductivity at all temperatures depends upon the distance between them. According to this theory, thicker films should show smaller activation energy, nearly approaching the value of bulk material and for thin films larger values of activation energy.

Thermoelectric power ($\alpha = \frac{dE}{dT}$) measured, was fairly constant and was independent of film thickness except for a very thin film, which was $400 \mu\text{m}$ C. Tellurium exhibited 'p' type semiconductor, which can be explained on the basis of energy band diagram, the film defects associated, which are mainly voids, imperfections of an annealed film must be the acceptor level very close to the upper edge of the valence band. As already pointed out in Chapter I, it is well known that the position of Fermi-level depends upon the concentrations and type of impurity. Since the thermoelectric power is constant at all temperature, it can be stated that, there is no change in the carrier concentration with the change of temperature.

The negative temperature coefficient of resistance (TCR) for tellurium films decreased with the increase of temperature. Negative TCR for all the films was found to be of the order of $\approx 10^{-2}$ (Table 3). This can be explained on the basis of island structure. According to Neugebauer (1962) TCR is given by:

$$\text{TCR} = \frac{d(d)}{dT} \left[\frac{4\pi \sqrt{2m\phi}}{h^2} + \frac{1}{d} \right] - \frac{C}{T^2} \quad \dots (37)$$

2. why does this differ from 38

where $C = \frac{2e^2}{e r} + \frac{\Delta E}{2k}$, and other symbols have their

usual meaning. Since on heating the size of islands increases

and distance between them decreases, the term $\frac{d(d)}{dT}$ must be negative, so that the final expression for TCR will be:

$$TCR = - \frac{d}{dT}(d) \left[\frac{4 \pi \sqrt{2m\phi}}{h^2} + \frac{1}{d} \right] - \frac{C}{T^2} \quad \dots(38)$$

The TCR for tellurium films decreased with the increase of temperature. This might be because of effective contribution by the first term of equation (38) and therefore there is a continuous decrease in TCR upto the maximum temperature of measurements. Unlike SnSe, Sn₂Se₃ and SnS described in Chapter V, negative TCR did not show any minimum value, but the nature seems to be similar to that obtained in case of SnSe, Sn₂Se₃ and SnS. It appears that ^{the} the temperature of measurement could have been raised, it is likely that TCR curve *would* follow the same as those of other curves.

Tellurium exhibited hexagonal structure throughout the temperature range of the present measurements i.e. upto $\approx 180^\circ\text{C}$. Deposit samples had *varying* film thickness from one end to other. All the films of different film thickness of same set exhibited more or less similar properties, which show that direction of deposition had practically no effect on the electrical properties like, resistivity (ρ), thermoelectric power (α), temperature coefficient of resistance (TCR) etc.

CHAPTER V

SEMICONDUCTING PROPERTIES OF SnSe,
Sn₂Se₃, SnS AND SnTe FILMS

A: INTRODUCTION

Generally sulphides and tellurides are found to be good semiconductors ^{and} used in semiconductor devices, especially in film transistors, photoconductors, etc. As early as in 1874 rectifying action ~~in case~~ of lead sulphide was reported by Braun (1874) ^{and} detailed studies on electrical properties of chalcogenides of lead ~~were~~ carried out by many workers, (Eisenmann 1940, Hintenberger, 1942, Lark-Horovitz 1954, Smith, 1951, 1953, 1955, Moss, 1955 and Scanlon 1954). These compounds are generally present as minerals, such as galena (PbS), Clausthalite (PbSe) and allatite (PbTe). Lawson (1951, 1952) applied the Bridgman-Stockbarger technique for growing the single crystals of lead sulphide, lead selenide and lead telluride. From the study of thermoelectric power measurements Stefan (1865) showed that PbS existed either as 'p' type or 'n' type semiconductor. Similar results were also recorded later by Eisenmann (1940) and Hintenberger (1942).

A comparative study of electrical properties of single crystals and films of lead sulphide, lead selenide and lead telluride was carried out by Silverman and Levinstein (1954). Measurements between the temperature range 77°K to 300°K showed

that all the films were showing 'n' type characteristic behaviour, irrespective of original crystal, whether 'n' type or 'p' type. The carrier concentration decreased after annealing of lead sulphide (PbS) and lead selenide (PbSe) films, which was 1/5th of bulk material value. A detailed study on the semiconducting properties of thin films especially of PbS, PbSe, PbTe, Bi_2Se_3 , Bi_2Te_3 has recently done by Koli (1965).

Kelly (1939) studied selenides and tellurides of manganese (MnSe, MnTe). Electrical measurements were carried out by Landau (1933), Squire (1939), Lindsay (1951), Palmer (1954).

Systematic investigations have been recently made of IV-VI group, intermetallic compounds, with respect to electrical properties and crystal structure. The crystal structure of SnSe has already been reported ^{to be} orthorhombic (Okazaki 1964) and preliminary experiments on electrical properties have shown that SnSe behaves as an ordinary 'p' type semiconductor. Single crystals for above investigations were prepared by mixing tin and selenium, and heating to 1000°C for a long time. The melt was slowly cooled, and single crystals of SnSe, having size $2 \times 3 \times 10 \text{ mm}^3$ were used. Studies on electrical properties were also undertaken and reported by

many workers (Albers and Bass 1962, Asanabe and Okazaki, 1959, Asanabe 1959, Albests et.al. 1960, Matukura, Yamamoto and Okazaki 1953).

The aim of the investigation was to obtain such physical quantities, as the energy gap between conduction and valence band, its temperature dependence, the effective mass of electrons or holes, the ionization energy of impurity levels etc. for SnSe single crystals. It was found that Hall coefficient exhibited an anomalous hump at 200°C for most of the crystals. Resistivity measurements between the temperature range 100°K to \approx 800°K also showed, a change in the shape of $\log R$ vs $1/T$ curves at 200°C. The electrical resistivity, Hall coefficient and thermoelectric power of SnSe single crystals were investigated, but it was not possible to analyse the results on a semiconductor model. The reason is that ~~the~~ conventional assumption, that ^{the} hole density in the valence band is equal to ~~sum~~ of electron density in the conduction band and acceptor density, does not hold on account of acceptor formation ~~at high formation~~ at high temperatures. Only qualitatively the experimental results were interpreted on a single model of acceptor formation.

Impurity band conduction model or two holes model also did not explain the results of SnSe, because the model is expected to imply only reversible phenomena with temperature

but for SnSe it was found irreversible. This behaviour was found to be similar to that exhibited by GaAs, GeSe, PbS, PbSe, etc. (Smith 1954).

Recently Yabumoto (1958), Philips (1960) studied the electrical properties and optical properties of tin mono-sulphide (SnS). Metal tin (spectrographically pure) was distilled in vacuum to exclude the impurities like copper, iron, etc. Sulphur was crystallized from carbon bi-sulphide (CS_2) and distilled in vacuum. Such tin metal and sulphur in the stoichiometric ratio of SnS, was put into a silica tube, evacuated in high vacuum and then sealed and heated to $\simeq 1000^\circ C$ for 6 hours and then cooled. X-ray diffraction studies showed that SnS had orthorhombic structure. Resistivity was of the order of $\simeq 10^6 \Omega \cdot cm$ which was found to be much low as compared to the resistivity of GeS which was $\simeq 10^{10} \Omega \cdot cm$. Graphs of conductivity vs $1/T$ for bulk single crystal SnS samples, exhibited two regions namely from $25^\circ C$ to $\simeq 130^\circ C$ and $130^\circ C$ to $\simeq 250^\circ C$. In the first region of low temperature activation energy was found to be $\simeq 0.26$ eV whereas the second region of graph showed the value of activation energy $\simeq 0.54$ eV. The energy gap determined from the optical properties was $\simeq 1.6$ to 1.7 eV at higher temperatures. The values of energy gap ~~for~~ were found to be 1.8, 1.6, 0.4 for GeS, SnS and PbS respectively.

Electrical properties on single crystals of SnTe were also studied by many workers, [Haken (1910), Hoshimoto (1956)]. Samples of SnTe were prepared by heating the mixture of tin and tellurium in stoichiometric proportion in vacuum sealed silica tube; the heating was continued for about 15 hours at temperature about 850°C . X-ray diffraction studies showed that SnTe had NaCl type cubic structure $a_0 = 6.32\text{\AA}$ at room temperature. Resistivity and Hall coefficient were found almost ^{the} same and moreover temperature coefficient of resistance (TCR), Hall constant ^{etc.} were positive at all temperature range of measurements, namely 100°C to $\approx 1000^{\circ}\text{C}$. Thermoelectric power was $\approx 26 \mu\text{volts}/^{\circ}\text{C}$. Measurements on zone melt samples of SnTe also revealed that resistivity and Hall coefficient both are same at all the temperatures, but the thermoelectric power at room temperature was $\approx 29 \mu\text{volts}/^{\circ}\text{C}$ to $\approx 33.3 \mu\text{volts}/^{\circ}\text{C}$. Thermoelectric power was also ^{the} same at all temperatures. The value already observed by Haken (1910) agrees well with $26 \mu\text{volts}/^{\circ}\text{C}$, a change of sign from positive to negative, at $\approx 250^{\circ}\text{C}$. Ston, Bis and Gubner (1961) studied single crystals of Sn telluride. Carrier concentration was found to be, $\approx 8 \times 10^{20}/\text{cm}^3$. Allsaler and Schele (1961) carried out the measurements on resistivity, as well as, Hall coefficient. The behaviour of SnTe was found to be semi-metal type.

B: EXPERIMENTAL**Preparation of tin selenides**

Both SnSe and Sn₂Se₃ were prepared by melting tin (AR) and selenium (BDH) in vacuo. To prepare SnSe, Tin (AR) and selenium highly pure were mixed in the atomic proportions (1:1) and the mixture was melted in a vacuum sealed silica-tube. The tube used was first cleaned with nitric acid, then with distilled water and finally, with distilled alcohol, followed by drying. The tube thus cleaned was then closed at one end by fusing. The mixture of tin and selenium in their atomic ratio was poured into it and was carefully evacuated, and when the vacuum was of the order of $\approx 10^{-5}$ mm Hg., the tube was sealed by fusing. The vacuum sealed silica tube thus obtained was then inserted in a vertical electric furnace the temperature of which was raised in stages, the maximum temperature being $\approx 950^{\circ}$ C. This temperature was raised during three hours and heating at maximum temperature (950°) was continued for about 6 hours and then cooled. The compound SnSe was obtained in the form of solid rod of dia. ≈ 1 cm. and length ≈ 2.5 cm. This bulk material was then used for evaporation during the study of semiconducting properties, as well as, the structure of films by electron diffraction technique.

Sn_2Se_3 was also prepared by the same method using tin and selenium in the atomic ratio (2:3).

Preparation of SnTe

This was also prepared by melting tin powder and pure tellurium in the atomic proportion (1:1) and the mixture was heated to maximum temperature about 900°C and the heating was continued for about six hours and then cooled as in case of SnSe and Sn_2Se_3 .

Preparation of stannous sulphide (SnS)

Stannous chloride (Riedel-de-Hoen; AG) was dissolved in 1:1 hydrochloric acid (AR) by warming for some time in the presence of granular tin metal in order to prevent the oxidation. H_2S gas, washed with distilled water, was passed through the clear solution for about eight hours, the precipitate thus obtained was washed with distilled water till it was free from chloride. The material thus obtained was then washed with ethyl alcohol and finally dried in a vacuum dessicator. The yellowish-brown powder material was then used for evaporation during the study of semiconducting properties of vacuum deposited films of SnS.

C: RESULTS

(1) Resistivity and activation energy

SnSe : Resistance of SnSe films was measured by the method described before. The variation of resistance with thickness was similar to that observed in the case of

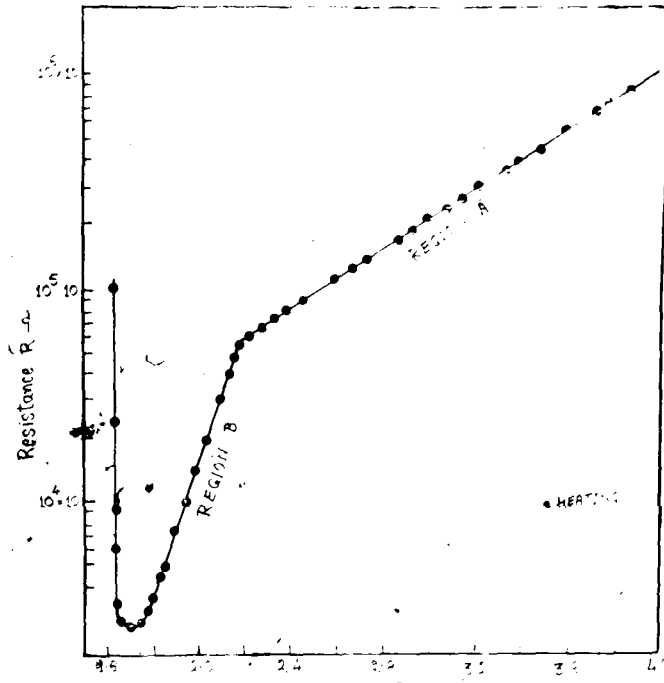


Fig 31.

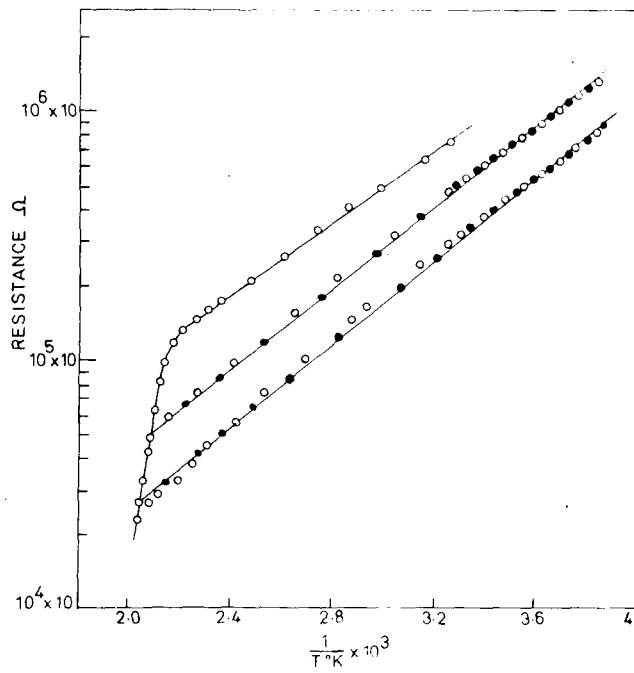


Fig 32.

of film thickness and finally became asymptotic showing nearly a constant value of resistivity much different from the bulk material.

Fig.(26) shows the variation of $\log R$ with the reciprocal of absolute temperature starting from room temperature, for a film of tin selenide of film thickness $\simeq 21000\text{\AA}$. The discontinuity temperature (T_d) was found to be $\simeq 310^\circ\text{C}$.

It is interesting to see that $\log R$ vs $1/T$ curves (Fig.26) show two slopes corresponding to regions 'A' and 'B', when measured upto the T_d temperature. The change of slope occurred nearly 150°C to 180°C temperature range. It was also observed that if maximum temperature of measurement of resistance during heating cycles was 150°C , i.e. in the region 'A' the cooling curve followed the same path as that of heating curve. Fig.(27) shows such curve. This was also true for different film thickness and even for different heating and cooling cycles provided the maximum temperature was below 150°C . If, on the other hand, the film was heated to the temperature range 'B', i.e. beyond 180°C to nearly about the T_d temperature, it was found that cooling curves followed entirely a different path depending upon the maximum temperature of heating. Fig.(28) shows such cooling curves for a film thickness $\simeq 40000\text{\AA}$, when the maximum temperature of heating in the region 'B' was gradually changed. It is clearly seen that cooling curves for resistance, were again dependent on the maximum temperature. It is also

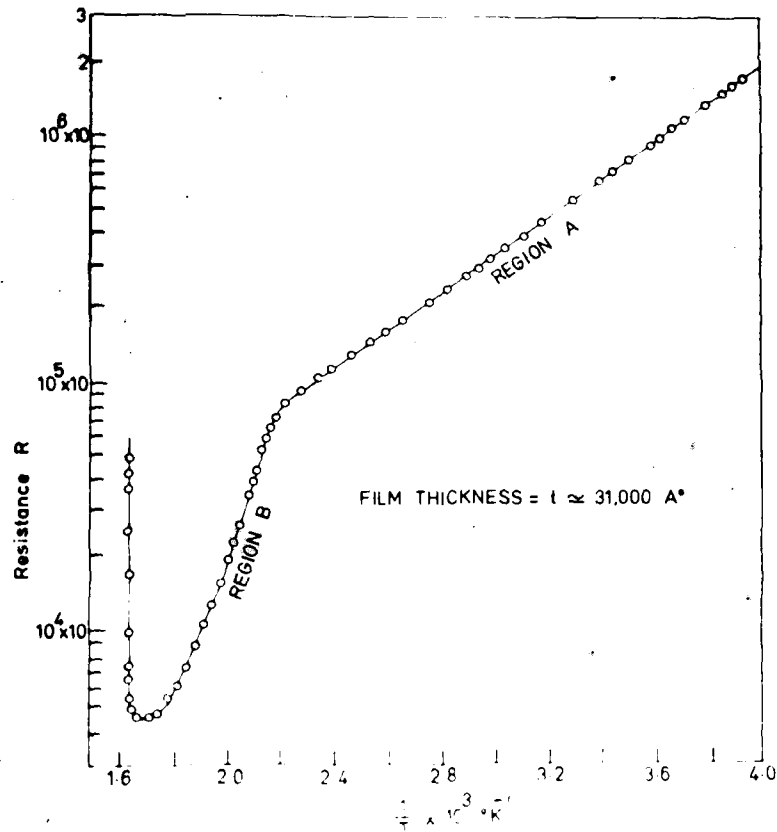


Fig 29.

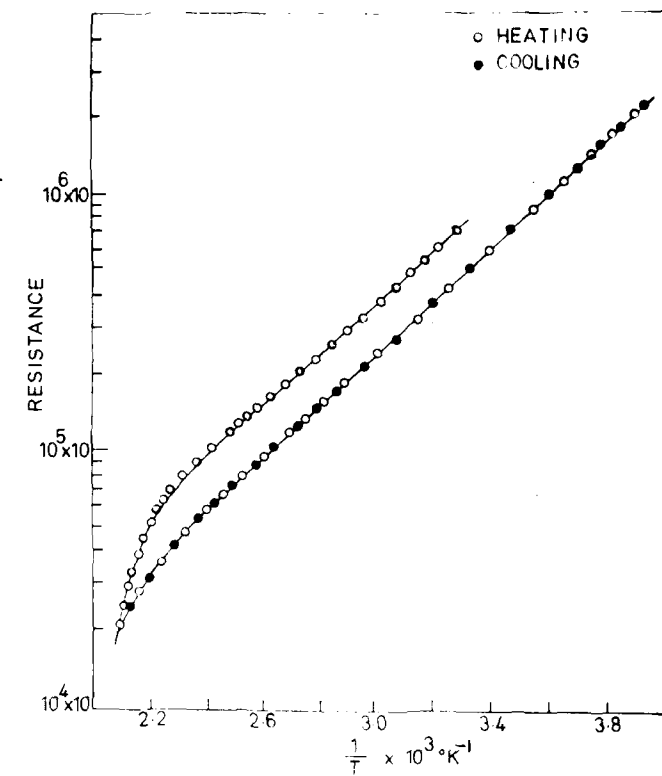


Fig 30.

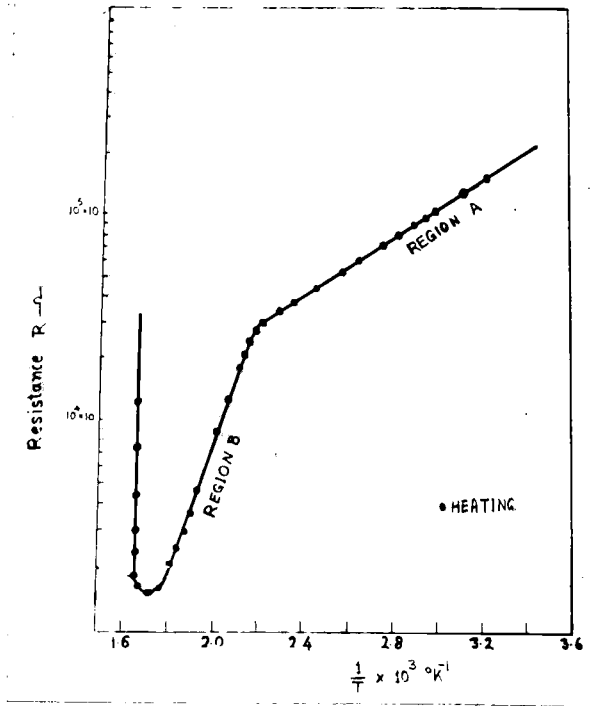


Fig 26.

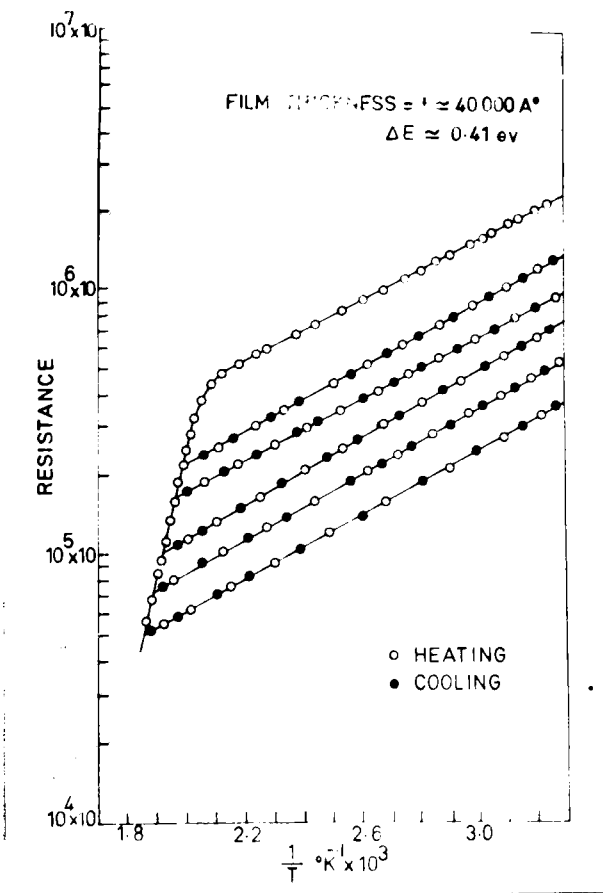


Fig 27. 1

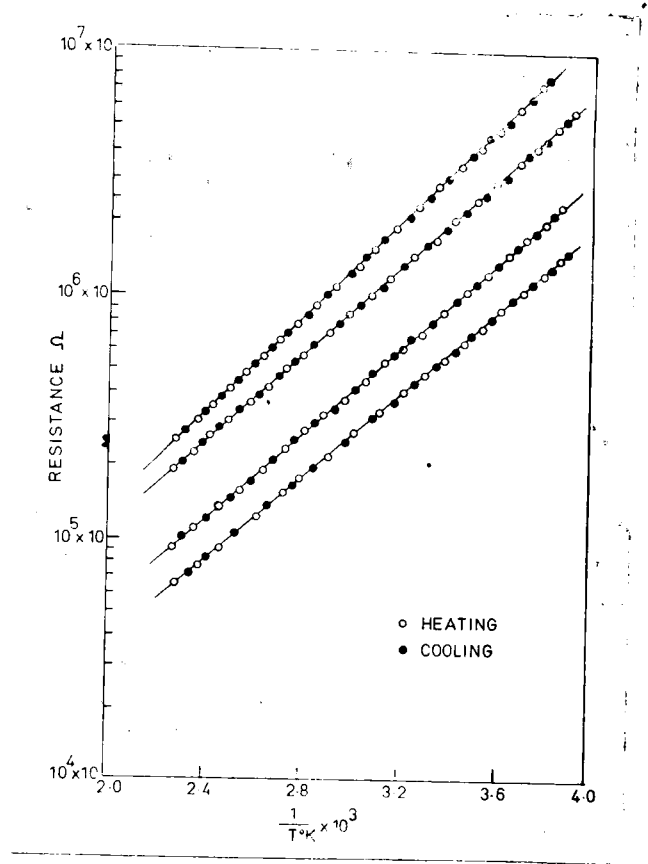


Fig 28.

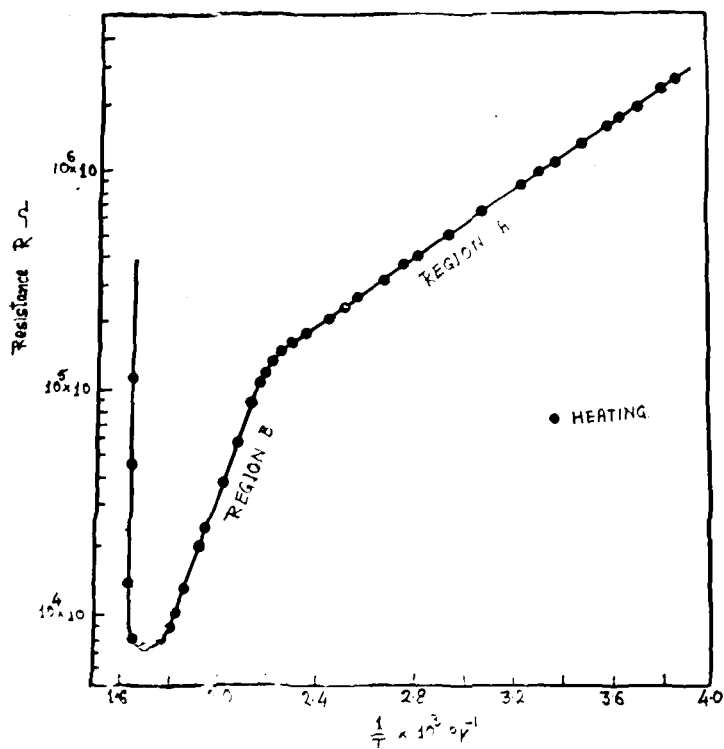


Fig 33.

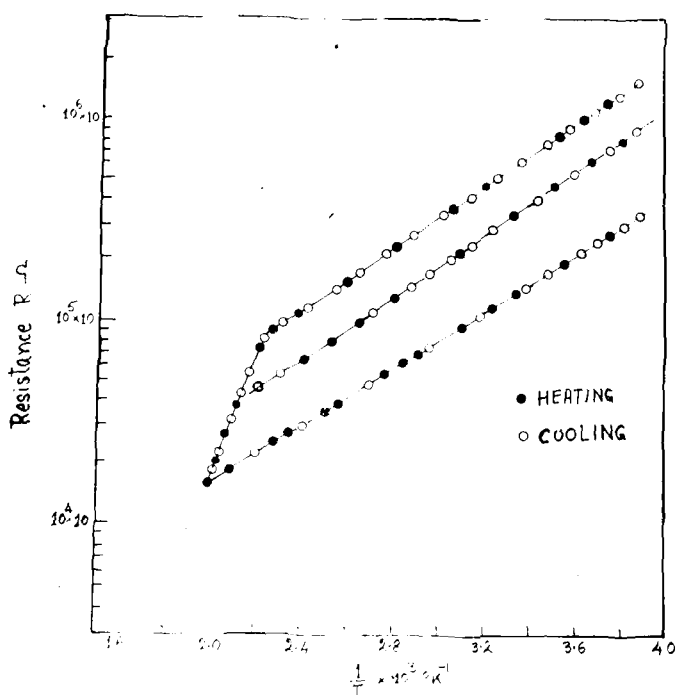


Fig 34.

interesting to note that even though the paths of the curve in the above figure changed with maximum temperature, their slopes remained nearly the same. Further during the subsequent heating and cooling cycles the maximum temperature did not exceed the previous limit. The curves followed almost the same path. This is better explained in the Fig.(28). Similar features were also observed for various film thickness ranging between 15000\AA to $\approx 40,000\text{\AA}$. In all cases the activation energy of the film heated to 'B' region of log R vs $1/T$ curves showed values ranging between 0.41 eV to 0.51 eV, the thinner films showing, however, the higher values similar to tellurium films. Resistance was also measured at temperatures, lower than room temperature upto about -12°C . Fig.(29) shows the variation of resistance from room temperature to $\approx -12^{\circ}\text{C}$ (cooling cycle) and then -12°C to $\approx 300^{\circ}\text{C}$ (heating cycle), showing again a change in slope at the temperature region $\approx 150^{\circ}\text{C}$ to 180°C as observed previously in Fig.(26). The cooling curve also had the same feature as mentioned previously (i.e. Fig.28). If cooling is further continued upto about -12°C the nature of the slope did not change. These results clearly show that conduction mechanism, operating near the room temperature region, did not materially change upto $\approx -12^{\circ}\text{C}$ (Fig.30).

Sn_2Se_3 - Resistivity measurements of Sn_2Se_3 films on glass substrate showed that the temperature of discontinuity (T_d)

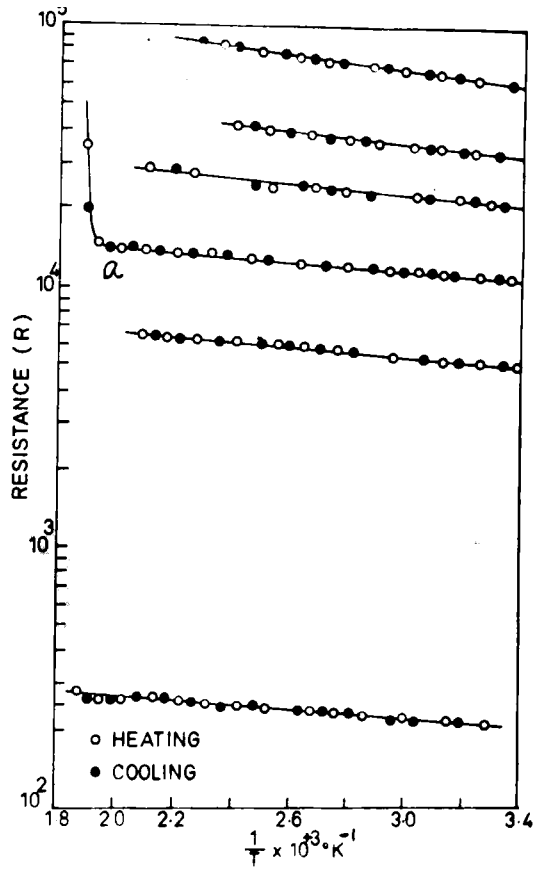


Fig 35

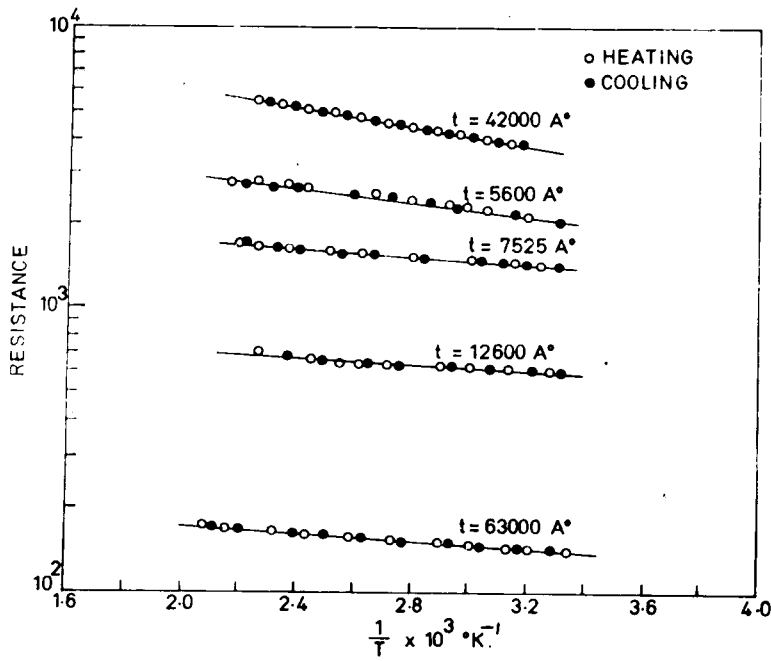


Fig 36.

Table 4

Film thickness \bar{Q}	Activation energy (ΔE) ev
25000	0.49
28000	0.47
35000	0.41
40000	0.41

Table 5

Film thickness \bar{Q}	Activation energy (ΔE) ev
22000	0.48
26000	0.48
32000	0.42
33000	0.42

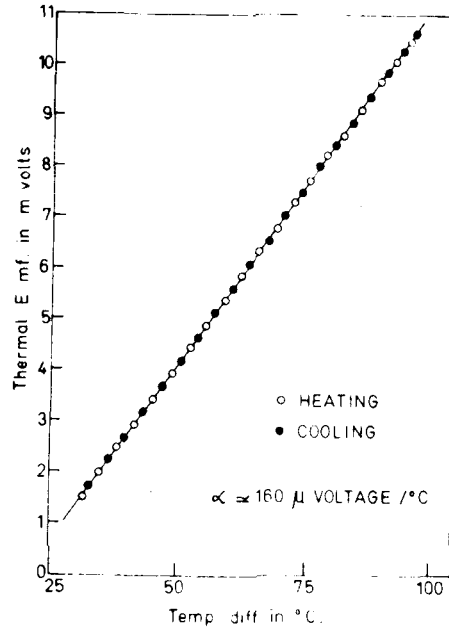


Fig 37

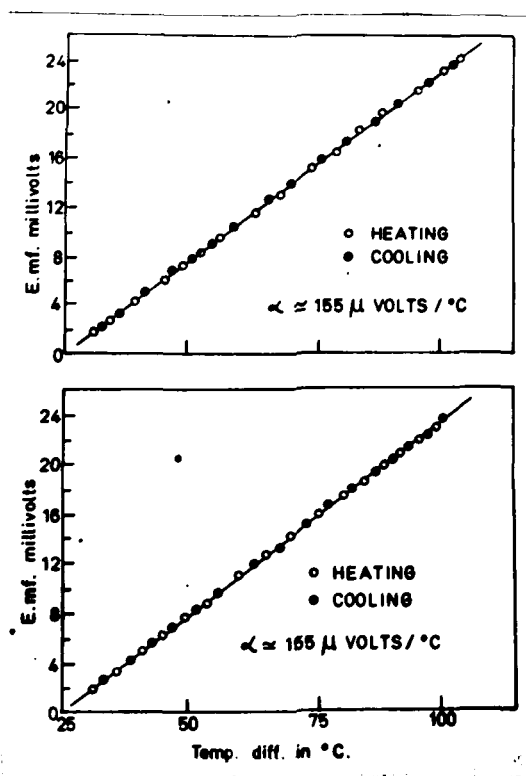


Fig 38.

was $\simeq 320^{\circ}\text{C}$. Log R vs $1/T$ curves, (Fig.31) shows that there are two slopes for temperature region studied between -12°C to $\simeq 330^{\circ}\text{C}$, the change in the slope occurring at about $150-180^{\circ}\text{C}$ as observed in the case of SnSe films. These curves also have similar characteristic as mentioned for SnSe films as can be seen from Fig. (32). It can again be seen that the path of the curve depends on the maximum temperature to which the film was heated. The values of activation energy (ΔE) varied between 0.41 ev to 0.51 ev, depending upon the film thickness, the thinner film, however, had higher values. Table (4) shows the variation of ΔE with film thickness.

SnS - Stannous sulphide films had considerably higher resistance compared to SnSe and Sn_2Se_3 films. The variation of log R vs $1/T$ was similar to the films of SnSe and Sn_2Se_3 . The T_d temperature was $\simeq 320^{\circ}\text{C}$ (Fig.33). The heating of SnS films in 'B' region of the log R vs $1/T$ curves caused a decrease in the resistivity without any appreciable change in the activation energy (Fig.34). Table (5) shows the variation of ΔE , the activation energy for different film thickness.

SnTe - All selenides and sulphides of tin so far discussed showed a fall of resistance with the increase of temperature, no doubt, a characteristic of a semiconductor. In the case of tin telluride films, however, the tendency was reverse, i.e. the resistance increased, though slightly,

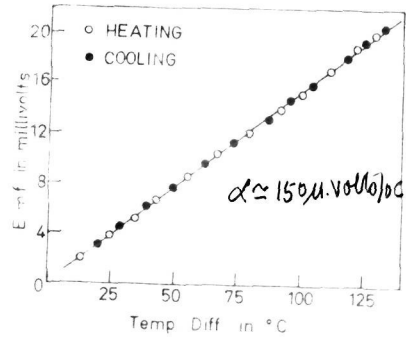
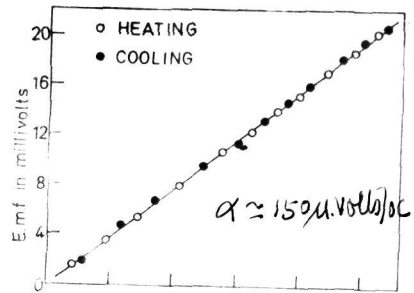


Fig 39.

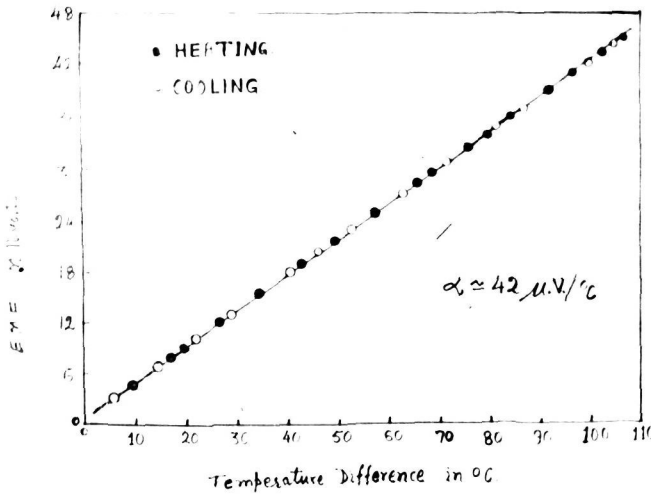


Fig 40.

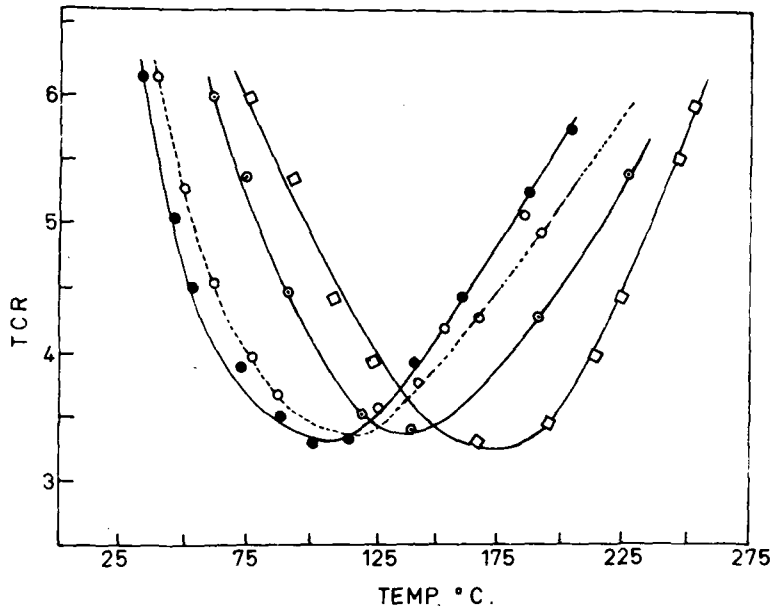


Fig 41

with the rise of temperature. The curve ('a') in Fig. 35 shows the variation of $\log R$ vs $1/T$, and the T_d temperature was $\approx 330^\circ \text{C}$. It may be pointed out here that unlike SnSe , Sn_2Se_3 and SnS films, the resistance of SnTe films both during heating and cooling cycles remained practically unaffected by annealing. Resistance measurement was, therefore, carried out after appropriate annealing as in the case of tellurium films. Figs. (35, 36) show a series of curves for different film thickness obtained in two sets of evaporation, carried out practically under similar evaporation conditions. The peculiar feature namely the increase of resistance with the increase in temperature is very much akin to the metallic character.

$$(ii) \text{ Thermoelectric power } (\alpha) = \frac{dE}{dT}$$

SnSe - The thermal e.m.f. between the two ends of a film was mostly studied by the integral method. Since the resistance of the films was very high, no significant measurable e.m.f. was developed, even when the hot end temperature was as high as 130°C . The films were, therefore, heated in the set-up in a vacuo to temperature $\approx 150^\circ \text{C}$ and then a temperature gradient was introduced by further heating the film, at one end, with the help of a micro-heater as discussed before (Chapter III). Fig. (37) shows the variation of e. m.f. with the difference of temperature between two ends when cold end

was maintained at 150°C . The thermoelectric power (α) was found to be fairly constant $\approx 150 \mu\text{volts}/^{\circ}\text{C}$ for film thickness ranging between 21000\AA and $40,000\text{\AA}$ prepared under more or less the same evaporation condition. The value of α measured in the present case was for region 'B' of log R vs $1/T$ curves as discussed previously in the resistivity measurements. Thermoelectric power (α) however could not be measured, for the temperature range of region 'A' of the curve log R vs $1/T$, because of high resistance of the films.

The type of semiconducting films was determined from the polarity of the sample either at hot or cold junction. In all cases the samples were found to be 'p' type.

Sn_2Se_3 - Since Sn_2Se_3 films also did not show any measurable thermal e.m.f. even when heated to temperature range namely room temperature to $\approx 150^{\circ}\text{C}$ i.e. in the 'A' region of the curve log R vs $1/T$, the measurements were carried out at 'B' region of temperature as mentioned before for SnSe films. Fig.(38) shows the variation of e.m.f. with the temperature difference between the two ends. The average thermoelectric power (α) for all the films was $\approx 155 \mu\text{volts}/^{\circ}\text{C}$, when the cold end was maintained at 150°C . All the samples were 'p' type as before.

SnS - Thermoelectric power of stannous sulphide films was measured in the same way as for SnSe and Sn_2Se_3 .

and the value of thermoelectric power was found to be $\approx 180 \mu\text{volts}/^\circ\text{C}$, for all the samples prepared under more or less same condition of deposition. All the samples were found to be 'p' type (Fig.39).

SnTe: As tin telluride films were conducting, compared to selenides and sulphide of tin, the thermal e.m.f. could be measured easily, even when, the cold end was maintained at room temperature. Fig.(40) shows variation e.m.f. with temperature difference between two ends of the film for film thickness ranging between 3000\AA to 18000\AA . The thermoelectric power was $\approx 42 \mu\text{volts}/^\circ\text{C}$, in all the films. This low value of thermoelectric power is in very much contrast to those for SnSe , Sn_2Se_3 and SnS , films. On the other hand, such value suggests that the electron transport process was similar to the metallic conductor.

(iii) Temperature coefficient of resistance (TCR)

SnSe - In the case of SnSe films the plots of resistance against temperature for annealed samples, the value of $\frac{1}{R} \cdot \frac{dR}{dT}$ known as temperature coefficient of resistance (TCR), was calculated at different temperatures. It is found that TCR is negative between the temperature range studied, namely from 30°C to $\approx 250^\circ\text{C}$. In every case TCR decreased with

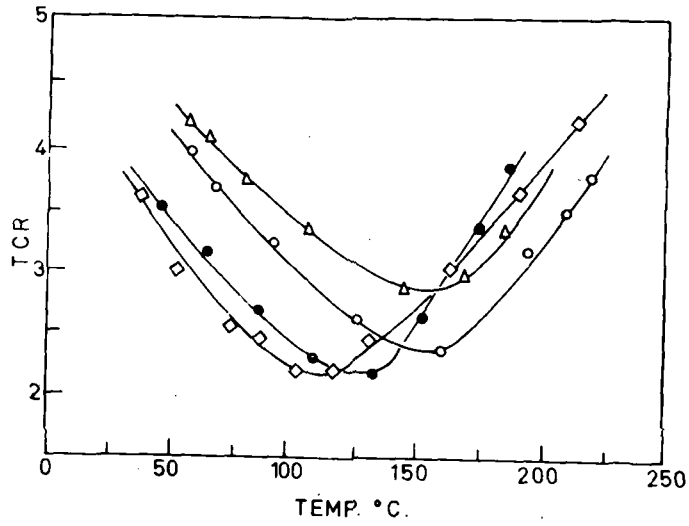


Fig 42.

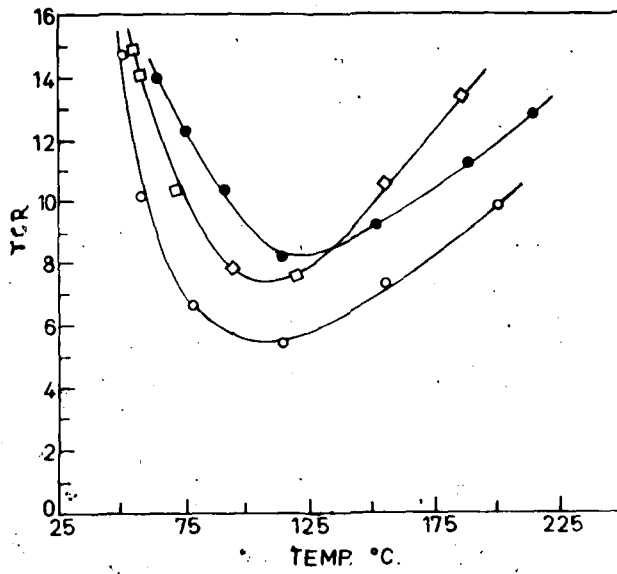


Fig 43

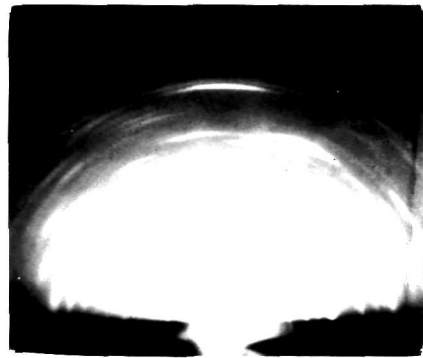
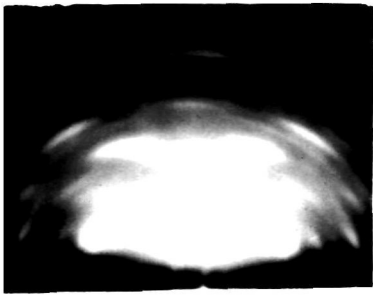
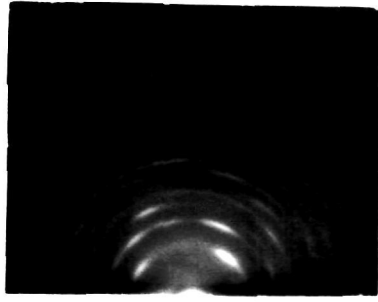


Fig 44.

the increase of temperature, attained a minimum negative value at a particular temperature, and then increased with higher temperatures. The temperature at which minimum value of negative TCR occurs, depends upon the thickness of the films, when the films are prepared under more or less similar evaporation conditions. It is further noted that the temperature, at which minimum value of TCR occurred, shifted towards the higher temperature side, for the films of lower thickness. Fig.(41) shows the such curves for different film thickness indicating the shift of minima on the temperature axis.

Sn₂Se₃ - In the case of Sn₂Se₃ also, a similar phenomena of negative TCR and minimum TCR at a particular temperature was observed. Fig.(42) shows such curves giving the dependence of TCR on the temperature for a different film thickness.

SnS - In consistence with resistivity, thermoelectric power, it was found that negative TCR also varied in the similar manner as in the case of SnSe and Sn₂Se₃. Fig.(43) shows the variation of TCR with the temperature for different film thickness.

(iv) Electron diffraction patterns

In order to have a control on the nature of the films, which were studied for semiconducting properties the electron diffraction patterns of these films were also studied, both

before and after measurements of semiconducting properties. Further, to see if there is a relation between the structure, and electrical properties of films, detailed electron diffraction study was carried out and these results are described in the Chapter VI.

B: DISCUSSION

From the above study it will be seen that $\log R$ vs $1/T$ graphs had two regions 'A' and 'B'. The change of slope occurred at $\approx 200^\circ\text{C}$ and conductivity increased with the rise of temperature in all films of SnSe , Sn_2Se_3 and SnS , maximum temperature being (T_d) temperature. If the heating was stopped in the region 'B' and cooled back to room temperature, the graphs obtained during cooling were nearly parallel to the region 'A', but for cooling at each stage of first heating in region 'B' the room temperature resistance decreased. This effect can be called as 'annealing effect'. In the formation of a vacuum deposited film as discussed in Chapter II, it was seen that voids, stress and other defects in the film do appear as a result of evaporation condition with the increase of temperature and keeping for some time these defects not only get annealed out, but also the small island formed earlier due to evaporation condition, assume larger crystal sizes. All these effects contribute to increase in conductivity.

It has been reported in Chapter VI that SnSe exhibits a normal orthorhombic structure with $a_0 \approx 4.19\text{\AA}$, $b_0 \approx 4.46\text{\AA}$ and $c_0 \approx 11.67\text{\AA}$, in the temperature range from room temperature

to $\approx 200^{\circ}\text{C}$, but at temperatures higher than 200°C it was found that a new phase (cubic structure $a_0 \approx 5.9\text{\AA}$) appeared both for SnSe and Sn_2Se_3 films. It is likely that such a structural change occurring at or about 200°C will also modify the electrical conductivity of the films. This effect was invariably observed in all the samples of SnSe, Sn_2Se_3 and SnS. It has already been reported by Badachhane and Goswami (1963) that in the case of SnS films phase change occurred, from ^{the} normal orthorhombic to a cubic form.

Thermoelectric power of all the films of SnSe, Sn_2Se_3 and SnS was found to be more or less same, ranging between $150 \mu\text{volts}/^{\circ}\text{C}$ to $160 \mu\text{volts}/^{\circ}\text{C}$, when the films were heated to 'B' region.

The minima of negative TCR observed in all samples of SnSe, Sn_2Se_3 and SnS can be explained from equation (38) Chapter IV, on the basis of island structure of films. It is quite possible that the factor C/T^2 is more effective and therefore, instead of decrease in TCR there is increase in TCR. For the films of higher thickness, since the minimum negative TCR occurs at comparatively lower temperature than corresponding thin films, it can be stated that the temperature at which the factor C/T^2 becomes effective is less for thick films and more in the case of thin films. Electron diffraction patterns

for SnSe, Sn₂Se₃ and SnS films on glass showed that tilted orientation did not affect the semiconductor parameters (Fig. 44).

In case of SnTe, unlike other chalcogenides of tin, it was found that all the films, of all sets of evaporation showed metallic behaviour. This is also supported by the results, low value of thermoelectric power (Fig. 40), increase of resistance with rise of temperature (Figs. 35, 36), etc. Because of this metallic behaviour it may be concluded that the system was a degenerate one and conduction was due to the electrons, similar to the conduction in metals.

According to periodic table of elements, the properties slowly change from insulator to a metallic conductor (Po) and therefore, when these elements combine with tin, it is quite possible that the properties of these also will gradually change from an insulator to metal, through an intermediate stage of a semi-metal. Thus SnS films had high resistivity, whereas SnSe, Sn₂Se₃ low resistivity, SnTe on the other hand showed metallic conduction.

CHAPTER VI

ELECTRON DIFFRACTION STUDIES OF GROWTH
OF SnSe, Sn₂Se₃ AND SnTe FILMS

A: GENERAL INTRODUCTION

In order to have a better understanding of the properties of thin films, it is essential to know their state of aggregation, structures, crystal size, orientation, etc., as many of the properties are structure sensitive. Vapour deposited films exhibit a wide range of structures from irregular amorphous mass to single crystals. The optical and electrical properties are also expected to depend upon, not only on the crystalline state, but also on the development of preferred axial direction. Regular arrangements of atoms in the ^{three} dimensions extended in space give rise to the formation of crystals. An atom contains a nucleus at the centre and extra nuclear electrons at its periphery. Consequently there will be an intense potential field concentrated at the centre of the atom, but slightly modified by the surrounding electrons. This is somewhat analogous to the potential field inside a spherical condenser, with the highly concentrated positive charge at the centre and negative charge at the periphery. Because of this intense field inside an atom or ion, negatively charged electrons are highly scattered and, scattering amplitude of the electron beam is about 10^5 times

more, compared to that of x-rays for a single atom. The intensity of ^{the} diffracted electron beam will therefore be much more than the corresponding x-rays. Consequently, electron diffraction technique has found applications in many fields especially in thin films, surface structure, crystal growth process, etc. (Thompson and Cochrane 1939, Finch and Wilman 1937, Pinsker 1953, Raether 1951, 1957), when the usual methods of structure analysis by x-rays are not suitable.

There are certain features which are characteristic of the diffraction of electrons, and the physics of diffraction of electrons have been studied in detail by many workers in Japan (Miyaake 1950, 1954), Australia (Cowley and Moodie, 1957, 1959) and Russia (Pinsker, 1953, 1959, Vainshtein, 1949, 1964). The technique has also been found useful to determine the complicated structures of organic as well as inorganic compounds. This method is particularly suitable for finding the positions of light atoms such as hydrogen, carbon, etc, in organic compounds (Pinsker, 1953, Vainstein 1964).

As electrons are highly scattered by matter, only a few layers of atoms of a crystalline material are quite sufficient to give a coherent diffraction pattern. On the other hand, with

x-rays comparatively much thicker samples (about 0.1 mm) are necessary for the diffraction. In the reflection pattern since the penetration of electrons in the direction normal to the beam and perpendicular to the surface is very low, a film thickness of the order of $5-10\text{\AA}$ is sufficient to give coherent diffraction patterns. Pashley and Newman (1955) claimed to have studied the films of gold and copper with thickness as small as 2 to 5\AA .

This technique has been extensively used for the study of structures of surface layers, electrodeposited films, phase change, crystal growth and corrosion etc., in England by Finch and Wilman (1937, 1939), Pinsker (1953) in USSR, many workers in Japan (Miyake, 1954) and Goswami and his co-workers in this laboratory (1955, 1957). Simultaneous investigations of film structures by electron diffraction along with the semiconducting properties will, however, provide much clearer insight on the physics and chemistry of solids, since often physical and electrical properties of films depend considerably upon their crystalline state. In fact, semiconducting properties of selenium depend upon the state of crystallinity (Smith 1873), Washman (1957) suggested that photoconductivity of lead sulphide depends on the crystalline structure and further investigation showed that the oxidation of material and presence of oxidised state contributes to photoconductivity.

Crystal growth

In an ideal crystal, atoms or ions are arranged regularly in ~~three~~ dimensions, in space. These atoms or ions normally should occupy positions conforming to minimum potential energy state. During the growth process, crystal grows atom by atom and layer by layer and often before the first layer is completed, the next layer starts growing, the growth may take place simultaneously either on same or different layers. It is possible that before a layer is completed, another layer may form over it. At the junction of two or more crystallites, atoms may not be in their ideal periodic position, as they should be in the ideal case. This gives rise to faults, such as intergrain-boundaries, dislocations, stacking faults, twinning etc.

During the last forty years the theories of crystal growth have been developed by many workers especially by Kossel (1927, 1928), Volmer (1939), Stranski and his co-workers (1949). Theories taking into consideration the imperfections arising from dislocations, have already been developed (see Burton, Cabera and Frank, 1949, 1951). It has been observed that in vapour phase deposition process, the substrate temperature is an important factor, which favours the epitaxial growth.

Evaporation conditions, such as rate of deposition, substrate temperature, etc., also affect the nature of the deposits, crystal structure, phase change, orientation etc. with the growth of films (Krustinson, 1941, Goswami, 1961, 1962, Aggarwal and Goswami, 1963, Badachhane and Goswami, 1964).

Increase of crystal size with film thickness, as well as the substrate temperature, has also been observed by many workers, (Evans and Wilman 1952, Wilman, 1955, Kuwabara 1957). Similar observations have also been made for crystal growth by electrodeposition, anodic process, by Goswami and his co-workers (1955).

The habit of growing crystals often depends upon the surrounding conditions, though, their structures normally remain unchanged. For example sodium chloride crystals grow normally, crystals grow normally with a cubic habit, from the neutral solutions, but develop octahedral faces, in the presence of urea in the solution.

Epitaxy

Epitaxial growth, or oriented over growth of crystals, was first observed by Wallerant (1902) and Mügge (1903) in naturally occurring minerals. The term 'Epitaxy' was first used by Royer (1928, 1936). After making extensive study on the growth of crystals on different substrates, he came

to the conclusion that the deposit atoms or ions developed orientations as to follow the substrate structure, such that there was a close fit between the two dimensional network of deposit and substrate at the inter-face. He also found that in such a case there was one densely populated lattice row in the deposit, parallel to one that of the substrate. Epitaxy was possible only if their relative identity spacing did not differ more than 15%. Frank and Van-der-Merwe(1949) considered the substrate as two dimensional network and arrived at similar conclusions emphasizing that no epitaxy was possible if lattice misfits were higher than 16%. It is now well known from many experiments that epitaxial growth can take place even when, the misfit is as high as 50% or more (Pashley 1956, Goswami, 1962). Hence the idea of Van-der-Merwe(1949) is no longer valid, at least for the epitaxial growth.

Further^a new type of orientated over growth was observed by Goswami (1961) on one degree orientated substrates. These results seems to be the 1st example of this kind.

Phase transition and polymorphism

Recent studies on ~~xxxx~~ structure of thin films have shown that the phenomenon of polymorphism is observed in metal deposits as well as the deposits of many other compounds. Schulz (1951), showed that rubidium bromide having normal NaCl type structure

developed CsCl type structure, when deposited on silver substrate. It was also recorded by Schulz (1951) that some halides having CsCl structure developed NaCl type structure, when grown from vapour phase, on appropriate single crystal substrates. Goswami and Trehan (1959) observed two new cubic structures ~~in case~~ of copper sulphides during the study, on ^{the} reaction of sulphur vapour on copper single crystals. Aggarwal and Goswami observed some hexagonal phase even from β form of ZnS and CdS. Figgot and Wilman (1958) also observed some superstructures of some sulphides.

It is well known that on heat treatment often a new phase appears. At a certain temperature ^{the} transition of one phase to another phase takes place. In case of thin films, this temperature at which transition takes place is much lower than that of bulk material.

It will be of great interest to investigate the structure of thin films of chalcogenides, their crystal growth process, phase changes, orientations, etc., and if possible to correlate them, with the semiconducting properties, which have simultaneously been studied, in the present work.

In the previous Chapter historical survey on the electrical and structural properties have already been made.

Tin is known to have two well defined sulphides namely stannous sulphide (SnS) ASTM Card 1-0984 and stannic sulphide (SnS_2) ASTM Card No: 1-1010. Another sulphide of tin, however, less established, is tin sesqui-sulphide Sn_2S_3 (Mellor 1930), Hoffman (1934) suggested that SnS had deformed structure similar to galena. Wells (1958) suggested that the structure of stannous sulphide consisted of very buckled hexagonal nets in which alternate atoms are tin and sulphur.

Clark and Anderson (1943) reported that stannous sulphide is a semiconductor at all temperatures. According to them at about 750°C the ionic component is less than 1% of total and also even fused SnS is a probable semiconductor. Anderson and others (1945) presented an evidence to confirm the suggestion that high temperature conduction of SnS represent the intrinsic electrical conductivity of the crystal lattice. Yurkov (1953) has studied the rectifying properties of SnS crystals. Grimm and Neseldov (1956) have given data on the conductivity of sulphides and selenides of tin for mass and thin layers.

SnSe is reported as orthorhombic structure with lattice constants, $a_0 \approx 4.19\text{\AA}$, $b_0 \approx 4.43\text{\AA}$, $c_0 \approx 11.57\text{\AA}$ (Palatnik and Levitin, 1954, Pearson, 1958), however, Sn_2Se_3 is reported as tetragonal $a_0 \approx 5.38\text{\AA}$ and $c_0 \approx 6.77\text{\AA}$.

Along with tetragonal structure, a cubic structure is also reported $a_0 \approx 5.99\text{\AA}$ (Okazaki and Ueda 1956, Palatnik and Levitin, 1954). SnTe had only one structural phase of NaCl type cubic as already mentioned in Chapter V.

A detailed study has also been made on crystal growth process at various substrate temperatures on different faces of NaCl and also on mica, glass, colladion. The results are presented in the following chapter.

B: EXPERIMENTAL

Preparation of specimen

The apparatus used for preparing the deposit films was as shown in Fig.(45). A pyrex tube of dia. ≈ 6.25 cms. and length ≈ 30 cms. was clamped horizontally and rubber bungs were fitted at the two ends. Two terminals were taken out and were used for heating the filament containing the sample. The whole system was evacuated by rotary pump and oil diffusion pump and the vacuum was of the order of 10^{-3} mm. Hg to $\approx 10^{-4}$ mm Hg. Substrates were kept nearly 2-3 cms. away from the filament. When the deposition at higher than room temperature was required the tube was heated by a cylindrical furnace placed around the pyrex tube. The temperature of substrate was indicated by a thermocouple. Before

evaporation the filament was first flushed to white (hot) several times and then the bulk sample which was to be evaporated was put into it. The rate of evaporation was controlled by an external variac. After the deposition was over, the heater was removed and the substrate was cooled down to room temperature in vacuo. These films were then examined by electron diffraction camera (Finch type), fabricated in this laboratory. Filaments used were from tungsten wire. The initial flushing of the filament was essential in order to get rid of surface impurities of the filament.

Preparation of substrates

Substrates used for depositing films were (100), (110), (111) faces of rock salt, cleavage face of mica, polycrystalline NaCl and amorphous glass surfaces.

(100) faces of rock salt were prepared by cleaving single crystals along with cube edge direction, with the help of a clean and sharp edged knife by applying sudden pressure. Untouched cleaved surfaces were used as substrates. Sometimes the particles adhering to the surface were removed by using a camel-hair brush. Proper precautions were taken to avoid any contamination of grease with the substrate surfaces.

(110) and (111) faces of rock salt were prepared by grinding the crystals very carefully with different grades of emery paper down to 0000. Afterwards the surface was etched with running water and dried immediately by pressing between fresh filter papers. Mica substrates were prepared by cleaving them and immediately used.

Glass substrates were prepared by cutting "Gold-seal" slides into convenient sizes and grinding sharp edges. These were then treated with nitric acid and finally washed with distilled water. The glass substrates were then dried by pressing them between filter papers and finally heated in an oven at $\approx 110^{\circ}\text{C}$ and cooled.

The substrates thus prepared, were then transferred in the deposition chamber where the deposition was carried out as described before.

Examination of specimen

Deposits obtained on various substrates were studied by reflection or transmission electron diffraction techniques. Deposits obtained on rock salt or polycrystalline NaCl were first examined by reflection and then by transmission method. For the latter, the deposit-films were removed from the substrates in the following way. The deposits, along with substrate was slowly dipped, keeping the deposit-film surface horizontal in a large petri-dish containing distilled water.

: 100 :

Water slowly dissolved the top layers of the substrate in contact with the film and thus leaving the film to float on the water, The deposits were then collected carefully on a collodian film placed on grids.

The electron beam used in the camera was accelerated by voltage $\simeq 50$ to $\simeq 60$ KV. The specimen were examined at different angles of azimuths by rotating the film with respect to the beam direction. For the analysis of the pattern, colloidal graphite was used as internal standard and 'd' values of various reflections were measured.

The method of interpretation was similar to those already discussed by early workers, especially, Finch and Wilman (1937), Thomason and Cochrane (1939), Wilman (1948, 1949, 1952), Pinsker (1953) and others. The details of the methods of interpretation is already given in Chapter II.

C: RESULTS

SnSe and Sn₂Se₃

On (100) NaCl - Evaporation was carried at different substrate temperatures ranging from room temperature to $\simeq 450^{\circ}\text{C}$ on (100) faces of NaCl crystals for different period of time. During the several trials of evaporation it was found that higher substrate temperature conditions, favoured the epitaxial

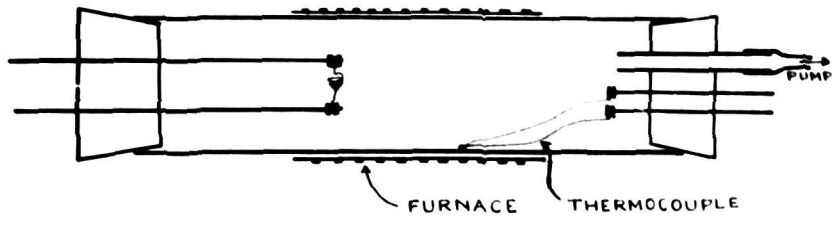


Fig 45.

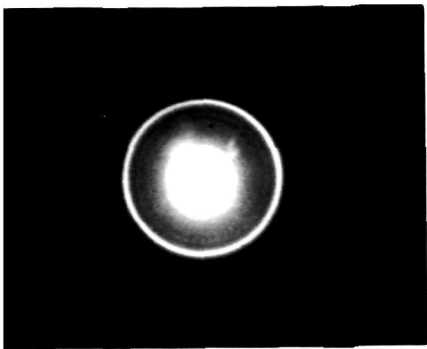


Fig 46.

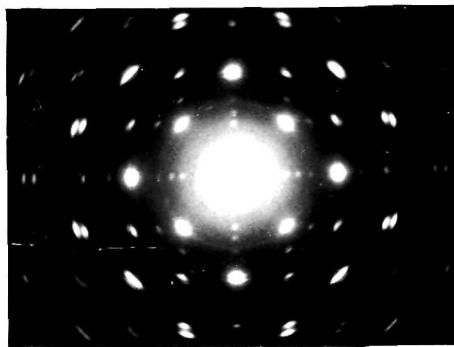


Fig 47.

growth. The deposit films exhibited different types of patterns conforming to polycrystalline materials with or without preferred orientation of the deposit crystal, or two degree orientations of them. Even though, reflection patterns did not always yield characteristic of *2-d* orientation, the basic pattern indicated that SnSe films grew epitaxially on NaCl crystals, when deposited in vacuo, at higher substrate temperature. The pattern (Fig. 46) at 100°C showed the polycrystalline nature of the deposits and the d_{hkl} values of different reflections correspond to the normal orthorhombic structure of SnSe. Similar patterns were also observed upto 200°C . Patterns obtained mostly at higher temperatures namely from 250°C to $\simeq 450^{\circ}\text{C}$ showed that the deposits developed *2-d* orientation, some times accompanied with rings (Fig. 47).

The above diffraction pattern is rather complex. The general disposition of the pattern shows that spots are arranged in a square net work, with spot at the centre of each diagonal. Closer examination, however, revealed that each of three bright *spots* at the corner of square net work of pattern, consisted of two individual spots very close to each other. These spots were clearly resolved when looked through a magnifying glass (especially in the negative).

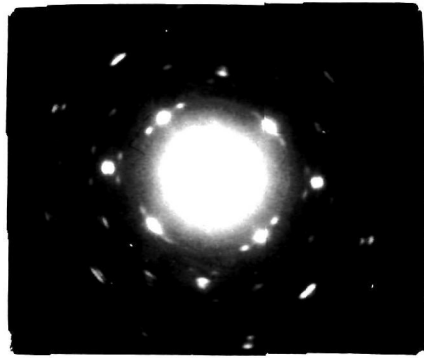


Fig 48.

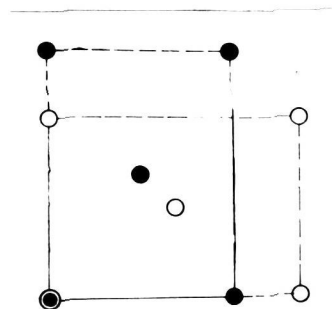
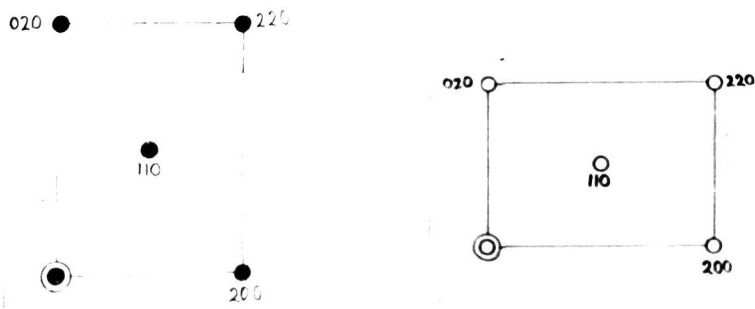


Fig 49.

Further these pairs of spots at the corners, instead of forming a square net work, form two sets of rectangles with undiffracted spot at the origin. This is most clearly seen in Fig. (48) when highly enlarged. The appearance of two clear spots (well resolved) at a distance of 3.1\AA , however, falls on the centre of a diagonal originating from undeflected spot for two rectangles. The ' d_{hkl} ' values of these two spots i.e. along with spot rows at right angles to each other are 2.24\AA and 2.08\AA , respectively. Thus such net work of spots forming rectangles had ' d_{hkl} ' values 2.08\AA , 1.55\AA and 2.24\AA corresponding to 200, 220 and 002 reflections of orthorhombic structure of SnSe. Further the appearance of second set of spots close to the previous one, were no doubt, due to the rotation of the crystal by 90° with undeflected beam at the origin.

The above disposition of spots, is however, consistent with the deposit developing $\{001\}$ orientation with azimuthal rotation 90° i.e. $\{001\}$ plane of the deposit was parallel to (100) face of rock salt, such that a^* and b^* of the reciprocal lattice which are right angles to each other would lie on plane of the photographic plate. Fig. (49) shows the analysis of spots with their respective indices. It is evident from the above figure (49) that r^*_{110} of one crystal, will be slightly away from r^*_{110} of the other crystal, which was actually observed in the pattern. It is also

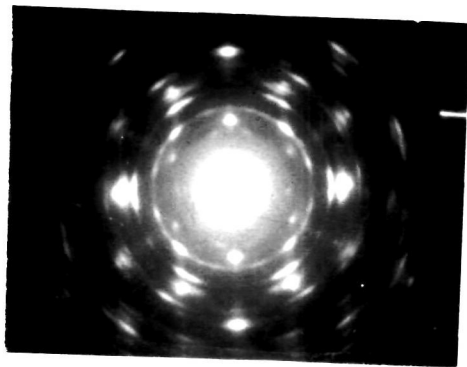


Fig 50

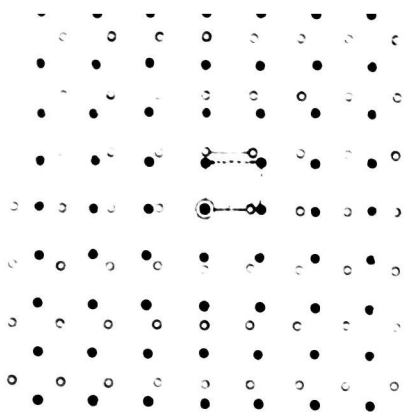


Fig 51.

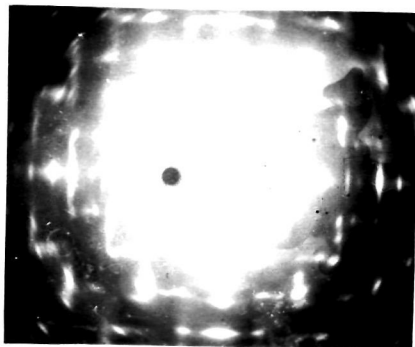


Fig 52 .

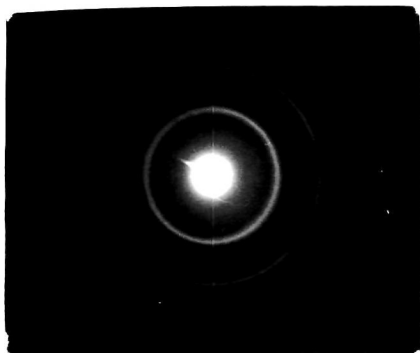


Fig 53.



Fig 54.

interesting to note that even though the lattice dimensions and arrangement of atoms of SnSe of orthorhombic structure $a_0 \approx 4.19\text{\AA}$, $b_0 \approx 4.46\text{\AA}$ and $c_0 \approx 11.57\text{\AA}$ are vastly different from that of the substrate. There are, however, present a few extra spots such as 100, 010, etc. in the pattern observed. Further, from the disposition of spots from SnSe deposits with respect to axial direction of NaCl, it was found that $\langle 100 \rangle$ or $\langle 010 \rangle$ of SnSe deposits was parallel to $\langle 110 \rangle$ of NaCl and vice a versa Fig.(48).

On (111) face - The deposits formed on (111) face of NaCl yielded patterns similar to Fig.(50). These patterns are also complex. It is also seen that quite a number of spots are disposed in hexagonal arrays. There are also two pair of spots, which are in the hexagonal arrangement and these reflections appear to arise from two individual crystals but not from the same crystal. This suggests that the deposit crystal developed two hexagonal structures and a_0 values of each of them was found to be 4.19\AA and 4.46\AA respectively. 'C' axis of these crystals were along with beam direction as seen from the hexagonal disposition of the spot pattern. It was, however, not possible to find out the c_0 for each of them and to decide unambiguously whether the deposits were of hexagonal close type structures. From the pattern, further it is seen that there are also a few additional spots appearing in pairs just inside r^*_{200} or r^*_{020} with

' d_{hkl} ' values 2.41\AA corresponding to (111) of a structure with a_0 4.18\AA to 4.25\AA . Thus indicating the formation of cubic or tetragonal structure with a_0 between 4.18\AA to 4.25\AA . Since beam direction was along 'C' axis in the case of transmission patterns, it was not possible to decide uniquely the 'C' axis of the crystal and hence whether the structure was cubic or tetragonal. The detailed analysis can also explain the appearance of most of the spots including faint spots, some of which can be seen in Fig.(5), obtained at substrate temperature $\approx 350^\circ\text{C}$ during deposition.

On (110) face - Deposits of SnSe formed on (110) face of rock salt at $\approx 300^\circ\text{C}$ and above yielded patterns which on casual looking appeared to be complex. There are some features such as rows of spots at right angles to each other giving rise to step-like appearance through out the region of pattern. A closer examination of these spot rows, however, revealed that the intense strong spots at a distance 2.08\AA and 2.24\AA form $\sqrt{2}$ type of rectangles, rotated by 90° . Fig.(51) shows the theoretical pattern, which explains most of the prominent spots in the pattern (Fig. 52). In addition to the basic pattern there are some extra spots, possibly due to hexagonal modification.

On collodion and NaCl tablets(polycrystalline)

SnSe deposits at different temperatures, from room temperature to about 200°C yielded ring patterns corresponding to polycrystalline deposits, ' d_{hkl} ' values of all the rings

Table. 6.

Analysis of Fig. (46)
 SnSe polycrystalline $a \approx 4.19\text{\AA}$,
 $b_0 \approx 4.46\text{\AA}$, $c_0 \approx 11.57\text{\AA}$

Intensity I/I_0	d \AA (observed)	d \AA (calculated)	h,k,l .
f	4.18	4.06	011
		4.15	101
m.s.	3.57		
s	3.10	3.1	110
s	2.94	2.94	111
m.f.	2.36	2.33	121
s	2.18	2.17	311
s	2.08	2.14	131
m.s.	1.95		
m.s.	1.85		
f	1.81		
f	1.78	1.77	331
v.f	1.72		
s	1.64		
s	1.49		
m.s.	1.403		
m.s.	1.345		
f	1.28	1.31	013
v.f	1.202		
f	1.18	1.17	212
v.f	1.08		
f	1.035		
v.f	0.97		
v.f	0.95		
v.f	0.86		

in the pattern correspond to ' d_{hkl} ' values of normal orthorhombic structure (Table 6) as already mentioned before.

Deposits of SnSe on collodion at $\simeq 300^{\circ}\text{C}$ yielded ring patterns (Fig. 53). It is seen that reflections consisted essentially either all odd or even indices (hkl) with $a_0 \simeq 6.15\text{\AA}$, a characteristic of F.C.C. type structure. Further it is also seen that 111 reflection was strongest, whereas 200 practically absent and 220 of medium intensity. These characteristic suggest that the deposit developed ZnS (zinc blend) type structure, similar to SnS as observed by Badachhape and Goswami(1964).

Reflection patterns on glass and mica substrates at room temperature were diffuse, whereas at higher substrate temperatures yielded patterns (Fig. 54) showing a characteristic of one degree orientation of SnSe deposit crystals.

Sn_2Se_3 deposits on (100), (110) and (111) faces of NaCl and on glass and mica yielded patterns similar to those of SnSe patterns discussed above.

SnTe

On (100) NaCl.

SnTe deposits on (100) face of NaCl yielded ring patterns due to polycrystalline material (Fig. 55) practically at all the temperatures ranging from room temperature to $\simeq 200^{\circ}\text{C}$. At higher substrate temperatures from 250°C to $\simeq 450^{\circ}\text{C}$ deposits yielded patterns (Fig. 56) characteristic

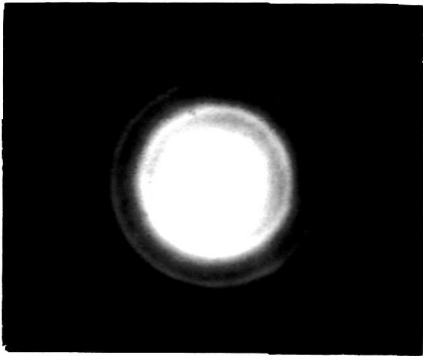


Fig 55

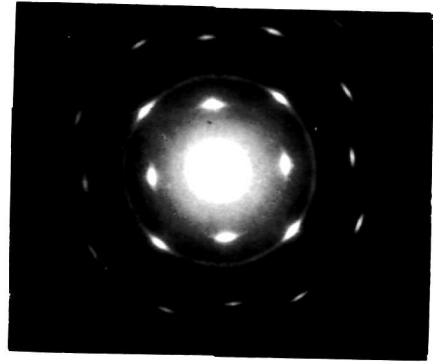


Fig 56.



Fig 57.



Fig 58.

Table 7

Analysis of Fig. (55) SnTe cubic

Intensity I/I ₀	d Å ⁰	d(x-ray)	I/I ₀ x-ray	hkl
s	3.11	3.13	70	200
V.s.	2.21	2.22	100	220
m.s.	1.81	1.82	60	222
V.f.	1.56	1.58	40	400
s	1.40	1.41	90	420
s	1.28	1.285	80	422
V.f.	1.13	1.12	30	440
m.f.	1.04	1.06	70	442 600
m.f.	0.98	0.999	60	620

mean $a_0 \approx 6.31\text{Å}$

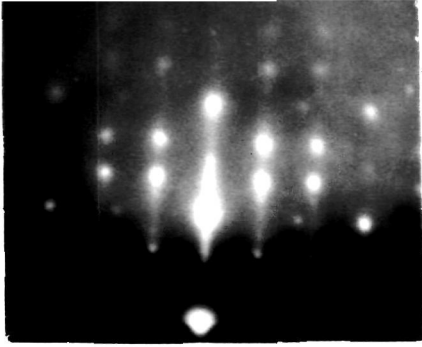


Fig 59.

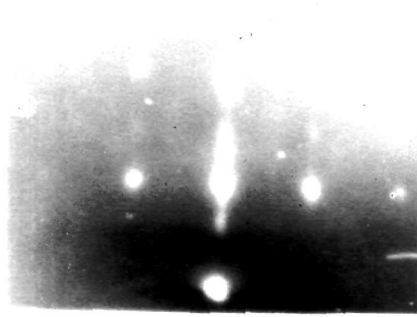


Fig 60.

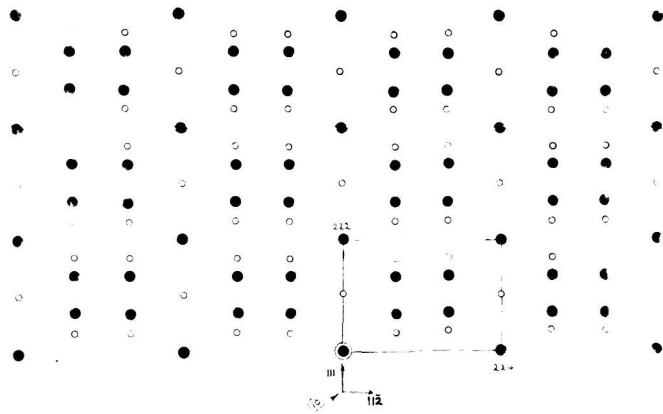


Fig 61.

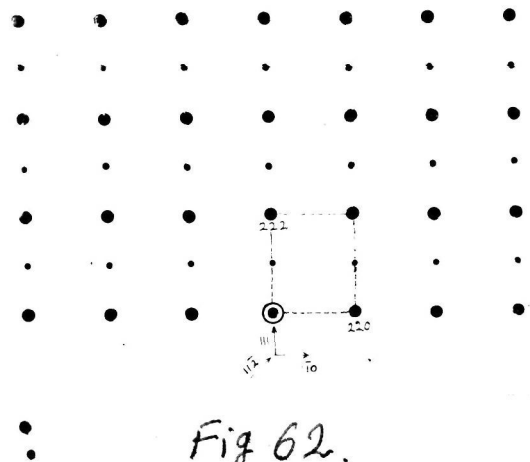


Fig 62.

of 2nd orientation by transmission methods. It is seen that spots formed a square arrangement. The analysis of spot patterns as well as polycrystalline ring patterns (Fig.55) indicated the formation of cubic structure having $a_0 \simeq 6.31 \text{ \AA}$. From the polycrystalline patterns it was also seen that 111 reflection of SnTe was practically absent unlike SnSe or SnS. Intensity distribution of different reflections conformed the above fact that 111 reflection was practically absent. This suggests that SnTe developed NaCl type structure. Since Sn and Te have practically the same electron scattering factor, the absence of 111 reflection is quite understandable.

On (111) face of rock salt - Deposits of SnTe on (111) face of NaCl particularly at higher temperatures i.e. from 250°C to $\simeq 450^\circ\text{C}$ yielded patterns, often forming arcs, disposed hexagonally (Fig.57) no doubt, due to $\{111\}$ orientation on (111) face of NaCl.

On (110) face - Deposits formed on (110) face of NaCl yielded patterns exactly similar to those formed on (100) face of NaCl, thus indicating the development of (100) orientation on (001) face. (Fig58).

On mica - Deposits formed on mica (0001) yielded very interesting patterns. Fig. (59) shows the pattern when the beam was along a certain direction of cleavage face of

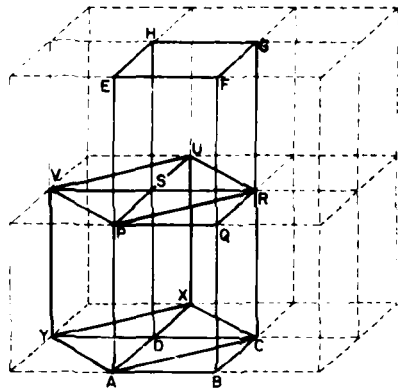


Fig 63.

mics and Fig. (60) when the specimen was rotated by 30° . Both the patterns however repeated themselves when rotated by 60° . Further it is seen that in Fig.(59) the diagonal of rectangle had spots at $1/3$ and $2/3$ distance. This however suggests that deposit developed $2d \{111\}$ orientation. But the measurement of spot-row along with plane of incidence and horizontal direction in Fig(59), are in the ratio $1: \sqrt{2}$, whereas it should have been in ratio $\sqrt{3}: \sqrt{24}$ ($1:2\sqrt{2}$). Similarly for 30° azimuthal direction of the pattern the ratio of spot-rows in the two directions would have in the ratio $\sqrt{3}: \sqrt{8}$, but they are in the ratio $\sqrt{12}: \sqrt{8}$. Thus theoretical patterns for $2d \{111\}$ orientation are as shown in Fig.(61,62). To resolve this difference negative was closely examined.

It was also found that in addition to the strong spots there were many spots comparatively faint which were in between the strong spots. Considering their disposition it was found that instead of strong spot forming the first reflection in the plane of incidence corresponding to $\{111\}$ reflection was considerably faint, and 222 reflection was very strong, thus giving rise to strong spots corresponding to even reflections only.

D: DISCUSSIONS

Deposit films exhibited patterns corresponding to normal orthorhombic structure ($a_0 \approx 4.10\text{\AA}$, $b_0 \approx 4.46\text{\AA}$ and $c_0 \approx 11.57\text{\AA}$) upto $\approx 200^\circ\text{C}$ but at higher substrate temperatures

there was a phase transition taking place to give rise to a cubic or tetragonal structure. A similar transformation of orthorhombic SnS to cubic and h.c.p. has also been reported by (Badachhape and Goswami, 1964). They have also shown the new values of hkl on such transformation. In addition a cubic modification of ZnS type with $a_0 \approx 6.15 \text{ \AA}$ has also been found. This modification was similar to that observed for SnSe. This phase transition from orthorhombic to cubic is possible generally when one axis out of three is large, practically double to either of the two remaining axes. The formation of such a cubic structure is illustrated in Fig.(63).

Epitaxial growth

It is also interesting to point out that the arrangement of atoms in SnSe, Sn_2Se_3 which have orthorhombic structure is vastly different from that of NaCl which has a cubic structure. Even though the lattice spacing and atomic arrangement of deposit and the substrate are so vastly different, the deposits of chalcogenides of Sn grew epitaxially at appropriate high temperature (above 200°C). Such growth took place on all the three different faces. For such epitaxial growth it is but natural that the deposit film would be subjected to a considerable stress because of misfits of atoms between the deposit and substrate layers. Under the influence of inter-atomic forces, as well as the considerable substrate temperature, it is quite likely that the deposit atoms may slightly rearrange.

This will result in developing a new phase during the epitaxial growth process. It is also interesting to note that ' a_0 ' and ' b_0 ' of the orthorhombic phase are nearly equal and hence with a slight rearrangement of atoms both the axes have same value. Further the development of complete cubic structure of $a_0 \approx 6.15 \text{ \AA}$ also involves the rearrangement of the 'c' axis. Badachhane and Goswami (1964) have already shown how such rearrangement takes place in the case of SnS deposits. It is also to be noted that most of the modified structure was observed in the case of epitaxially grown films. This, no doubt, clearly shows the influence of interatomic forces in structure and phase change of thin films.

For 2nd $\{111\}$ orientation of f.c.c. crystals by reflection methods, it has already been observed by many workers that reflections upto 3rd, even of higher orders have more or less same intensity. But in the present case it was however noticed that all even (hkl) reflections were very strong whereas all odd (hkl) reflections were very weak. These strong reflections gave rise to rectangular disposition of spots with sides in the ratio of $2\sqrt{3} : \sqrt{24}$, $(1 : \sqrt{2})$ as observed in the present case. This peculiar intensity-distribution, is, however, not clearly understood as yet.

CHAPTER VII

SUMMARY AND CONCLUSIONS

In the present investigations on semiconducting properties of vacuum deposited films and also on crystal growth process, by electron diffraction, an attempt has been made to standardize the measurement of semiconductor parameters for thin films, evaporation condition and other factors, controlling these properties, and at the same time, study the surface structures. Solids in thin film state often have distinctive structural and physical properties absent in ^{the} bulk form.

In order to investigate these properties of films a new device was developed. After many trials, the method was adopted for measurements of semiconducting parameters. Many of the difficulties involved in this film measurements, namely flimsy character, their contact problem, evaporation of films, oxidation etc. with temperature, which consequently cause unreliability of the measurements, had considerably been removed in this device. The measuring techniques for different parameters of the semiconductors, were standardized and the practical limits of maximum temperature of heating of the specimen governed by the temperature of discontinuity (T_d) of the individual film, was determined and the annealing temperature in each case also found out.

A detailed study has been made by this device on the different semiconductor parameters, namely resistivity (ρ), energy band-gap (ΔE), thermoelectric power (α), temperature coefficient of resistance (TCR) etc. at different temperature region, for the vacuum deposited films of tellurium and sulphide, selenides and telluride of tin, with thickness varying from 500\AA to $\approx 40,000\text{\AA}$. Corresponding structural features were also determined by electron diffraction methods.

The discontinuity temperature (T_d) of tellurium films was about 180°C and the variation of resistance of tellurium films with the temperature both during heating and cooling cycles was determined. Resistance of films decreased with the increase of temperature, which was a characteristic feature of semiconductors. From the slope of straight line curves ($\log R$ Vs $1/T$), the energy band-gap or activation energy (ΔE) was calculated. It was found that the activation energy (ΔE) varied from 0.32 eV to $\approx 0.44\text{ eV}$ for the films of thickness ranging from $13,000\text{\AA}$ to $\approx 500\text{\AA}$. Higher value was, however, observed for thinner films, whilst lower value for thicker films. In order to study the film properties with corresponding bulk properties, experiments were also carried out on compressed bulk

material obtained from tellurium powder. Activation energy (ΔE) for such bulk material was ≈ 0.325 eV. Thermoelectric power (α) for tellurium films was determined and found to be nearly constant for all film thickness ($\approx 340 \mu\text{volts}/^\circ\text{C}$), except for very thin films ($\approx 500\text{\AA}$) for which it was $\approx 400 \mu\text{volts}/^\circ\text{C}$. Negative temperature coefficient of resistance was of the order of $\approx 10^{-2}/^\circ\text{C}$ and it decreased, with the rise of temperature.

In the case of SnSe, Sn_2Se_3 and SnS films $\log R$ Vs $1/T$ curves showed two regions of slope. Films heated to higher temperature region showed irreversible change in the conductivity and the room temperature resistance was less compared to unheated specimen. This appears to be due to a phase-change of the specimen namely ^{the} change of ^{the} orthorhombic structure to the cubic one. The activation energy for these films were found to vary from 0.47 eV to 0.51 eV. Here in these cases also thinner film had higher ΔE compared to thicker films. Temperature of discontinuity (T_d) for all the films of SnSe, Sn_2Se_3 and SnS was 310°C , 320°C and 330°C respectively. All the films were found to have much higher resistance ($\approx 1\text{M}\Omega$ to $\approx 100\text{M}\Omega$) SnS films showed the maximum resistance. SnSe, Sn_2Se_3 and

SnS films were found to be 'p' type semiconductors having thermoelectric power $\approx 155 \mu$ volts/ $^{\circ}$ C, 160μ volts/ $^{\circ}$ C and 150μ volts/ $^{\circ}$ C, respectively. Negative temperature coefficient of resistance decreased with the rise of temperature after reaching to a minimum, again increased with the further rise of temperature. This behaviour seems to be due to the contribution of the factor C/T^2 at higher temperatures in the expression for TCR. The temperature at which minima took place was dependent on film thickness. The shift of minima on higher temperature side was for thin films.

SnTe films unlike SnSe, Sn_2Se_3 and SnS did not show any fall of resistance with increasing temperature in $\log R$ Vs $1/T$ curves. The curves on the other hand, showed a slight increase of resistance with increasing temperature, suggesting a degenerate system similar to that of a metallic conductor. Low thermoelectric power ($\alpha \approx 42 \mu$ volts/ $^{\circ}$ C) independent of film thickness, also confirmed the above view.

An electron diffraction study was also carried out on the crystal growth process of SnSe, Sn_2Se_3 and SnTe films on (100), (110) and (111) faces of rock salt, cleavage face of mica and also on collodion films, at different temperatures, ranging between room temperature

to $\approx 450^{\circ}\text{C}$. Even though the films had structures dissimilar from the single crystal substrates, they grew epitaxially on them, often with the formation of new phases, depending on ^{the} substrate temperature. Deposits of SnSe developed a normal orthorhombic structure with the lattice constant $a_0 \approx 4.19\text{\AA}$, $b_0 \approx 4.46\text{\AA}$ and $c_0 \approx 11.57\text{\AA}$ upto 200°C . On the (100) face of rock salt, at higher temperatures deposits developed two structures ($a_0 \approx 4.18\text{\AA}$ and 4.46\AA) growing epitaxially, but rotated by 90° and possibly with the $\{001\}$; plane parallel to the substrate. On the (111) face, deposits developed again two phases with $\{111\}$ orientation. On (110) face also deposits developed two similar structures rotated by 90° to each other. A third structure (cubic, $a_0 \approx 6.15\text{\AA}$) was also observed on collodion at temperature $\approx 300^{\circ}\text{C}$. Deposit films of Sn_2Se_3 developed similar orientations as observed in SnSe.

SnTe deposits developed ^a f.c.c. structure with $a_0 \approx 6.31\text{\AA}$. Films grew epitaxially with suitable temperatures with $\{100\}$, $\{100\}$, $\{111\}$ orientations on (100), (110) and (111) faces of rock salt respectively. On mica, however, deposit crystals developed ~~2-d~~ $\{111\}$ orientation.

The above studies showed in many cases that the physical properties are depending on the surface structures of the deposit films. It has been observed in this Laboratory that there exists a better correlation between semiconducting properties and structures of thin films in the case of InSb single crystal films, grown on mica substrates. It is expected, therefore, that if a similar study could be made on epitaxially grown single crystal films of these sulphides, selenides and tellurides, under a suitable substrate temperature and deposition condition, a better conclusion regarding the electron transport process could be arrived. It may, therefore, be mentioned that at the present stage of the development of "Physics of Thin Films" none of the theories can satisfactorily explain many of the features of thin films. To account for these, one has to take into consideration certain characteristics, such as, defects, voids, surface asperities, etc. which are invariably present in films. A theoretical treatment taking into account of these factors will have a better chance to explain the experimental results quantitatively.

ACKNOWLEDGMENT

The author is deeply indebted to Dr.A. Goswami, Assistant Director, National Chemical Laboratory, Poona, for his supervision, encouragement, keen interest in the work, many helpful day-to-day discussions and also for his kindness in giving an opportunity to work in his "Electron Diffraction Laboratory".

The author is thankful to the Director, National Chemical Laboratory, Poona, for giving permission to work as voluntary worker and for the permission to submit the work in the form of a thesis.

---0---

J. G. M.
22/8/66.

117

REFERENCES

- (1) Adams, W. G. and Day, R. E. (1876)
Proc. Roy. Soc. (London) 25, 113.
- (2) Aggarwal, P.S. (1968)
Ph.D. Thesis, Poona University.
- (3) Albers, W., Hass, C. et.al. (1960),
J. Phys. Chem. Solids, 15, 306.
Albers, W., Hass, C. et.al. (1961),
J. Phys. Chem. Solids, 23, 215.
- (4) Albers, W., Hass, C., et.al. (1961),
J. Appl. Phys., 32, 220.
- (5) Allgaier, R.S. and Scheie, P.O. (1961),
Bull. Amer., 6, 436.
- (6) Andrade, E. N. dae and Martindale, J.G. (1935),
Trans. Farad. Soc. (London), 235A, 69.
- (7) Anderson and et.al. (1948),
Nature, 155, 112.
- (8) Appleyard, E.T.S. (1937),
Proc. Phys. Soc. (London), 49, 118.
- (9) Appleyard, E.T.S. and Bristow (1939),
Proc. Roy. Soc., A172, 530.
- (10) Asanabe, S. (1959),
J. Phys. Soc. Japan, 14, 281.
- (11) Asanabe, S. and Okazaki, A. (1959),
Proc. Phys. Soc. (London), 73, 824.
- (12) A.S.T.M. Card No: 1-0984.
- (13) A.S.T.M. Card No: 1-1010.
- (14) Austin, L.W. (1907),
Phys. Rev., 24, 508.
- (15) Bacquerel, A.E. (1839),
Academie des Sciences, 2, 711-724.
- (15a) Eadschape, S.B. and Goswami, A. (1964),
Ind. J. Pure & Appl. Phys. 2 250-253

(16) Benjamin, P. (1956),
Nature (London), 177, 1030.

(17) Bloch, F. (1928),
Z. Physik., 52, 555.

(18) Bloem, J. and Kroger, F.A. (1956),
Z. Phys. Chem., 7, 1.

(19) Bonfiglioli, ^{et al} (1956), J. Appl. Phys. 27, 201-203.

(20) Bose, J.C. (1904), U.S. Patent, 756840.

(21) Bottom, V. (1949),
Phys. Rev., 75, 1310.

(22) Bottom, V. (1962),
Science, 115, 570.

(23) Bradley, A. (1924),
Phil. Mag., 45, 477.

(24) Brattain, W. H. and Briggs, H.B. (1949),
Phys. Rev., 75, 1705.

(25) Braun, (1874),
Ann. Phys. Chem., 153, 556.

(26) Brebrick, R.F. and Allgaier (1960),
J. Chem. Phys., 32, 1826.

(27) Brebrick, R.F. and Gubner, (1962),
J. Chem. Phys., 36, 170.

(28) Brebrick, R.F. and Gubner, (1962),
Ibid, 36, 1283.

(29) Brebrick, R.F. and Strauss, A.J. (1962),
Bull. Amer. Phys. Soc. Ser. II, 7, 203.

(30) Fredmann, P.W. (1925),
Proc. Amer. Akad. Arts & Sci, 60, 305.

(31) Fredmann, P.W. (1938), *ibid*, 72, 157.

(32) Briggs, H.B. (1950),
Phys. Rev., 77, 287.

- 119
- and Frank,
- (33) Burton, W. K. and Cabrera, N. (1949),
Disc. Faraday Soc., No. 5 (Crystal Growth).
- (34) Cartwright, C. H. et al. (1933), Ann. Physik, 18, 666.
- (35) Cartwright, C. H. et al. (1934), Nature, 134, 287.
- (36) Cartwright, C. H. et al. (1935), Proc. Roy. Soc., 148A, 648.
- (37) Clark, E. D. (1955), Brit. J. Appl. Phys., 6, 158.
- (38) Clerk, M. C. and Anderson, J. C. (1943), Nature, 152, 75.
- (39) Cohen and Kröner, (1913), Ann. Chem. Phys. 82, 587.
- (40) Cowley, J. M. (1963), Acta. Cryst., 1, 516.
- (41) Cowley, J. M. (1963), *ibid*, 6, 846.
- (42) Cowley, J. M. (1966), *ibid*, 6, 653.
- (43) Cowley, J. M. (1969), *ibid*, 12, 367.
- (44) Cowley, J. M. and Moodie, (1967), Acta. Cryst., 10, 609.
- (45) Cowley, J. M. and Moodie, (1969), *ibid*, 12, 363.
- (46) Cowley, J. M. and Moodie, (1969), *ibid*, 12, 366.
- (47) Cowley, J. M. and Moodie, (1969), *ibid*, 12, 423.
- (48) Cowley, J. M., Rees, A. L. G. and Spink, J. A. (1951),
Proc. Phys. Soc., A64, 609.
- (49) Cowley, J. M., Rees, A. L. G. and Spink, J. A. (1951),
Proc. Phys. Soc., A64, 638.
- (50) Cowley, J. M., Rees, A. L. G. and Spink, J. A. (1963),
J. Sci. Instrum., 30, 33.
- (51) DeBoer and Kraak, H. H., (1936), Proc. Trav. Chim., 65, 941.
- (52) Dixit, K. R. (1933), Phil. Mag., 16, 1049.
- (53) Drude, P. (1894), Ann. d. Physik, 51, 77.
- (54) Drude, P. (1900), Ann. Phys. Lpz (4) 39, 789.
- (55) Eisenmann, L. (1940), Ann. Physik, 38, 121.
- (56) Faraday, (1877), Trans. Roy. Soc. (London), 147, 145.
- (57) Finch, C. I. and Wilman, H. (1937), Engl. Exact. Nature, 16, 353
- (58) Fowler, R. H. (1933), Proc. Roy. Soc., A140, 505.

(59) Frank, F.C. and Van-der-Merwe, J.H. (1949), Proc. Roy. Soc., A198, 126, 205, 216.

(60) Fuchs, K. (1938), Proc.Cambr.Phil.Soc., 34, 100.

(61) Garnett, J.C.M. (1904), Trans.Roy.Soc.(London), 203A, 385.

(62) Ghosh, S. K. (1961), J.Phys.Chem.Solids, 19, 61.

(63) Gillham and et.al. (1955), Phil.Mag. 46, 1051.

(64) Goldschmidt, (1927), Geochmische Verteilungsgesetze VIII.

(65) Gontier, and et.al. (1956), C.R.Acad.Sci.(Paris), Vol. 242, No.26, 3054-6.

(66) Goswami, A. (1961), Nature, 191, 160.

(67) Goswami, A. (1967), Jour.Sci. & Ind. Research, 16B.

(68) Goswami, A. and Jog, R. H. (1964), Indian J. Pure and Appl. Phys., 2, 407-408

(69) Goswami, A. and Trehan, Y. N. (1966), Indian Institute of Metals 10th Annual Meeting.

(70) Goswami, A. and Trehan, Y. N. (1969), Trans.Parad.Soc., 155, 2122.

(71) Goswami, A. and Trehan, Y. N. (1969), Proc.Nat.Inst. Sci. Ind., 25, 210.

(72) Haken, W. (1910), Ann.Phys. 32, 291, micro card.

(73) Ham, F.S. and Mattis, D.C. (1960), I.B.M. J.Rev.Dev. 4, 158.

(74) Hashimoto and Hirakawa, (1957), J. Phys.Soc. Japan, 11, 716.

(75) Hawley, C., Cartwrite, Harberfeld-Schwarz (1948), Proc. Roy. Soc., 148A, 648.

(76) Heikes, R.R. and Miller, F.C. and Ure, R.W.(Jr.), "Thermoelectricity", p.406, Interscience Publishers, New York

(77) Helmut and Schwaz, (1962), Z.Physik, 132, 402.

(78) Hennig, (1956), Z.Physik, Vol. 144, 1-3, 296-310.

(79) Hintenbergen, H. (1942), Z.Physik, 119, 1.

(80) Hippel, A.V. (1936), Zeits, f. Physik, 101, 680.

(81) Hippel, A.V. (1948), J.Chem. Phys., 6, 372.

(82) Hippel, A.V. and Rittner, E.S. (1946), J.Chem.Phys., 14, 370.

(83) Hofmann, W. (1935), Z.Kristallogr., 92, 161.

(84) Holmes (1923) Ann Chem Phys. 91, 501.

(85) Holland, L. (1956) "Vacuum Deposition Thin Films" (London), Chapman and Hall.

(86) Houston, B.B., Bis, R.F. and Gubner, E. (1961), Bull.Amer.Phys.Soc., 6, 436.

(87) Howarth, D. H. and Sondheimer, (1953), Proc.Roy.Soc.A219,53.

(88) Ioffee, A.F. (1957), "Semiconductor thermoelements and thermoelectric cooling", Infosearch. Ltd, (London), 149.

(89) Ioffee, A.F. (1960), "Physics of Semiconductors", Infosearch. Ltd, (London).

(90) Kelley, K. K. (1939), J.Amer.Chem.Soc., 61. 203.

(91) King, (1917), Phys.Rev., 2, 291.

(92) Koli, S.S. (1965), Ph.D. Thesis, Poona University.

(93) Kossel, W. (1927), Nachr.Ges. Wiss. Göttingen, 135.

(94) Kossel, W. (1928), Quanten theorie und Chemie, p.46, Leipzig.

(95) Kuwabara, (1959), J. Phys.Soc. Japan, 14, 1206.

(96) Lange and Hiller, (1929). Z.Phys., 30, 419.

(97) Landau, L. (1933). Phys. Zeits, 6, 675.

(98) Lark-Horowitz, (1954) "The Present State of Physics" American Association for the Advance of Science, Washington (1954).

(99) Lashkarev, (1933) "Electron Diffraction", G.T.T.I.Moscow, Leningrad.

(100) Lawson, W.D. (1961), J. Appl. Phys.22, 1444.
(1962), J. Appl. Phys.23, 495.

(101) Lennard, (1932), Trans.Farad.Soc. 28, 333.

(102) Leonard, W.F. and Ramey, F.L. (1964), J.Appl. Phys.35, 2963.

(103) Levinstein, H. (1949), J.Appl. Phys. 20, 306.

Lindsay, (1951), Phys.Rev., 84, 569.

- 122
- (104) Loferski, J., (1952), Phys.Rev., 87, 906.
- (105) Loferski, J., (1954), Phys.Rev., 93, 707.
- (106) Longden, (1900), Phys.Rev., 1. xi, p.40 and p.84.
- (107) Lorentz, H.A. (1904-1906), Proc.Acad.Sci. Amst., 7, p.438, 585, 684.
- (108) Louis-Harris, (1946), J. Appl. Phys. 17, 757.
- (109) Mathew, J.W. (1959), Phil. Mag., 4, 1017.
- (110) Mathew, and Phillips, (1962), Phil. Mag., 7, 915.
- (111) Matukura, Yamamoto and Okazaki, (1953), Mem.Fac.Sci. Kyusyu. Univ. Ser.B1, 98.
- (112) Mayer, H. (1955), Physik Duenner Schichten wissenschaftliche Verlagsgesellschaft m.b.H. Stoff-gart, p.178-273.
- (113) Mayer, H. (1959), "Structure and Properties of Thin Films". p.225, Wiley, New York.
- (114) Mayer, H. (1961), Symposium on Electrical and Magnetic Properties of Metallic Thin Layers, Louvain Belg.
- (115) McKay and Gravelle, (1961), Can.J. Phys. 39, 534.
- (116) McHugh, J. P. and Tiller, W.A. (1960), A.I.M.E. 218, 187.
- (117) Mellor, J.W. (1930), Comprehensive treatise on Inorganic and Theoretical Chemistry, Vol.7, Longman Green and Co., London, New York.
- (118) Miller, R.F., (1925), J.Opt. Soc. Amer., 10, 621.
- (119) Miyake, S. et.al. (1954), Acta. Cryst., 2, 218.
- (120) Miyake, S. et.al. (1954), *ibid*, 2, 220.
- (121) Miyake, S. et.al. (1950), *ibid*, 3, 314.
- (122) Moss, T.S. (1949), Proc.Phys.Soc.(London), A62, 264.
- (123) Moss, T.S. (1951), Proc.Phys.Soc.(London), A64, 590.
- (124) Moss, T.S. (1952), Proc.Phys.Soc.(London), A65, 62 and 147.
- (125) Mott, T.S. and Chasmer, R.P.(1948), Nature, 161, 244.

- 123
- (126) Mugge, O. (1903), Jahrbuch Mineralogie Beil, Bd. 16, 335.
- (127) Nassbaum, A. (1953), Ph.D. Thesis, Pennsylvania.
- (128) Nassbaum, A. (1954), Phys.Rev., 94, 337.
- (129) Naugebauer, C.A. (1962), Z.Angew.Phys. 14, 182,
- (130) Naugebauer, C.A. (1964), "Physics of Thin Films", Vol.2, p.11(Academic Press, New York, London).
- (131) Naugebauer, C.A. and Webb, M.B. (1962), J.Appl.Phys., 33, 74.
- (132) Okazaki, A. (1959), J.Phys.Soc. Japan, 14, 281.
- (133) Okazaki, A. and Veda, I. (1956), J.Phys.Chem.Japan, 11, 470.
- (134) Okazaki, A. and Veda, I. (1956), Mem.Fac.Sci.Nyusyu Univ. Ser. B2, 46-49.
- (135) Olshausen, S.V. (1925), Zeits. Krist, 61, 463-514.
- (136) Palatnik and Levitin(), Doklady Akad. Nauk. SSSR. 25, 215.
- (137) Palmer, W.C. (1954), J.Appl. Phys. 25, 216.
- (138) Pashley, D.W. (1964), Adv.Phys. 5, 176.
- (139) Pashley, D.W. (1959), Phil.Mag., 4, 316, 324.
- (140) Patterson, (1900), Phil. Mag., 4, 652.
- (141) Pauling, L. (1947), J.Am. Chem. Soc., 69, 542.
- (142) Phillips, V.A. (1960), Phil. Mag., 5, 571.
- (143) Philip and Trompette, (1955), C.R.Acad.Sc.(Paris), Vol. 241, No.8, 627-629.
- (144) Picard, R.G. and Luffendack, C.S. (1943), J.Appl.Phys., 14, 291
- (145) Pierce, W.G. (1907), Phys.Rev., 25, 31.
- (146) Pierce, W.G. (1909), Phys.Rev., 28, 153.
- (147) Pierce, W.G. (1909), Phys.Rev., 29, 478.
- (148) Piggott, M.R. and Wilman, H. (1958), Acta.Cryst., 11, 93.
- (149) Pinsker, Z. G. (1953) "Electron Diffraction"(Butterworth, London).
- (150) Pinsker, Z. G. (1959) "Advances in Electronics and Electron Physics", Reprints from Academic Press. Inc. New York.
- (151) Quarrel, A.G. (1937), Proc.Phys.Soc.(London), 49, 279.

- 124
- (152) Raether, H. (1951), *Ergeb. Exakt. Natur*, 24, 64.
 - (153) Raether, H. (1957), *Hand buch der Physik*. (Eds. Plugg) Vol. 32, 443, Berlin, Göttingen, Heidelberg, Springer Verlag.
 - (154) Rajgopalan and Ghosh, S. K. (1963), *Physica.*, 29, 234.
 - (155) Ramanjanov, (1962), *Solid State (Sovient Physics)*, 3, No.8.
 - (156) Peimer, (1957), *Z.Naturforsch*, 12a, No.6, #25-6.
 - (157) Roth, H. (1959), *J.Phys.Chem. Solids*, 2, 525.
 - (158) Royer, L. (1928), *Bull. Soc. Franc. Min.* 61, 7.
 - (159) Royer, L. (1936), *Compt. rend.* 202, 1687.
 - (160) Sagar, A. and Miller, B.C. (1962), *Bull.Amer.Phys.Soc.*, Sr.II, 7, 203.
 - (161) Sakurai, T. P. (1956), *J.De. Physique. Radium*, 17, 274.
 - (162) Sakurai, T. P. & Nunesue, S. (1952), *Phys.Rev.*, 85, 921.
 - (163) Scanlon, (1948), Ph.D.Thesis, Purdue University.
 - (164) Scanlon, W.W. and Lark-Horvitz (1947). *Phys. Rev.*, 72, 530.
 - (165) Schaidt, E. and Steffalbach, F. (1937), *Ann.Physik*, 29, 274
 - (166) Schmidt and Wassermann, (1927), *Zeitz. f. Physik*, 46, 663
 - (167) Schutz, (1951), *Acta.Cryst.*, 4, 483.
 - (168) Schwrz, H. (1962), *Z.Physik.*, 162, 402.
 - (169) Seebeck, (1822).
 - (170) Silverman, S. J. and Levinstein, (1954), *Phys.Rev.*, 94, 871.
 - (171) Slattery, M. K. (1925), *Phys.Rev.*, 21, 378.
Slattery, M. K. (1925), *Phys.Rev.*, 25, 333.
 - (172) Smith, W. (19), *Jour.Soc.Telegraph.Engineers*, 2, 31-33.
 - (173) Snennett, R.S. and Scott, W.G.(1950), *J.Opt.Soc.Am.*, 40, 203.
 - (174) Smith, R.A. (1951), "Semiconducting Materials", p.198, (Butterworths Scientific Publications).
 - (175) Smith, R. A.(1953), *Advances in Phys.*, 2, 321.
 - (176) Smith, R. A. (1954), *Physica*, 20, 910.
 - (177) Sondheimer, E. H. (1950), *Phys.Rev.*, 80, 401.

(178) Sondheimer, E. H. (1962), *Advances in Phys.* 1, 1.

(179) Sommerfeld, A. (1928), *Zeitschrift.Fur Physik*, 47, 1.

(180) Sommerfeld, A. (1928), *ibid*, 47, 43.

(181) Squire, C.F. (1939), *Phys. Rev.*, 56, 960.

(182) Steffen, J. (1865), *Ann.Physik.*, 124, 632.

(183) Steinberg, J.C. (1923), *Phys.Rev.*, 21, 22.

(184) Stranski, I. N. (1949), *Disc. Faraday Soc.*, No.6, p.13 (Crystal Growth).

(185) Tartakovski, P.S. (1932), "Experimental Basis of Wave Theory of Matter" G.T.T.I. Moscow, Leningrad.

(186) Thomson, G. P., Cochran, W. (1939), "Theory and Practice of Electron Diffraction" (McMillan, London).

(187) Tolansky, S. (1948) "Multiple beam interferometry" (London), Oxford University Press.

(188) Uyeda, R. (1951), *Acta.Cryst.*, 1, 227.

(189) Uyeda, R. (1951), *Acta.Cryst.*, 1, 229.

(190) Vainshtein, B. K. (1949), *Dokl. Acad.Nauk SSSR*, 68, 301.

(191) Vainshtein, B. K. (1964), "Structure Analysis by Electron Diffraction" Translated and edited by E.Feigl & J.A.Spink.

(192) Vanshtein, B. K. and Pinsker, Z.G. (1949), *J.Phys.Chem. USSR*, 23, 1068.

(193) Vanshtein, B. K. and Pinsker, Z.G. (1950a) *J.Phys.Chem. USSR*, 24, 432.

(194) Vanshtein, B. K. and Pinsker, Z.G. (1950b), *J. Dokl.Akad. Nauk SSSR*, 72, 83.

(195) Van-Dyke, G.D. (1922), *J. Opt.Soc.Amer*, 6, 917.

(196) Verwey, E. J., Haayman, P.W. and Romeyn, F.C. (1948), *Chem. Weekbl.* 44, 705.

(197) Vincent, (1900), *Ann.d. chim. et Phys.*, 7, 421.

(198) Volmer, M. (1939), *Kinetic der Phasenbildung*, Steinkopff, Dresden and Leipzig.

(199) Wait, G.R. (1922), Phys.Rev., 19, 616.

(200) Wallerant, F. (1902), Bull.Soc.Franc.Mineral., 25, 180.

(201) Wayne, S. and Lark-Horovitz, (1947), Phys. Rev. 72, 530.

(202) Weber and Costerhuis, (1917), K.Akad.Amsterd.Proc. 19, 597.

(203) Weiner, F. K. (1964), Proc. I.E.E.E., 52, 608.

(204) Williman, R.C. and Bauckus, R.C. (1949), J.Appl.Phys., 20, 98.

(205) Wilman, H. (1948), Proc. Phys. Soc. (London). 60, 341. 61, 416.

(206) Wilman, H. (1955), Proc.Phys.Soc.(London), 68B, 474.

(207) Wilson, A. H. (1931), Proc.Roy.Soc., 133A, 458.

(208) Wilson, A. H. (1931), Proc.Roy.Soc., 134A, 277.

(209) Wilson, A. H. (1936), "Theory of Metals".

(210) Wold, (1916), Phys.Rev., 7, 163.

(211) Yin Shih-tuan and Regel, H. (1962), Solid State(Soviet Physics), 3, 2627.

(212) Yurkov, V.A. (1963), Zhur.Fekh.Fiz., 23, 1464.